

Design of Nonlinear Circuits
The Linear Time-Varying Approach

Design of Nonlinear Circuits
The Linear Time-Varying Approach

Proefschrift

ter verkrijging van de graad van doctor
aan de Technische Universiteit Delft,
op gezag van de Rector Magnificus prof.dr.ir. J.T. Fokkema,
voorzitter van het College voor Promoties,
in het openbaar te verdedigen op 9 september 2003 om 15:30 uur

door

Fransiscus Christianus Maria KUIJSTERMANS

elektrotechnisch ingenieur
geboren te Oud en Nieuw Gastel.

Dit proefschrift is goedgekeurd door de promotor:
Prof.dr.ir. A.H.M. van Roermund

Samenstelling promotiecommissie:

Rector Magnificus	Voorzitter
Prof.dr.ir. A.H.M. van Roermund	Technische Universiteit Delft, promotor
Dr.ir. A. van Staveren	Technische Universiteit Delft, toegevoegd promotor
Prof.dr. J.R. Long	Technische Universiteit Delft
Prof.dr.ir. P.P.J. van den Bosch	Technische Universiteit Eindhoven
Prof.dr.-Ing. W. Mathis	Universität Hannover
Prof.dr.-Ing. W. Schwarz	Technische Universität Dresden
Dr.ir. J.-W. Eikenbroek	Ericsson EuroLab Netherlands B.V.

This work was supported in part by the Foundation for Technical Sciences (STW) under project DEL 66.4405.

ISBN 90-9017169-X

Copyright © 2003 by F.C.M. Kuijstermans

All rights reserved.

No part of the material protected by this copyright notice may be reproduced or utilized in any form or by any means, electronic or mechanical, including photocopying, recording or by any information storage and retrieval system, without prior written permission from the author: F.C.M. Kuijstermans, Leiderdorp, the Netherlands.

Printed in the Netherlands by PrintPartners IPSkamp B.V., Enschede

Contents

1	Introduction	1
2	Analysis and synthesis of dynamic nonlinear circuits	5
2.1	Classification of instantaneous nonlinear behaviour	5
2.2	Classification of nonlinear dynamic behaviour	7
2.3	General synthesis/analysis approach	9
2.3.1	High-level synthesis/analysis	10
2.3.2	Low-level analysis/synthesis	10
2.4	Conclusions	12
3	Modeling approaches for high-level synthesis/analysis	13
3.1	Objectives and desired properties	13
3.2	General modeling approaches	14
3.3	Approximation by a pre described method	14
3.3.1	Taylor-series expansion	14
3.3.2	Volterra functional expansion	15
3.3.3	Piece-wise linear modeling	16
3.4	Expansion in basic functions	17
3.5	Conclusions	18
4	Modeling approaches for low-level analysis/synthesis	21
4.1	Objectives and desired properties	21
4.2	General modeling approaches	22
4.3	Expansion in simpler systems	24
4.3.1	Taylor-series expansion	25
4.3.2	Volterra functional expansion	25
4.3.3	Expansion in basic functions	26
4.3.4	Piece-wise linear modeling	27
4.4	Input signal dependent modeling	27
4.4.1	Linear time-invariant small-signal modeling	27
4.4.2	Linear time-varying small-signal modeling	28

4.5	Conclusions	28
5	The linear time-varying approach	31
5.1	The linear time-varying approach	32
5.1.1	The linear time-varying small-signal model of a nonlinear circuit	33
5.1.2	The linear time-invariant small-signal model of a nonlinear circuit	34
5.1.3	Linear time-invariant circuits	35
5.2	Modeling of non-idealities in the LTV approach	36
5.2.1	Deviations in instantaneous behaviour	36
5.2.2	Internally generated noise	37
5.2.3	Deviations in dynamic behaviour	38
5.3	Theory of linear time-varying systems	38
5.3.1	General solution in terms of the matriciant	39
5.3.2	Linear systems with constant coefficients	42
5.3.3	Linear systems with periodic coefficients	44
5.3.4	Linear systems with arbitrary time-varying coefficients: quasi-static and dynamic eigenvalues and eigenvectors	45
5.3.5	Lyapunov characteristic exponents	49
5.4	First-order systems and their stability	52
5.4.1	The dynamic eigenvalue and eigenvector	52
5.4.2	Lyapunov and Floquet exponent and stability	53
5.5	Second-order systems and stability	54
5.5.1	Dynamic eigenvalues and eigenvectors using the Riccati equation	54
5.5.2	Lyapunov and Floquet exponents and stability	56
5.6	Higher-order systems and stability	57
5.7	Conclusions	58
6	The linear time-varying approach applied to a negative-feedback class-B output amplifier	61
6.1	Negative-feedback amplifiers and class-B output stages	62
6.2	Class-B output stage	63
6.2.1	Circuit description	63
6.2.2	Model division	65
6.2.3	Dynamic bias trajectory	67
6.2.4	Linear time-varying small-signal model	72
6.2.5	Floquet exponent	76
6.3	Application of a class-B output-stage in a negative-feedback amplifier	78
6.3.1	Specification	79
6.3.2	The basic configuration	79

6.3.3	Class-B implementation	80
6.3.4	Stability analysis of the amplifier	82
6.3.5	Implementation of the auxiliary circuitry	83
6.3.6	Measurement results	85
6.4	Conclusions	86
7	The linear time-varying approach applied to dynamic translinear circuits	89
7.1	Static and dynamic translinear circuits	90
7.1.1	The static translinear principle	90
7.1.2	The dynamic translinear principle	91
7.2	The linear time-varying approach applied to a first-order dynamic translinear filter	92
7.2.1	DTL synthesis and circuit description	92
7.2.2	The linear time-invariant and quasi-static approach	94
7.2.3	The linear time-varying approach	96
7.2.4	Comparison between the quasi-static and linear time-varying approach	98
7.3	The linear time-varying approach applied to a dynamic translinear oscillator	99
7.3.1	DTL synthesis of a second-order oscillator	100
7.3.2	The linear time-varying approach	102
7.4	Conclusions	106
8	The linear time-varying approach applied to a limiting differential pair	109
8.1	Circuit description	109
8.2	First-order dynamic behaviour	114
8.2.1	Dynamic bias-trajectory	115
8.2.2	Dynamic eigenvalue	116
8.2.3	Floquet exponent	118
8.3	Second-order dynamics	120
8.3.1	Dynamic bias-trajectory	122
8.3.2	Dynamic eigenvalues and eigenvectors	122
8.4	Conclusions	127
9	Conclusions	129
A	Lyapunov transformations	133
B	Dynamic eigenvalues using quasi-static similarity-transforms	137
C	Transformation of the Riccati differential equation	141

viii

Bibliography	143
Summary	147
Samenvatting	153
Acknowledgements	159
List of publications	161
Biography	163

List of Symbols

Symbol	Meaning
\mathbf{A}	time-invariant transition matrix
$\mathbf{A}(t)$	time-varying transition matrix
\mathbf{A}_x	transition matrix of the variational equation
$\mathbf{A} \in C(I)$	the elements of the matrix \mathbf{A} are continuous on the interval I
β	Floquet exponent
\mathcal{C}	set of complex numbers
\mathcal{C}^n	n -dimensional complex vector space
$\text{Ln } \mathbf{X}$	logarithm of the matrix \mathbf{X}
$\mathbf{L}(t)$	matrix defining a Lyapunov transformation
λ	algebraic eigenvalue
$\lambda(t)$	dynamic eigenvalue
$\lambda_{qs}(t)$	quasi-static eigenvalue
\mathcal{R}	set of real numbers
\mathcal{R}^n	n -dimensional Euclidean vector space
\mathbf{s}	algebraic eigenvector
$\mathbf{s}(t)$	dynamic eigenvector
$\mathbf{s}_{qs}(t)$	quasi-static eigenvector
T	period of a periodic function
t	time
$\mathbf{u}(t)$	vector of external sources
$\mathbf{u}_b(t)$	vector of deterministic part of external sources
$\mathbf{u}_\delta(t)$	vector of variations of external sources, for reasons of compactness also denoted as $\mathbf{u}(t)$
$\Omega_{t_0}^t \mathbf{A}$	matriciant of matrix \mathbf{A}
ω	spectral frequency in (rad/s)
$\mathbf{X}(t)$	fundamental matrix
$\mathbf{X}(t, t_0)$	fundamental matrix normalized at a point $t = t_0$
$\mathbf{x}(t)$	vector of state variables
$\mathbf{x}_b(t)$	dynamic bias trajectory of the state variables

$\mathbf{x}_\delta(t)$	vector of variations of the state variables, for reasons of compactness also denoted as $\mathbf{x}(t)$
$\dot{x} = \frac{d}{dt}x$	time derivative of x
$\mathbf{x} \in C(I)$	the elements of the vector \mathbf{x} are continuous on the interval I
χ	Lyapunov exponent

Introduction

Over the last years interest in the design of nonlinear electronic circuits has been steadily increasing. The reason for this is twofold. On the one hand, some of the basic constants and functions needed in signal processing are fundamentally nonlinear. Examples are frequency references (implemented by oscillators) and the limiting function. They can be inherently implemented by nonlinear circuits only. The ever-growing demand for higher performance has led to much interest in the structured design of this type of electronic circuits.

On the other hand, the vast amount of work done on structured design-methodologies for classic linear-based electronic circuits has led us to the stage where we are approaching the limits of what is theoretically possible, given a certain IC-process. Therefore, an evolutionary improvement of these linear-based circuits will only lead to slight improvements in performance. Using linear design methods we can only achieve big advances in performance by migrating to more advanced processes or technologies and that is a very expensive strategy. From a design methodology point of view the other option is to extend the linear paradigm and come up with a nonlinear paradigm, which involves using entirely new nonlinear circuit concepts. One example to demonstrate this option is the use of dynamic translinear circuits, which use the exponential relation as a primitive for synthesizing linear and nonlinear differential equations.

The use of nonlinear relations as primitives for the synthesis of electronics inherently implies that we have to deal with the analysis and synthesis of nonlinear electronic circuits. A structured design methodology exists for some circuits exhibiting weak nonlinearities, for example for oscillators. For these circuits often linear or quasi-static frequency-domain methods still provide a good approximation. This is no longer the case for circuits with a very strong non-linearity, such as limiters, and for these circuits no structured design approach is available.

This thesis presents a general approach to the structured design of nonlinear circuits. A good design should always start with a synthesis and optimization procedure at the highest possible hierarchical level. At this hierarchical level the designer should be able to quickly explore the design space in order to choose the right (type of) circuit for the job. When designing nonlinear circuits this hierarchical level should include the ideal nonlinear relations to be used as primitives for high-level analysis and synthesis. Therefore, this level will be specific to the type of nonlinear circuit to be designed. For some nonlinear design concepts, for example dynamic translinear circuits, such a high-level analysis and synthesis method already exists.

Once a specific circuit topology has been chosen the influence of non-idealities of the nonlinear relations and circuit implementation should be analyzed. The resulting deterioration of instantaneous behaviour, noise behaviour and dynamic behaviour should be determined. At this lower hierarchical level we encounter typical nonlinear issues such as signal-dependent dynamic behaviour, signal-dependent noise and signal-dependent transfers. To date, no suitable design-oriented analysis method has been found for this hierarchical level. This thesis presents the linear time-varying approach as a general method for analyzing deviations in instantaneous behaviour, noise behaviour and dynamic behaviour of nonlinear circuits in the context of lower-hierarchical-level analysis and synthesis.

The main contributions of this thesis are in the field of the application of the linear time-varying approach for analyzing the dynamic behaviour of nonlinear circuits in the context of low-level analysis/synthesis. For this first the low-level analysis/synthesis step is put in the perspective of a general design approach, which starts with a high-level synthesis/analysis step based on ideal models. When the linear time-varying approach is used in the low-level analysis/synthesis step, information obtained in the high-level step can be used to decrease the complexity in the low-level step. It is shown how the linear time-varying approach can be used to model and analyze deviations in instantaneous behaviour, noise behaviour and dynamic behaviour. The theory underlying the linear time-varying approach is treated. Much effort is done to relate the concepts of this theory to familiar concepts from LTI design. An important step in applying the linear time-varying approach is determining the dynamic eigenvalues by solving a Riccati differential equation. A transformation method is introduced which can obtain this solution even if it contains singularities. The linear time-varying approach is applied to various specific nonlinear circuits: a negative-feedback amplifier with class-B output stage, a dynamic translinear filter and oscillator and a differential pair used as limiter. These examples illustrate the usefulness and limitations of the linear time-varying approach for low-level analysis/synthesis.

This thesis is structured as follows. After the introduction, Chapter 2 gives a brief survey of the instantaneous behaviour and dynamic behaviour of nonlinear circuits. They are classified in order of increasing complexity of non-linearity, and the applicability and break-down of existing analysis methods is addressed. A general approach to the synthesis and analysis of nonlinear circuits is then presented. It consists of a high-level synthesis/analysis step, specific to the type of nonlinearity, and a low-level analysis/synthesis step, in which performance degradation due to small deviations of the ideal high-level behaviour is covered.

The high-level synthesis/analysis step is covered in Chapter 3. The possible approaches for this step are presented and our choice is given. In Chapter 4 we look into various modeling approaches for low-level analysis/synthesis and it is explained why we have chosen the linear time-varying approach. The linear time-varying approach is elaborated on in Chapter 5. It explains the fundamental concepts used in this model and shows how they relate to the familiar linear time-invariant concepts. The use of the linear time-varying small-signal model for the analysis of deviations in amplitude behaviour, noise behaviour and dynamic behaviour of nonlinear circuits is presented. The determination of the dynamic behaviour is identified as the first and most important step in this analysis, and the rest of the thesis focuses on this task.

The following chapters describe the use of our structured design approach in the design of certain specific nonlinear circuits. In Chapter 6 the linear time-varying approach is applied to a class-B stage, used as output stage in a negative-feedback amplifier. This is a generally used amplifier stage with a hard nonlinearity. Until now, the effects due to this nonlinearity have not been well understood. The linear time-varying small-signal model enables us to get some insight into the dynamic behaviour of this amplifier stage. First it is analyzed separately and then applied as an output stage in a negative feedback amplifier. In Chapter 7 the linear time-varying approach is applied to two dynamic translinear circuits: a dynamic translinear filter and a dynamic translinear oscillator. For this type of circuit a high-level synthesis/analysis method exists based on ideal behaviour, but non-ideal behaviour could not be analyzed because a suitable method was lacking. In Chapter 8 the linear time-varying approach is used to analyze the dynamic behaviour of a differential pair. When driven with a sufficiently large input signal, this commonly used amplifier stage implements the limiter function and inherently behaves strongly nonlinear.

The general design approach presented is reviewed and conclusions are drawn in Chapter 9.

2

Analysis and synthesis of dynamic nonlinear circuits

Over the last years interest in the design of nonlinear circuits has been steadily increasing. Research has been done in topics varying from circuits and systems exhibiting weak linearities [26], [51] up to strongly nonlinear ones [13], [32], [50] with varying methods of handling the design complexity.

In this chapter we start to summarize the different kinds of nonlinearities and of nonlinear dynamic behaviour which can occur in a circuit or system. In the first section we classify nonlinearities according to their instantaneous nonlinear behaviour. In the following section we give a classification of nonlinear dynamic behaviour. Then we present our general synthesis/analysis approach for handling these nonlinearities, and we give the limitations of this approach. We end with some conclusions.

2.1 Classification of instantaneous nonlinear behaviour

The most obvious way to distinguish between different types of nonlinearities is to consider their instantaneous behaviour. Based on the amount of amplitude domain nonlinearity relative to the signal amplitudes, here five classes are considered:

1. linear circuits,
2. affine circuits,
3. linearizable circuits,

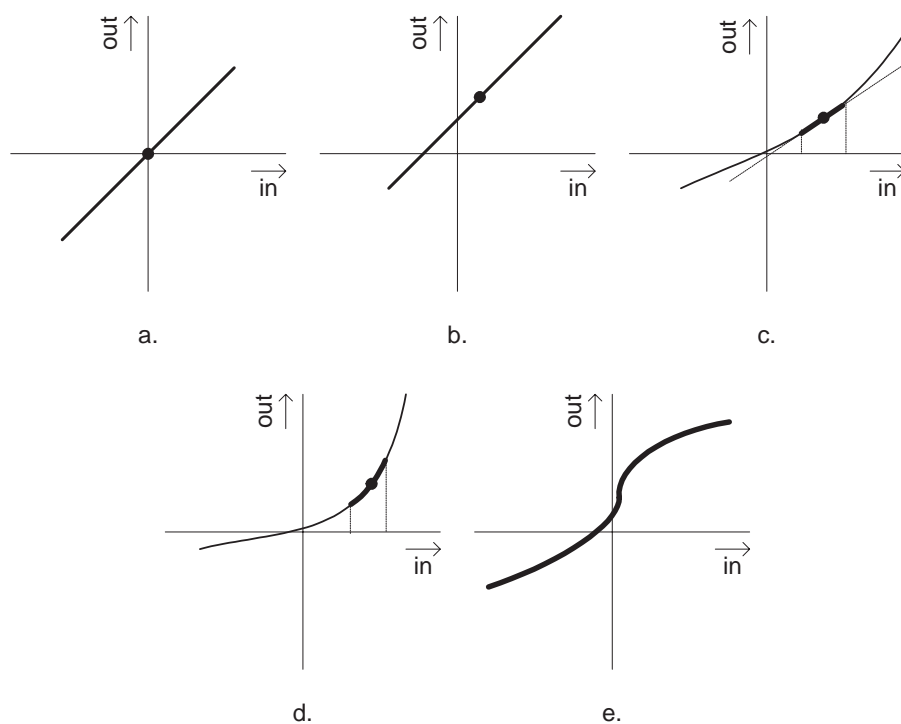


Figure 2.1: Classes of instantaneous nonlinear behaviour: a. linear circuits, b. affine circuits, c. linearizable circuits, d. weakly nonlinear circuits, e. strongly nonlinear circuits.

4. weakly nonlinear circuits,
5. strongly nonlinear circuits.

The first class is that of the *linear circuits*. An example of a linear input-output relation is given in Figure 2.1a. Linear circuits are characterized by the fact that they obey the superposition principle: their response to a linear combination of input signals equals the linear combination of the individual responses. This is one of the main properties which enables the use of a whole range of techniques for analyzing and synthesizing linear circuits and systems, and it makes their behaviour signal-amplitude independent.

Though the superposition principle is theoretically only applicable for “lines through the origin”, *affine circuits*, as depicted in Figure 2.1b., can easily be covered by a translation to the origin. This introduces a first notion of an “operating point”, indicated by the dot in Figure 2.1b. For linear and affine

systems the choice of the operating point has no influence on the linear model after translation to the origin, and there is no limitation on signal amplitudes.

Linearizable circuits can still be described by linear behaviour in the neighbourhood of an operating point. If a linear model is used in the operating point, we can still use linear techniques to describe the response to small variations around the operating point. The linear model is depicted by the thick line in Figure 2.1c., which is tangent to the transfer curve in the operating point. The distinction with intrinsically linear circuits is that the linear model will change as a function of the operating point and that the linear model is valid for a limited range of signal amplitudes only. Most of present-day circuits designed with linear techniques belong to this class of circuits.

For *weakly nonlinear circuits* we can still use the notion of an operating point. However, in order to adequately describe their behaviour in the vicinity of this bias-point a linearized model does not suffice. Since the nonlinearity is assumed to be weak, only a few orders of nonlinearity need to be taken into account in a series expansion in the operating point. This is shown as the curved thick line in Figure 2.1d. The distinction between linearizable circuits and weakly nonlinear circuits is determined by the signal amplitudes which need to be handled by the circuit relative to the circuit nonlinearity, and by the application requirements. For large signal amplitudes the behaviour of a linearizable circuit will start to deviate from its linear model, and it will need to be modeled as a weakly nonlinear circuit. On the other hand, if the signal amplitudes in a weakly nonlinear circuits are sufficiently small, its behaviour can be accurately described by a linear model.

Finally, for *strongly nonlinear circuits* a series expansion in an operating point is no longer suitable. For adequate precision large numbers of orders would need to be taken into account. Strongly nonlinear circuits are characterized by the property that higher-order nonlinear components are dominant over the first-order linear component in the transfer function, and that small variations in the signal amplitudes cause significant variations in behaviour. Therefore, for this type of circuits we would prefer methods which take the entire nonlinearity directly into account, without the intermediate step of an operating point, as depicted in Figure 2.1e. A method of accomplishing this is the use of an operating trajectory instead of an operating point.

2.2 Classification of nonlinear dynamic behaviour

The step from linear or linearized circuits to nonlinear circuits has a large consequence on the way we have to describe and design the dynamic behaviour of a circuit.

instantaneous behaviour	linear / affine	LTI	LTI
	linearizable		
	weakly nonlinear	quasi-static approach	dynamic approach
	strongly nonlinear		
		slowly-varying	fast varying
dynamic behaviour			

Figure 2.2: Approaches for analysis of dynamic behaviour for different classes non-linear circuits

For linear and linearized circuits the internal dynamics are independent of the signals. Since the superposition principle applies, a direct link exists between time domain and frequency domain description of the circuit, and we can apply all the familiar frequency domain design and analysis techniques. Dynamic behaviour can be described in terms of frequency domain poles and zeros, which are constant and independent of input signals.

For nonlinear circuits the superposition principle no longer holds. Therefore, we can not switch between time-domain and classic frequency-domain at will. Note that the frequency domain is merely a very convenient way of modeling time-domain behaviour. The time domain is what is happening in real life. For nonlinear circuits we have to take the time-domain behaviour as a starting point for describing their dynamic behaviour.

For nonlinear circuits the internal dynamics are dependent on the signals. Based on the relative time-scales of signal variations and of the internal dynamics (“time-constants”) of the circuits, different methods of modeling the dynamic behaviour of these nonlinear circuits need to be used. Two classes can be distinguished:

1. quasi-static approach,
2. dynamic approach.

For circuits in which the signal variations are slow compared to the internal dynamics, a *quasi-static approach* can be used. The circuit can be considered fast enough for the internal dynamics to instantaneously follow the slowly-varying

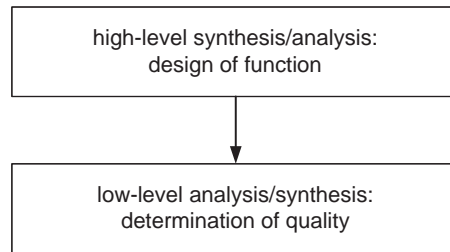


Figure 2.3: Division of design process in two steps

signals: the internal dynamics at a certain instant of time are dependent only on signals at that same instant of time (frozen time approach). Then still the concept of poles, being it time-varying poles, can be used. The pole locations will be dependent on the instantaneous signal values, but not on the dynamics of the signal. This concepts makes sense for the analysis of relatively small variations (e.g. noise) around the (slow) signal trajectory.

For nonlinear circuits in which the signals vary fast compared to the internal dynamics of the circuit, a quasi-static approach is no longer feasible. The internal dynamics at a certain instant of time will be dependent not only on the signals at that same instant of time, but also on the derivatives of the signals. Then a more general time-domain theory is necessary. The conventional pole concept is no longer applicable. The approaches necessary for different classes of nonlinear behaviour are summarized in Figure 2.2.

2.3 General synthesis/analysis approach

The design of nonlinear circuits becomes complicated by the fact that their behaviour is signal-dependent. In this thesis we propose to handle this design complexity by dividing the design process in two main steps, as depicted in Figure 2.3.

First, in a high-level synthesis/analysis step we design the function which needs to be implemented. We choose a hierarchical level such that signal-dependent behaviour is manageable for fast exploration of the design-space. We need to use simple models, which however should cover the fundamental nonlinear relations of the building blocks.

Second, in a low-level analysis/synthesis step we determine the quality of the solutions found. Relatively small deviations from the ideal high-level behaviour are investigated and performance degradation due to these small deviations is determined. More complex models are needed in order to cover the perturbed behaviour. However, at this stage only the effect of small deviations needs to be

modeled, since the overall behaviour is assumed to be covered in the high-level synthesis/analysis step. If the deviations are found to be too large, then we need to go back to the high-level synthesis/analysis step in order to cover this.

2.3.1 High-level synthesis/analysis

The main objective of the high-level synthesis/analysis step is to design the function we want to implement. We need to find circuit topologies which can implement the wanted nonlinear function, and which potentially meet all the specifications. We want to rule out topologies which cannot implement the function or meet the specifications in an early phase. We want to do this in such a way that the design-space can be explored relatively fast.

In order to obtain this goal, we need simple models, which however should cover the fundamental nonlinear relations (the wanted relation) of the building blocks. In these models we should get rid of all details, without losing the fundamental nonlinear relations.

The kind of models used in this step will be very specific to the type of nonlinear circuitry which is being designed. This is the only way to combine fast design-space exploration with adequate precision. Also the way the design-space is explored will depend on the type of nonlinear circuitry. Ideally, the nonlinear-circuit topology is being generated in a synthesis path, without the need for any analysis feedback loops.

An example is the design of filters using dynamic translinear circuits [32]. In dynamic translinear filters we use the exponential behaviour of a bipolar transistor (or a MOSFET in the subthreshold region) in combination with linear capacitors. By using the exponential relation as a primitive and a description in terms of collector currents and capacitor currents, a differential equation can be mapped onto a multivariable polynomial of currents, which then can be mapped onto a dynamic translinear topology. This synthesis path gives us the possibility to easily explore potential dynamic translinear topologies which can implement a wanted differential equation.

2.3.2 Low-level analysis/synthesis

After a circuit topology has been found implementing the nonlinear function, the quality of this solution needs to be determined. The effect of deviations from the simple models used needs to be investigated. The corresponding performance degradation due to these non-idealities needs to be determined. Performance can be degraded in three ways: the instantaneous behaviour can be affected, the signals can be deteriorated by internally generated noise and the dynamic behaviour can be affected.

Instantaneous behaviour

Firstly, the instantaneous transfer of signals from input to output might be affected by non-idealities. These deviations of the designed instantaneous behaviour can be modeled by distortion. If the deviations are signal-amplitude independent (e.g. an extra multiplicative term in the static transfer), the distortion is categorized as linear distortion. If the deviations do depend on signal amplitudes, the distortion is categorized as nonlinear distortion.

Noise

Secondly, noise needs to be considered. We can distinguish two types of noise. In the first place, noise is inherently present in the input signal. In a nonlinear circuit this noise will intermodulate with the signals. Part of this intermodulation is caused by the wanted nonlinear function implemented by the nonlinear circuit. In this case the intermodulation should be covered in the high-level design step. However, non-idealities in the nonlinear circuit might cause additional intermodulation, and this effect needs to be analyzed in the low-level analysis/synthesis step. This additional signal-noise intermodulation is a function of the deviations in instantaneous and dynamic behaviour, and can be analyzed using a model of the modified instantaneous and dynamic behaviour (no additional noise sources are necessary).

In the second place, noise will be generated internally in the circuit. In nonlinear circuits this noise generation can be signal-dependent. It can be analyzed by inserting additional signal-dependent noise sources on appropriate places in the circuit model. In strongly nonlinear circuits in the presence of high noise levels even signal transfer and dynamic behaviour might become noise dependent. However, noise-dependent signal transfer and noise-dependent dynamic behaviour will not be the topic of this thesis.

Dynamic behaviour

Thirdly, the dynamic time-domain transfer of signals from input to output will be affected by non-idealities. If a specific dynamic behaviour was designed in the high-level synthesis/analysis step, then non-idealities will cause the actual dynamic behaviour to be different from the wanted dynamic behaviour (in linear design: the actual pole locations might be different from the wanted pole locations). If a specific dynamic behaviour was not designed (only the instantaneous behaviour was designed in the high-level step), then often a specific lower limit on the speed of the circuit needs to be met (in linear design: a certain bandwidth needs to be obtained). Furthermore, it needs to be determined whether the circuit might go unstable, and what the safety margin is (in linear design: the phase margin needs to be determined).

2.4 Conclusions

In this chapter we classified nonlinearities according to their instantaneous behaviour and their dynamic behaviour. The instantaneous behaviour was classified on the basis of the nonlinearity relative to the instantaneous signal amplitudes, which determines the complexity of the models we need to use. For linear and affine circuits we can use generally valid linear models. For linearizable circuits we can use a linear model for a specific operating point and for a limited signal amplitude range. For weakly nonlinear circuits we need to model a few orders of nonlinearity, again for a specific operating point and a limited signal amplitude range. Finally, for strongly nonlinear circuits, we need to use models which take the entire nonlinearity directly into account.

The dynamic behaviour was classified on the basis of the time-scale of the signal variations relative to the time-scale of internal circuit dynamics. If the signals are relatively slowly-varying compared to the internal dynamics, a quasi-static approach can be used for modeling the dynamic behaviour. If this condition is not met, a more general time-domain theory is necessary.

Furthermore we presented a general synthesis/analysis approach. This approach handles the design complexity by dividing the design process in two main steps. In the first step, a high-level synthesis/analysis step, a topology which implements the wanted (nonlinear) function is found. Simple models, and a synthesis path specific to the nonlinearities, are used in order to perform a fast exploration of the design space. In the second step, a low-level analysis/synthesis step, the quality of the topologies is determined, and the effect of non-idealities on the instantaneous behaviour, noise behaviour and dynamic behaviour is determined.

3

Modeling approaches for high-level synthesis/analysis

In the previous chapter we briefly introduced the design approach presented in this thesis. It is based on a division of the design process in a high-level synthesis/analysis step, in which the desired function is designed, and a low-level analysis/synthesis step, in which the quality aspects of this solution are determined and designed.

In this chapter we cover the high-level synthesis/analysis step. First we describe the objectives of the high-level synthesis/analysis step, and from this we deduce the properties this step should have. Then we consider several modeling approaches which can be used to implement such a high-level synthesis/analysis step, and determine whether they have the desired properties.

3.1 Objectives and desired properties

The main objective of the high-level synthesis/analysis step is to design the function that we want to implement. We need to find circuit topologies which can implement the wanted nonlinear function, and want to rule out topologies which cannot implement the function or meet the specifications in an early phase. We want to do this in such a way that the design-space can be explored relatively fast.

In order to obtain this goal, we need simple models, which however should cover the fundamental nonlinear relations (the wanted relation) of the building blocks. In these models we should get rid of all details, without losing the fundamental nonlinear relations.

Furthermore, the nonlinear-circuit topology is ideally being generated in a

synthesis path, without iterations. This would enable a very fast exploration of the design space. The models used should preferably be suitable for such a synthesis path.

Finally, the designer would like models with a relation to physical laws governing the nonlinear building blocks being modeled. This gives the designer some insight where the behaviour of the model can be influenced in the nonlinear building block. For instance, it would be preferable if state variables in the model have a physical basis, such as capacitor charge or inductor current.

3.2 General modeling approaches

In general two types of approaches for modeling nonlinear circuits for high-level synthesis/analysis can be distinguished. Firstly, the approach can be based on some kind of approximation of the nonlinear transfer curves by a pre described method. Taylor-series expansion, Volterra functional expansion and piece-wise linear approximation belong to this category.

Secondly the approach can be based on expansion of the desired transfer in basic functions, where the basic function can be chosen based on either the type of transfer to be designed or the type of nonlinear building blocks used. For instance, in dynamic translinear circuits the desired transfer is expressed in terms of a multivariable polynomial of currents, since this can be mapped directly on dynamic translinear circuitry.

3.3 Approximation by a pre described method

In the first general type of approaches for modeling nonlinear circuits for high-level synthesis/analysis the model is based on some kind of approximation of the nonlinear transfer curves by a pre described method. Taylor-series expansion, Volterra functional expansion and piece-wise linear approximation belong to this category.

3.3.1 Taylor-series expansion

A very familiar method of modeling a nonlinear transfer is using a Taylor-series expansion. The 1-dimensional Taylor-series expansion $T_{q,p}(x)$ of order p of a nonlinear transfer function $f(x)$ for a certain bias point q is given by

$$T_{q,p}(x) = \sum_{n=0}^p \frac{d^n f(q)}{dx^n} \frac{1}{n!} (x - q)^n \quad (3.1)$$

The model is valid in the vicinity of the bias point q only, especially if only a few terms are used, and for strong nonlinearities a large number of terms is nec-

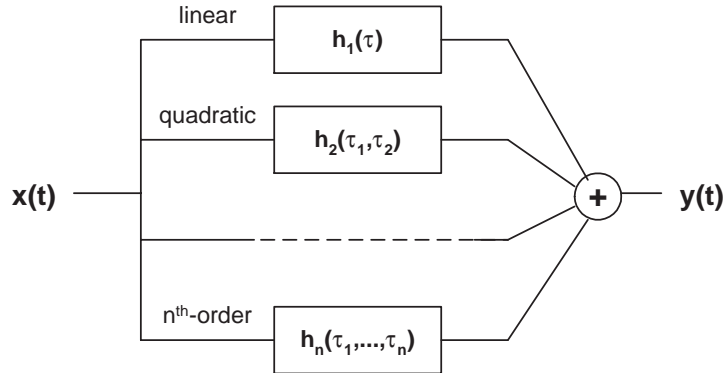


Figure 3.1: Volterra functional expansion

essary for adequate precision, which complicates the model. The Taylor-series expansion can be generalized to multi-dimensional transfers, but it is limited to instantaneous transfers only. Therefore, using Taylor-series only instantaneous transfers can be designed. Finally, for nonlinear circuits the Taylor-series expansion has no physical basis and gives the designer little insight. For linear and linearizable circuits however, the first-order Taylor-series expansion is equivalent to the static small-signal diagram, and can be useful in designing the instantaneous transfer.

3.3.2 Volterra functional expansion

A more general approach, which can also explicitly incorporate dynamic behaviour in the model, is the Volterra functional expansion. It is a generalization of the convolution integral used in linear system analysis.

The Volterra functional expansion represents some arbitrary nonlinear system by a sequence of systems connected in parallel as shown in Fig. 3.1. The first system is a linear system. Its output $y_1(t)$ is simply a convolution of the input $x(t)$ and the impulse response $h_1(t)$:

$$y_1(t) = \int_{-\infty}^{\infty} h_1(\tau) x(t - \tau) d\tau. \quad (3.2)$$

The second system is of quadratic nature, described by the two-dimensional convolution:

$$y_2(t) = \int_{-\infty}^{\infty} \int_{-\infty}^{\infty} h_2(\tau_1, \tau_2) x(t - \tau_1) x(t - \tau_2) d\tau_1 d\tau_2. \quad (3.3)$$

The total output $y(t)$ is, in general, an infinite sum of $y_i(t)$:

$$y(t) = \sum_{i=0}^{\infty} y_i(t) \quad (3.4)$$

where the i^{th} system is characterized by the i -dimensional kernel $h_i(\tau_1, \tau_2, \dots, \tau_i)$:

$$y_i(t) = \int_{-\infty}^{\infty} \int_{-\infty}^{\infty} \cdots \int_{-\infty}^{\infty} h_i(\tau_1, \tau_2, \dots, \tau_i) x(t - \tau_1) x(t - \tau_2) \cdots \\ \cdots x(t - \tau_i) d\tau_1 d\tau_2 \cdots d\tau_i.$$

The Volterra functional expansion can be considered a generalization of the Taylor-series expansion which also models dynamic behaviour and by taking the Laplace transform of (3.4) a frequency domain description can be obtained. However, for adequate precision large numbers of terms are necessary, especially for strong nonlinearities. Volterra series can in principle directly be mapped on circuits which implement the kernels (for synthesis) but these circuits become very complicated. If a Volterra expansion is used to model a general nonlinear circuit, the model gives little insight to conventional circuit designers, since it is very mathematically oriented. For linear and linearizable circuits however the first-order Volterra kernel is equal to the linear small-signal diagram and is very useful in designing both the instantaneous and dynamic transfer.

3.3.3 Piece-wise linear modeling

The piece-wise linear modeling approach takes a nonlinearity and divides it in small pieces in the amplitude domain. Then for each of these pieces a linear model is derived, as depicted in Fig. 3.2.

In principle every nonlinearity can be covered by this method. Dynamic behaviour can be modeled linearly in every linear piece of the piece-wise linear approximation. Stronger nonlinearities require a larger number of pieces for adequate precision.

Though the model used in every piece is very simple (a linear model), handling the boundaries between the pieces makes analytical use of the piece-wise linear model difficult. It is more suitable for time-domain numerical analysis. The overall fundamental nonlinear relations of the building blocks are lost, making it difficult to use a piece-wise linear approximation in a synthesis path.

Though the overall nonlinear relations are lost, the model does give the designer some local insight for the behaviour of building blocks, since locally (staying within one piece of the model) the modeling is identical to conventional linear modeling.

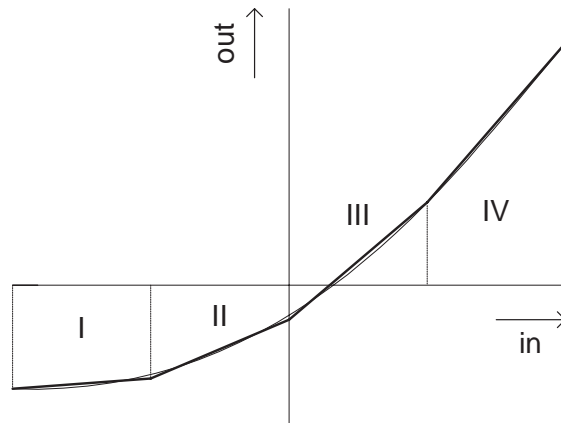


Figure 3.2: Piecewise linear model using 4 linear pieces

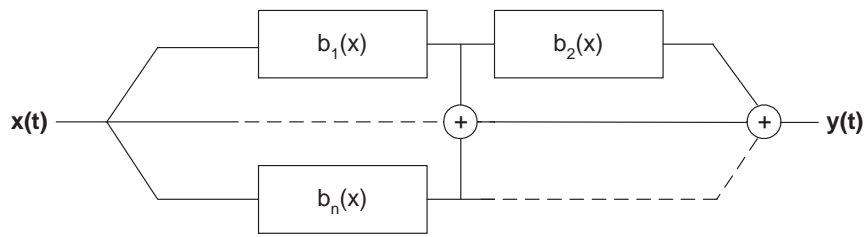


Figure 3.3: Expansion in basic function $b_i(t)$ ($i = 1 \dots n$)

3.4 Expansion in basic functions

A more physical approach can be obtained if the desired transfer is expressed in terms of basic functions, which are chosen based on either the type of transfer to be designed or the type of nonlinear building block used. This expansion is depicted in Fig. 3.3, where it is shown that the basic functions $b_i(t)$ ($i = 1 \dots n$) can be series-connected, parallel-connected or a combination of this, in order to implement the overall transfer function.

If the choice of the basic functions is made with respect to the type of transfer to be designed, then expressing the desired transfer in terms of these basic functions should be very easy. If the basic functions then can easily be mapped on nonlinear building blocks, a two step synthesis path without iterations is very feasible. However, mapping an arbitrary basic function on a nonlinear building block is not always straightforward.

A better approach would be to choose the basic functions based on the nonlinear building block to be used. Then mapping the basic functions on the functions of the nonlinear building blocks should be quite easy. The type of basic functions then determines which category of desired transfers can be synthesized. Since this approach inherently results in a close relationship between basic functions and physical building block, the designer gets lots of insight about the circuit to be designed. If the basic functions for a specific building block also match the type of desired transfer, then a close link between desired transfer and underlying nonlinear building block exists. This should enable relatively easy generation of nonlinear-circuit topologies and confidence that the circuit designed is a good choice for the transfer required.

The advantage of this approach is also its main problem: it is not as generally applicable as other methods. Since the basic functions should match both the nonlinear building block and the desired transfer, it is not always possible to find suitable basic functions for every possible combination of nonlinear building blocks and type of transfer, under the restriction that we want to have a limited number of basic blocks and functions. However, if such a match is found, then a close relation between the function to be implemented and the underlying physics can be obtained.

3.5 Conclusions

The main objective of the high-level synthesis/analysis step is to design the function that we want to implement. We need to find circuit topologies which can implement the wanted nonlinear function and want to rule out topologies which cannot meet the specifications, in a fast exploration of the design space.

In order to accomplish this, we need simple models, which should cover the fundamental nonlinear relations of the building blocks. Ideally the nonlinear-circuit topology is being generated in a synthesis path, without iterations. The models preferably have a relation to the physical behaviour of the nonlinear building blocks, in order to give the designer some insight.

Of the approaches considered, the Taylor-series expansion appears to be the worst choice. It is valid in the vicinity of a bias-point only, needs a large number of terms for adequate precision, is limited to instantaneous transfers only and has no physical basis.

The Volterra functional expansion has slightly better properties, since it is able to explicitly model dynamic behaviour. However, again large numbers of terms can be necessary for adequate precision, and it doesn't have a physical basis.

The piece-wise linear modeling approach uses very simple sub-models, but requires lots of pieces to cover an entire nonlinear curve. Though the model does have a local physical basis, and gives the designer some local insight, the

overall nonlinear relations are lost, which makes it more suitable for numerical analysis.

An expansion in basic functions, chosen to fit the nonlinear building blocks used, appears to be the best option. The type of basic functions then determines which category of desired transfers can be synthesized. Since there is a direct link between basic functions and physical building blocks, the designer inherently gets insight. If the basic functions for a specific building block also match the type of desired transfer, nonlinear-circuit topologies can be generated relatively easily. The challenge for the designer is to identify basic functions which match both the nonlinear building blocks and the desired type of transfer.

The specific high-level description will depend on the nonlinear function we want to implement (and on the nonlinear building blocks used). An example is the design of filters using dynamic translinear circuits [32]. In this thesis we will not elaborate on the high-level synthesis/analysis step. We will focus on the low-level analysis/synthesis step and proceed with modeling approaches suitable for this step.

4

Modeling approaches for low-level analysis/synthesis

In the previous chapter we covered the high-level synthesis/analysis step of the design approach proposed in Chapter 2. We saw that the main objective of this step is to identify circuit topologies which can implement the wanted nonlinear function and to rule out in an early phase topologies which cannot meet the specifications. In order to obtain this goal we need simple models, which enable synthesis of the nonlinear-circuit topology and which have a relation to the physical behaviour of the nonlinear building blocks, in order to give the designer insight. We concluded that an expansion in basic functions appears to be the best modeling approach since it potentially has all of these properties.

In this chapter we cover the second step of our proposed design approach as outlined in Chapter 2. It consists of a low-level analysis/synthesis step, in which we determine the quality of the solutions found in the high-level synthesis/analysis step. First we give a more detailed description of the objectives of this low-level analysis/synthesis step and deduce the properties it should have. Then we review the modeling approaches we can use, and determine which one suits our requirements best.

4.1 Objectives and desired properties

After a circuit topology has been found implementing the wanted nonlinear function, the quality of this solution need to be determined. We need to determine the effect of deviations from the simple models used in the high-level synthesis/analysis step. We need to analyze the effect of the following non-idealities:

- deviations in the instantaneous behaviour,
- internally generated noise,
- deviations in the dynamic behaviour.

The performance degradation caused by these non-idealities needs to be determined. Therefore, in the low-level analysis/synthesis step we need to use *more detailed models* than in the high-level step, in order to cover the perturbed behaviour. However, the low-level analysis method itself needs to be *simplified* as much as possible in order to arrive at estimates of quality useful in practical circuit design.

One way to overcome this contradiction is to make use of the fact that at this stage *only the effect of small deviations* needs to be investigated, since the large-signal behaviour is assumed to be covered in the high-level synthesis/analysis step. Furthermore, since we are aiming to design high-performance circuits, the deviations from the intended behaviour cannot be large by definition. If we discover that the deviations are large after all, then we need to go back to the high-level synthesis/analysis step in order to incorporate these effects.

Also in the low-level analysis/synthesis step we would like a modeling approach which gives us a *close relation between the model and the physical layer*. Then the designer knows where and how to take measures when the performance degradation is too high. Ideally the designer gets analytical expressions (or at least approximations) describing the relation between circuit parameters and performance measures and can obtain the insight she or he was used to in conventional linear design.

4.2 General modeling approaches

The modeling approach used in the low-level analysis/synthesis step needs to be able to handle the combination of nonlinear complexity and detailed models in a way useful in practical circuit design. The complexity needs to be reduced by somehow expressing the nonlinear behaviour in terms of more simple functions and by using knowledge of the large-signal behaviour obtained in the high-level synthesis/analysis step. The degree to which this reduction in complexity is obtained to a large extent determines the suitability of a specific approach for low-level analysis/synthesis.

The design of nonlinear circuits becomes complicated by the fact that their behaviour is signal-dependent. In order to accurately determine the quality of a circuit topology, this signal-dependent behaviour needs to be incorporated in the model for low-level analysis/synthesis. Based on the method in which the nonlinear complexity and resulting signal-dependent behaviour is handled

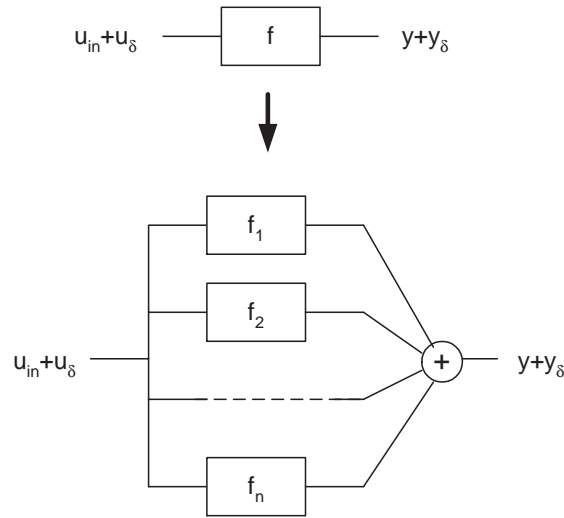


Figure 4.1: Modeling by expansion in simpler systems

in the modeling approach, we can distinguish the following two general types of approaches for modeling nonlinear circuits for low-level analysis/synthesis.

First, the approach can handle the nonlinear complexity by expressing the nonlinear system as a combination of simpler systems. For the simpler systems the signal-dependent behaviour hopefully is easier to handle. This general idea is shown in Figure 4.1. Here, in order to analyze the effect of the nonlinear transfer function f on the input signal u_{in} and small deviations of the input signal u_δ , f is expressed as a sum of simpler transfer functions f_1, f_2, \dots, f_n . This hopefully makes it easier to determine the resulting output y and small deviations in the output y_δ . The following modeling approaches belong to this category:

- Taylor-series expansion,
- Volterra functional expansion,
- expansion in basic functions,
- piecewise linear modeling.

The first three methods expand the nonlinear system in simpler systems which contribute to the output over the entire input-signal range. In the latter method the input-signal range is divided into pieces and for each piece a linear model of the nonlinear system is derived.

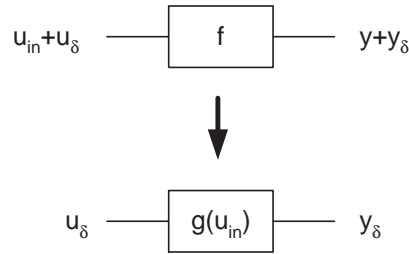


Figure 4.2: Modeling by input signal dependent model

Second, the approach can handle the nonlinear complexity by letting the model be dependent on the input signals and only model the effect of small deviations of the input signal or model. In this way the signal-dependent behaviour is explicitly incorporated in the model. This general idea is shown in Figure 4.2. From the nonlinear transfer function f and the input signal u_{in} we derive a signal-dependent transfer function $g(u_{in})$, which models the systems response to small deviations u_{δ} in the input and can be used to analyze the resulting small deviations y_{δ} in the output. In this approach the model will be different for each class of input signals. However, in deriving the model, we can make use of the knowledge about the large-signal behaviour obtained in the high-level synthesis/analysis step. The following two modeling approaches belong to this category:

- linear time-invariant (LTI) small-signal modeling,
- linear time-varying (LTV) small-signal modeling.

In LTI small-signal modeling the response of the nonlinear circuit to the DC input signals is determined and an LTI small-signal model is derived for this DC bias point. In LTV small-signal modeling the response of the nonlinear circuit to the (deterministic) large-signal part of the input signals is determined and an LTV small-signal model is derived for this dynamic bias trajectory.

In the following sections the different modeling techniques are discussed in more detail.

4.3 Expansion in simpler systems

The first category of modeling approaches for low-level analysis/synthesis handles the nonlinear complexity by expressing the nonlinear system as a combination of simpler systems. Taylor-series expansion, Volterra functional expansion, expansion in basic functions, and piecewise linear modeling belong to this category. In the following paragraphs these approaches are discussed in more detail.

4.3.1 Taylor-series expansion

The Taylor-series expansion, as outlined in Section 3.3.1, expresses a nonlinear static input-output relation $f(x)$ as a sum of functions $(x - q)^n$:

$$T_{q,p}(x) = \sum_{n=0}^p \frac{d^n f(q)}{dx^n} \frac{1}{n!} (x - q)^n \quad (4.1)$$

The number of systems $(x - q)^n$ is determined by the required accuracy.

The Taylor-series expansion is a functional expansion in the amplitude domain only. Therefore, only instantaneous transfers can be handled and dynamic behaviour cannot be incorporated. Noise can be handled, though dynamic noise transfers cannot be described.

As any functional expansion, the Taylor-series does not explicitly make use of the fact that in the low-level analysis/synthesis the large-signal behaviour is already known. Therefore, in low-level analysis at least the same number of terms is necessary as in the high-level step, and probably even a larger number of terms, since now more detailed models are necessary to cover the perturbed behaviour. Thus the knowledge of large-signal behaviour doesn't result in a reduction of complexity.

Finally, the Taylor-series expansion has no physical basis and gives the designer little insight. The exception is again linear and linearizable circuits, for which the first-order Taylor-series expansion is equivalent to the static small-signal diagram.

4.3.2 Volterra functional expansion

The Volterra functional expansion, as outlined in section 3.3.2, expands a nonlinear dynamic system in a set of systems connected in parallel, as shown in Fig. 3.1. The general expression is repeated below:

$$y(t) = \sum_{i=0}^{\infty} y_i(t) \quad (4.2)$$

where the i^{th} system is characterized by the i -dimensional kernel $h_i(\tau_1, \tau_2, \dots, \tau_i)$:

$$y_i(t) = \int_{-\infty}^{\infty} \int_{-\infty}^{\infty} \cdots \int_{-\infty}^{\infty} h_i(\tau_1, \tau_2, \dots, \tau_i) x(t - \tau_1) x(t - \tau_2) \cdots \\ \cdots x(t - \tau_i) d\tau_1 d\tau_2 \cdots d\tau_i.$$

These systems are generalizations of the convolution integral used in linear system analysis. The first system is simply the linear system (3.2), characterized by the impulse response $h_1(t)$. The second system is of quadratic

nature and is described by the two-dimensional convolution (3.3), using the second-order Volterra kernel $h_2(t_1, t_2)$. Generally, the i^{th} system uses the i -dimensional convolution (4.2), characterized by the i -dimensional Volterra kernel $h_i(t_1, t_2, \dots, t_i)$.

The Volterra functional expansion is a functional expansion in both amplitude domain and time domain (or alternatively, frequency domain). Therefore, both deviations in instantaneous behaviour and deviations in dynamic behaviour can be covered. The effect of noise can also be investigated.

The main drawback of the Volterra functional expansion for low-level analysis/synthesis is that no explicit use can be made of the knowledge of large-signal behaviour obtained in the high-level synthesis/analysis step. The complexity of the model is at least the same as in the high-level step: at least the same number of terms is necessary, since the same input range needs to be covered. Probably the complexity is even larger, since now more detailed models are necessary to cover the perturbed behaviour together with the intended behaviour.

The Volterra functional expansion has no physical basis. It gives the designer little insight: a certain parasitic component might manifest itself spread over several Volterra kernels.

An exception is the analysis of nonlinear distortion in weakly nonlinear systems with an intended linear behaviour [26]. For such systems the intended behaviour is modeled by the first-order Volterra kernel, and the nonlinear effects (causing nonlinear distortion) are concentrated in the higher-order kernels. If the deviations from the intended linear behaviour are small, a limited order of terms is necessary for accurately predicting the nonlinear distortion and they can be related to the parameters describing the linear behaviour. Those have a clear relation to the physical layer.

4.3.3 Expansion in basic functions

As described in Section 3.4, a more physical modeling approach can be obtained if the nonlinear system is expanded in basic functions, chosen to fit the nonlinear building blocks used. Depending on the type of basic functions, instantaneous behaviour, dynamic behaviour and noise behaviour can be covered.

As was the case for the Volterra functional expansion, in the low-level analysis/synthesis step no use is made of the knowledge of large-signal behaviour obtained in the high-level synthesis/analysis step for decreasing modeling complexity. The same or even a larger number of terms is necessary for equal precision.

Moreover, since the basic functions were chosen in the high-level step in order to model intended nonlinear behaviour, they might not be very suitable for inclusion of perturbed behaviour. A contradiction might arise between the simple models needed to speed up high-level synthesis/analysis and the precision required to cover the perturbed behaviour in low-level analysis/synthesis.

An advantage of the basic functions modeling approach is that there exists a direct link between basis functions and physical building blocks, which inherently gives the designer insight.

4.3.4 Piece-wise linear modeling

The piece-wise linear modeling approach, as outlined in Section 3.3.3, takes a nonlinear transfer function and divides the input-signal range in small pieces. Then for each of these pieces a linear model is used. The resulting piece-wise linear model can be seen as a combination of linear systems, only one of which contributes to the output for each piece of input amplitude.

Deviations in instantaneous behaviour and dynamic behaviour can be modeled linearly in every piece of the input range. The effect of noise sources can also be handled.

Again this expansion in linear pieces does not make use of the knowledge obtained in the high-level design step in order to decrease complexity in the low-level design step. At least the same number of linear pieces is necessary and each linear submodel will need to be more complex in order to include non-idealities.

The designer does get local insight in the behaviour, since locally the modeling is identical to conventional linear modeling. However, handling the boundaries between the pieces complicates analytical use of the piece-wise linear model.

4.4 Input signal dependent modeling

The second type of modeling approaches for low-level analysis/synthesis handles the nonlinear complexity by letting the model be dependent on the input signals and only model the effect of small deviations of the input signal or model. Linear time-invariant (LTI) small-signal modeling and linear time-varying (LTV) small-signal modeling belong to this category, and are described in more detail below.

4.4.1 Linear time-invariant small-signal modeling

A first type of modeling approach which handles the nonlinear complexity by letting the model be dependent on the input signal is conventional linear time-invariant small-signal modeling. An LTI small-signal model characterizes a nonlinear system for a specific (DC-input dependent) bias point. For sufficiently small deviations around this DC bias point, instantaneous behaviour, dynamic behaviour and noise behaviour can be described accurately by the LTI model.

For linear time-invariant small-signal modeling it is evident that a large reduction in low-level analysis/synthesis complexity can be obtained by letting

the model be only dependent on the DC input signals. All nonlinear complexity is dealt with when calculating the DC bias point and the low-level model is completely linear. This explains the success of conventional linear design.

The LTI model also gives a close relation between the model and the physical layer. It is easy to include parasitic effects in the model, and the designer knows exactly where to take measures when the resulting performance degradation is too high.

The obvious drawback of linear time-invariant small-signal modeling is that the signals need to be limited to small deviations around the DC bias point only. However, in linear design methodology, measures can be taken to make this assumption valid [49].

4.4.2 Linear time-varying small-signal modeling

A more general approach which uses an input-signal dependent model is the linear time-varying approach. It generalizes the linear small-signal modeling approach, by describing the behaviour of a nonlinear circuit in the neighbourhood of an (input-signal dependent) *dynamic bias trajectory* rather than a (DC-input dependent) *bias point*. For this the approach uses a linear time-varying model, in which the input signals and resulting dynamic bias trajectory are implicitly present.

Using the linear time-varying small-signal model, deviations in instantaneous behaviour, deviations in dynamic behaviour and the effect of internally generated noise can be analyzed.

The linear time-varying model makes explicit use of the knowledge of large-signal behaviour obtained in the high-level synthesis/analysis step, by using it to define the input-signal dependent dynamic bias trajectory. Small deviations from this intended overall system behaviour are explicitly modeled. In this way the complexity of the linear time-varying model is kept as small as possible, while nonlinear circuit behaviour is still implicitly incorporated in this model for low-level analysis/synthesis.

If the time-variations of the LTV model due to input-signal dependency are handled accordingly, the model gives a lot of insight. Due to the linear type of modeling it gives a similar relation to the physical behaviour as the conventional LTI model.

4.5 Conclusions

The main objective of the low-level analysis/synthesis step is to determine the quality of topologies found in the high-level synthesis/analysis step. We need to investigate deviations in instantaneous behaviour, deviations due to internally

generated noise and deviations in dynamic behaviour for predicting the resulting performance degradation.

In the low-level analysis/synthesis step we might need to use more detailed models than in the high-level step, in order to cover the perturbed behaviour. However, since large-signal behaviour is covered in the high-level step, only the effect of small deviations needs to be modeled, and knowledge from the high-level step should be used to decrease complexity. Also we would like a modeling approach which provides a close relation between the model and the physical layer, in order to give the designer insight in what to do to improve performance, if required.

In the context of low-level analysis/synthesis, two types of modeling approaches can be distinguished. The distinction is made based on the way the nonlinear complexity and the resulting signal-dependent behaviour is handled in the modeling approach.

The first type of modeling approach expresses the nonlinear system as a combination of simpler systems, for which the signal-dependent behaviour hopefully is easier to handle. *Taylor-series expansion*, *Volterra functional expansion*, *expansion in basic functions* and *piece-wise linear modeling* belong to this category. All these modeling approaches have in common that they do not make explicitly use of the knowledge of overall system behaviour from the high-level step in order to decrease the model complexity in the low-level step. They need at least the same number of terms in the expansion (or pieces in the piece-wise linear model) as in the high-level step, since the input range is the same, and probably even more in order to cover the non-idealities.

The second type of modeling approach handles the nonlinear complexity by letting the model be dependent on the input signals and only modeling the effect of small deviations. *Linear time-invariant small-signal modeling* and *linear time-varying small-signal modeling* belong to this category. By using knowledge obtained in the high-level step in order to define the DC bias point or dynamic bias trajectory, and only modeling deviations, the complexity can be kept as low as possible. These linear type of modeling approaches also give the designer the insight he is used to from conventional linear design.

The conclusion is that for general nonlinear circuits the linear time-varying small-signal model (or, if the signals are sufficiently small, the LTI small-signal model) appears to be a good modeling candidate in the context of low-level analysis/synthesis. Therefore, the rest of this thesis will focus on the LTV approach for low-level analysis/synthesis of nonlinear circuits.

5

The linear time-varying approach

In the previous chapter we identified the linear time-varying approach as a good modeling candidate for low-level analysis/synthesis. We saw that the main objective for this low-level analysis/synthesis step is to determine the quality of topologies found in the high-level synthesis/analysis step. This is done by investigating the performance degradation resulting from deviations in instantaneous behaviour, deviations due to internally generated noise and deviations in dynamic behaviour. In order to cover this perturbed behaviour, on the one hand we need to use more detailed models, but on the other hand knowledge from the high-level step can be used to decrease model complexity. The linear time-varying approach has these properties, since it can reduce model complexity by using knowledge from the high-level design step and by only modeling the deviations from the intended behaviour. It might also give the designer the insight and close relation to the physical layer that he was used to in conventional linear design methodologies.

The linear time-varying approach generalizes the linear small-signal modeling approach, by describing the behaviour of a nonlinear circuit in the neighbourhood of an (input-signal dependent) *dynamic bias trajectory* rather than a (DC-input dependent) *bias point*. For this, the approach uses a linear time-varying model, in which the input signals and resulting dynamic bias trajectory are implicitly present. Using the linear time-varying small-signal model, deviations in instantaneous behaviour, the effect of internally generated noise and deviations in dynamic behaviour can be analyzed. The linear time-varying model makes explicit use of the knowledge of the large-signal behaviour obtained in the high-level synthesis/analysis step, by using it to define the input-signal dependent dynamic bias trajectory. Small deviations from this intended overall system

behaviour are explicitly modeled. In this way the complexity of the linear time-varying model is kept as small as possible, while nonlinear circuit behaviour is still implicitly incorporated in this model for low-level analysis/synthesis.

In the first section of this chapter we describe the basic approach used in the linear time-varying modeling of nonlinear systems. We will derive the *linear time-varying (LTV) small-signal model* and show how it relates to the conventional *linear time-invariant (LTI) small-signal model* and to *linear time-invariant circuits*, which are special cases of the general LTV small-signal model. When using the LTV small-signal model for low-level analysis/synthesis, we need to analyze the effect of deviations in instantaneous behaviour, the effect of internally generated noise and the effect of deviations in dynamic behaviour. In Section 5.2 we show how these non-idealities are incorporated in the LTV model, and we indicate why we concentrate on the dynamic behaviour in the rest of this thesis. Then in Section 5.3 we give an overview of the theory of linear time-varying systems and relate this theory to the familiar theory of linear time-invariant systems. We show how the linear time-varying approach can be used to describe the dynamic behavior of nonlinear circuits by time-varying eigenvalues, and relate these to Lyapunov and Floquet exponents. Finally in the last sections of this chapter we apply these concepts to the LTV small-signal models of nonlinear circuits. In Section 5.4 we treat nonlinear circuits exhibiting first-order dynamic behaviour (equivalent to one pole in linear time-invariant systems). In Section 5.5 we show how to overcome the complications in calculating the dynamic eigenvalues and Floquet exponents for nonlinear circuits with second-order dynamic behaviour, as described in more detail in the paper by van der Kloet et al. [21]. A generalization to higher-order dynamics is briefly introduced in Section 5.6, more details about this topic can be found in [22].

5.1 The linear time-varying approach

The linear time-varying approach consists of separating the behaviour of a dynamic nonlinear circuit in a *signal dependent bias trajectory* and a *linear time-varying small-signal model*. It is a generalization of the familiar concept of DC bias point and linear small-signal circuit known from conventional circuit design. It enables the explicit incorporation of signal-dependent behaviour in the analysis and synthesis of nonlinear circuits.

The linear time-varying small-signal model of a nonlinear circuit is obtained by linearizing the behavior of the nonlinear circuit in its signal-dependent bias trajectory. It enables the analysis of deviations in the instantaneous behaviour, the analysis of the effect of noise and the analysis of deviations in the dynamic behaviour (or the entire dynamic behaviour, if not present in the high-level step) for the nonlinear circuit in the vicinity of the dynamic bias trajectory. Note that this analysis is exact, despite of the (time-varying) linearization in-

involved, because the next point in the linearization is determined by the signal dependent bias-trajectory, which incorporates the large-signal behaviour of the nonlinearities in the time evolution of the state variables. The only limitation is that the influence of deviations on the signal dependent bias-trajectory is neglected. Therefore, circuits in which the behaviour is dominantly changed by small deviations (e.g. chaotic circuits) can not be handled.

The *linear time-varying small-signal model* is a generalization of the conventional *linear time-invariant small-signal model* of a nonlinear circuit. The latter enables the small-signal analysis of a nonlinear circuit as if it was a *linear time-invariant circuit*. In order to show the relations between these three models, below we first derive the linear time-varying small-signal model of a nonlinear circuit, and then show how the model simplifies for linear time-invariant modeling of nonlinear circuits and finally for linear circuits.

5.1.1 The linear time-varying small-signal model of a nonlinear circuit

The linear time-varying small-signal model is obtained in the following way. We begin with the tableau equations which can be written down for any circuit composed from capacitors, inductors, resistors and other electronic elements. These equations have the node voltages and branch currents as variables. The currents through inductors and the voltages over capacitors yield dynamic equations, whereas the other circuit-variables yield algebraic equations and can be eliminated from the tableau equations, resulting in the well known state-space description

$$\frac{d}{dt}\mathbf{x}(t) = \mathbf{f}[\mathbf{x}(t), \mathbf{u}(t), t] \quad (5.1)$$

$$\mathbf{y}(t) = \mathbf{g}[\mathbf{x}(t), \mathbf{u}(t), t] \quad (5.2)$$

Here $\mathbf{x}(t)$ represents the vector of all inductor currents and all capacitor voltages, $\mathbf{u}(t)$ represents external sources, $\mathbf{y}(t)$ represents the output vector and t is the time. The time-parameter t will only be explicitly present in \mathbf{f} and \mathbf{g} if the parameters of some of the circuit elements are varying with time independent of the state variables or inputs (for instance if the value of a resistor or capacitor is mechanically altered). The dynamical part of the state-space description (5.1) can be used to calculate the dynamic bias trajectory $\mathbf{x}_b(t)$ of the state variables as function of the external sources $\mathbf{u}_b(t)$. The dynamic bias trajectory of the output $\mathbf{y}_b(t)$ then immediately follows from the instantaneous output function of the state-space description (5.2).

The dynamic behaviour of the nonlinear circuit in the vicinity of the dynamic bias trajectory can be studied by analyzing the response of the system when the state variables are perturbed slightly away from the dynamic bias trajectory.

For this we consider small variations in the state variables. The effect of small deviations in the instantaneous behaviour and the effect of noise can be studied by considering small variations in the modeled input. If we denote these variations as $\mathbf{x}_\delta(t)$ and $\mathbf{u}_\delta(t)$, respectively, and if we denote the resulting variations in the output as $\mathbf{y}_\delta(t)$, we can model them by substituting $\mathbf{x}(t) = \mathbf{x}_b(t) + \mathbf{x}_\delta(t)$, $\mathbf{u}(t) = \mathbf{u}_b(t) + \mathbf{u}_\delta(t)$ and $\mathbf{y}(t) = \mathbf{y}_b(t) + \mathbf{y}_\delta(t)$ in equations (5.1) and (5.2). Linearizing these state-space equations around $\mathbf{x}_b(t)$ and $\mathbf{u}_b(t)$ yields

$$\begin{aligned} \frac{d}{dt} [\mathbf{x}_b(t) + \mathbf{x}_\delta(t)] &= \mathbf{f} [\mathbf{x}_b(t) + \mathbf{x}_\delta(t), \mathbf{u}_b(t) + \mathbf{u}_\delta(t), t] && \iff \\ \frac{d}{dt} \mathbf{x}_b(t) + \frac{d}{dt} \mathbf{x}_\delta(t) &= \mathbf{f} [\mathbf{x}_b(t), \mathbf{u}_b(t), t] + && (5.3) \\ &+ \left. \frac{\partial \mathbf{f}}{\partial \mathbf{x}} \right|_{\mathbf{x}=\mathbf{x}_b(t), \mathbf{u}=\mathbf{u}_b(t)} \cdot \mathbf{x}_\delta(t) + \left. \frac{\partial \mathbf{f}}{\partial \mathbf{u}} \right|_{\mathbf{x}=\mathbf{x}_b(t), \mathbf{u}=\mathbf{u}_b(t)} \cdot \mathbf{u}_\delta(t) \end{aligned}$$

and

$$\begin{aligned} \mathbf{y}_b(t) + \mathbf{y}_\delta(t) &= \mathbf{g} [\mathbf{x}_b(t) + \mathbf{x}_\delta(t), \mathbf{u}_b(t) + \mathbf{u}_\delta(t), t] && \iff \\ \mathbf{y}_b(t) + \mathbf{y}_\delta(t) &= \mathbf{g} [\mathbf{x}_b(t), \mathbf{u}_b(t), t] + && (5.4) \\ &+ \left. \frac{\partial \mathbf{g}}{\partial \mathbf{x}} \right|_{\mathbf{x}=\mathbf{x}_b(t), \mathbf{u}=\mathbf{u}_b(t)} \cdot \mathbf{x}_\delta(t) + \left. \frac{\partial \mathbf{g}}{\partial \mathbf{u}} \right|_{\mathbf{x}=\mathbf{x}_b(t), \mathbf{u}=\mathbf{u}_b(t)} \cdot \mathbf{u}_\delta(t) \end{aligned}$$

Since $\mathbf{x}_b(t)$ is the solution of Equation (5.1) for $\mathbf{u}(t) = \mathbf{u}_b(t)$ and $\mathbf{y}_b(t)$ is the resulting solution of Equation (5.2), we obtain the following *variational equations* for the variations $\mathbf{x}_\delta(t)$ in the states, the variations $\mathbf{u}_\delta(t)$ in the sources and the resulting variations $\mathbf{y}_\delta(t)$ in the outputs.

$$\frac{d}{dt} \mathbf{x}_\delta(t) = \mathbf{A}_x [\mathbf{x}_b(t), \mathbf{u}_b(t), t] \cdot \mathbf{x}_\delta(t) + \mathbf{B}_u [\mathbf{x}_b(t), \mathbf{u}_b(t), t] \cdot \mathbf{u}_\delta(t) \quad (5.5)$$

$$\mathbf{y}_\delta(t) = \mathbf{C}_x [\mathbf{x}_b(t), \mathbf{u}_b(t), t] \cdot \mathbf{x}_\delta(t) + \mathbf{D}_u [\mathbf{x}_b(t), \mathbf{u}_b(t), t] \cdot \mathbf{u}_\delta(t) \quad (5.6)$$

The matrix \mathbf{A}_x is the Jacobian of \mathbf{f} and the matrix \mathbf{C}_x is the Jacobian of \mathbf{g} with respect to the state-space vector in its dynamic point of operation. The matrix \mathbf{B}_u is the Jacobian of \mathbf{f} and the matrix \mathbf{D}_u is the Jacobian of \mathbf{g} with respect to the input vector.

Since $\mathbf{u}_\delta(t)$ is used to model variations in the sources, it suffices to deal with $\mathbf{u}_\delta(t) = 0$ in studying the dynamics, e.g. stability. This is described in the next sections and in more detail in [21]. In noise problems however, the noise sources are modelled by $\mathbf{u}_\delta(t)$ and we have to deal with the complete equation (5.5). This is demonstrated in [33] and [50].

5.1.2 The linear time-invariant small-signal model of a nonlinear circuit

The classic linear small-signal circuit is a special case of the variational equations (5.5) and (5.6). It models the behaviour of a nonlinear circuit in the

vicinity of a DC bias point. Variations of the parameters of circuit elements independent of the state-variables or the inputs can only be modeled parametrically by definition, so t should not explicitly be present in the state-space description (5.1),(5.2) and it reduces to:

$$\frac{d}{dt}\mathbf{x}(t) = \mathbf{f}[\mathbf{x}(t), \mathbf{u}(t)] \quad (5.7)$$

$$\mathbf{y}(t) = \mathbf{g}[\mathbf{x}(t), \mathbf{u}(t)] \quad (5.8)$$

This state-space description is used to calculate the DC bias point \mathbf{x}_{DC} as function of the DC part of the external sources \mathbf{u}_{DC} .

The dynamic behaviour of the nonlinear circuit in the vicinity of this DC bias point can be studied by considering small variations in the state variables, denoted by $\mathbf{x}_\delta(t)$. The small-signal transfer and noise behaviour can be studied by considering small variations in the external sources, denoted by $\mathbf{u}_\delta(t)$, and the resulting variations in the output $\mathbf{y}_\delta(t)$. If we substitute $\mathbf{x}(t) = \mathbf{x}_{DC} + \mathbf{x}_\delta(t)$, $\mathbf{u}(t) = \mathbf{u}_{DC} + \mathbf{u}_\delta(t)$ and $\mathbf{y}(t) = \mathbf{y}_{DC} + \mathbf{y}_\delta(t)$ in equations (5.7) and (5.8) and linearize around \mathbf{x}_{DC} and \mathbf{u}_{DC} we obtain the variational equations

$$\frac{d}{dt}\mathbf{x}_\delta(t) = \mathbf{A}_x(\mathbf{x}_{DC}, \mathbf{u}_{DC}) \cdot \mathbf{x}_\delta(t) + \mathbf{B}_u(\mathbf{x}_{DC}, \mathbf{u}_{DC}) \cdot \mathbf{u}_\delta(t). \quad (5.9)$$

$$\mathbf{y}_\delta(t) = \mathbf{C}_x(\mathbf{x}_{DC}, \mathbf{u}_{DC}) \cdot \mathbf{x}_\delta(t) + \mathbf{D}_u(\mathbf{x}_{DC}, \mathbf{u}_{DC}) \cdot \mathbf{u}_\delta(t). \quad (5.10)$$

In this case the matrices \mathbf{A}_x , \mathbf{B}_u , \mathbf{C}_x and \mathbf{D}_u are independent of time. The variational equations are linear time-invariant, enabling a transition to the frequency domain using Laplace transforms. It should be noted that, by definition (linear time-invariant assumption), the influence of the non-DC part of the signal sources on the dynamic and noise behaviour can not be determined from equations (5.9) and (5.10), since \mathbf{A}_x , \mathbf{B}_u , \mathbf{C}_x and \mathbf{D}_u do not contain this information about the signal sources. Also the accuracy of the linear time-invariant small-signal model is limited to relative small signals or weak nonlinearities only.

5.1.3 Linear time-invariant circuits

For linear time-invariant circuits the variational equation is obtained very easily. For these circuits the state-space description (5.1),(5.2) is already linear and has the form:

$$\frac{d}{dt}\mathbf{x}(t) = \mathbf{A} \cdot \mathbf{x}(t) + \mathbf{B} \cdot \mathbf{u}(t) \quad (5.11)$$

$$\mathbf{y}(t) = \mathbf{C} \cdot \mathbf{x}(t) + \mathbf{D} \cdot \mathbf{u}(t) \quad (5.12)$$

The superposition principle can be used and consequently the variational equation is identical to the state-space description.

5.2 Modeling of non-idealities in the LTV approach

When using the linear time-varying small-signal model for low-level analysis/synthesis we need to incorporate the effect of non-idealities in the model. In this subsection we show how *deviations in instantaneous behaviour*, *internally generated noise* and *deviations in dynamic behaviour* can be covered in the LTV small-signal model. For brevity we only consider the dynamic part of the state-space equation as given by Equation (5.1). The output part of the state-space equation, as given by Equation (5.2), is easily included and only results in some additional instantaneous relations.

5.2.1 Deviations in instantaneous behaviour

In order to include small deviations in instantaneous behaviour in the LTV small-signal model we have to slightly modify the variational equation (5.5) and its derivation as given in Equation (5.3). We will see that the resulting extended variational equation still resembles Equation (5.5) and that the effect of deviations in instantaneous behaviour can be analyzed in a similar way as the effect of noise sources.

Small deviations in instantaneous behaviour may effect the state-space description (5.1) in two ways. One possibility is that the deviations are caused by small variations in the parameters of devices already included in the state-space description. This type of effect can be modeled by explicitly including these parameters \mathbf{p} in the state-space description. The other possibility is that deviations in instantaneous behaviour are caused by additional (small) parasitic devices. This type of effect will result in extra (possibly nonlinear) terms in the state space-description. These small additional terms can be modeled by adding an extra function $\mathbf{f}_\delta[\mathbf{x}(t), \mathbf{u}(t), t]$ to the state-space description. Both types of effects combined results in the following extended state-space description (assuming that the additional terms do not change the order of the state-space description):

$$\frac{d}{dt}\mathbf{x}(t) = \mathbf{f}[\mathbf{x}(t), \mathbf{u}(t), \mathbf{p}, t] + \mathbf{f}_\delta[\mathbf{x}(t), \mathbf{u}(t), t]. \quad (5.13)$$

If the deviations in instantaneous behaviour are sufficiently small, the original state-space description (5.1) can still be used to calculate the dynamic bias trajectory $\mathbf{x}_b(t)$ of the state variables as function of the external sources $\mathbf{u}_b(t)$ with unperturbed parameters \mathbf{p}_b . Again denoting variations in the state variables as $\mathbf{x}_\delta(t)$ and variations in the modeled input as $\mathbf{u}_\delta(t)$, denoting the small variations

of parameters as \mathbf{p}_δ and linearizing around the dynamic bias trajectory yields

$$\begin{aligned}
\frac{d}{dt} [\mathbf{x}_b(t) + \mathbf{x}_\delta(t)] &= \mathbf{f} [\mathbf{x}_b(t) + \mathbf{x}_\delta(t), \mathbf{u}_b(t) + \mathbf{u}_\delta(t), \mathbf{p}_b + \mathbf{p}_\delta, t] \\
&+ \mathbf{f}_\delta [\mathbf{x}_b(t) + \mathbf{x}_\delta(t), \mathbf{u}_b(t) + \mathbf{u}_\delta(t), t] \quad \iff \\
\frac{d}{dt} \mathbf{x}_b(t) + \frac{d}{dt} \mathbf{x}_\delta(t) &= \mathbf{f} [\mathbf{x}_b(t), \mathbf{u}_b(t), \mathbf{p}_b, t] + \mathbf{f}_\delta [\mathbf{x}_b(t), \mathbf{u}_b(t), t] \quad (5.14) \\
&+ \left. \frac{\partial \mathbf{f}}{\partial \mathbf{x}} \right|_{\mathbf{x}=\mathbf{x}_b(t), \mathbf{u}=\mathbf{u}_b(t), \mathbf{p}=\mathbf{p}_b} \cdot \mathbf{x}_\delta(t) + \left. \frac{\partial \mathbf{f}}{\partial \mathbf{u}} \right|_{\mathbf{x}=\mathbf{x}_b(t), \mathbf{u}=\mathbf{u}_b(t), \mathbf{p}=\mathbf{p}_b} \cdot \mathbf{u}_\delta(t) \\
&+ \left. \frac{\partial \mathbf{f}}{\partial \mathbf{p}} \right|_{\mathbf{x}=\mathbf{x}_b(t), \mathbf{u}=\mathbf{u}_b(t), \mathbf{p}=\mathbf{p}_b} \cdot \mathbf{p}_\delta \\
&+ \left. \frac{\partial \mathbf{f}_\delta}{\partial \mathbf{x}} \right|_{\mathbf{x}=\mathbf{x}_b(t), \mathbf{u}=\mathbf{u}_b(t)} \cdot \mathbf{x}_\delta(t) + \left. \frac{\partial \mathbf{f}_\delta}{\partial \mathbf{u}} \right|_{\mathbf{x}=\mathbf{x}_b(t), \mathbf{u}=\mathbf{u}_b(t)} \cdot \mathbf{u}_\delta(t).
\end{aligned}$$

Denoting the additional Jacobians as \mathbf{A}_p , $\Delta \mathbf{A}_x$ and $\Delta \mathbf{B}_u$, respectively, we obtain the following characteristic equation:

$$\begin{aligned}
\frac{d}{dt} \mathbf{x}_\delta(t) &= \mathbf{A}_x [\mathbf{x}_b(t), \mathbf{u}_b(t), \mathbf{p}_b, t] \cdot \mathbf{x}_\delta(t) + \Delta \mathbf{A}_x [\mathbf{x}_b(t), \mathbf{u}_b(t), t] \cdot \mathbf{x}_\delta(t) \\
&+ \mathbf{B}_u [\mathbf{x}_b(t), \mathbf{u}_b(t), \mathbf{p}_b, t] \cdot \mathbf{u}_\delta(t) + \Delta \mathbf{B}_u [\mathbf{x}_b(t), \mathbf{u}_b(t), t] \cdot \mathbf{u}_\delta(t) \\
&+ \mathbf{A}_p [\mathbf{x}_b(t), \mathbf{u}_b(t), \mathbf{p}_b, t] \cdot \mathbf{p}_\delta \quad (5.15) \\
&+ \mathbf{f}_\delta [\mathbf{x}_b(t), \mathbf{u}_b(t), t]
\end{aligned}$$

Assuming that the deviations in instantaneous behaviour are small, the cross-terms $\Delta \mathbf{A}_x \cdot \mathbf{x}_\delta(t)$ and $\Delta \mathbf{B}_u \cdot \mathbf{u}_\delta(t)$ can be neglected and we finally arrive at the following state-space description extended for small deviations in instantaneous behaviour:

$$\begin{aligned}
\frac{d}{dt} \mathbf{x}_\delta(t) &= \mathbf{A}_x [\mathbf{x}_b(t), \mathbf{u}_b(t), t] \cdot \mathbf{x}_\delta(t) + \mathbf{B}_u [\mathbf{x}_b(t), \mathbf{u}_b(t), t] \cdot \mathbf{u}_\delta(t) \\
&+ \mathbf{A}_p [\mathbf{x}_b(t), \mathbf{u}_b(t), \mathbf{p}_b, t] \cdot \mathbf{p}_\delta + \mathbf{f}_\delta [\mathbf{x}_b(t), \mathbf{u}_b(t), t] \quad (5.16)
\end{aligned}$$

We see that this description is very similar to Equation (5.5). The small deviations in instantaneous behaviour are modeled by the extra non-homogeneous terms $\mathbf{f}_\delta [\mathbf{x}_b(t), \mathbf{u}_b(t), t]$ and $\mathbf{A}_p [\mathbf{x}_b(t), \mathbf{u}_b(t), \mathbf{p}_b, t] \cdot \mathbf{p}_\delta$. The effect of these non-homogeneous terms can be analyzed in a similar way as the effect of the non-homogeneous noise term $\mathbf{B}_u [\mathbf{x}_b(t), \mathbf{u}_b(t), t] \cdot \mathbf{u}_\delta(t)$.

5.2.2 Internally generated noise

The effect of internally generated noise can be incorporated in the LTV small-signal model using the complete equation (5.5), which is repeated below:

$$\frac{d}{dt} \mathbf{x}_\delta(t) = \mathbf{A}_x [\mathbf{x}_b(t), \mathbf{u}_b(t), t] \cdot \mathbf{x}_\delta(t) + \mathbf{B}_u [\mathbf{x}_b(t), \mathbf{u}_b(t), t] \cdot \mathbf{u}_\delta(t) \quad (5.17)$$

The term $\mathbf{u}_\delta(t)$ represents small variations in the sources, and can be a stochastic variable for noise calculations. If internal noise is generated at a location where a source was not present in the original state-space description (5.1), then an additional noise source $u_n = u_{b_n}(t) + u_{\delta_n}(t)$ needs to be added to the source vector $\mathbf{u}(t)$, with $u_{b_n}(t) = 0$. This modification changes neither the dynamic bias trajectory of the state-variables, nor their dynamic behaviour.

5.2.3 Deviations in dynamic behaviour

For studying the deviations in dynamic behaviour of a nonlinear circuit using the LTV small-signal model, we can set $\mathbf{u}_\delta(t) = 0$ in the variational equation (5.5), since $\mathbf{u}_\delta(t)$ is used to model small deviations in the sources. We only need to consider the homogenous part of the variational equation:

$$\frac{d}{dt}\mathbf{x}_\delta(t) = \mathbf{A}_x[\mathbf{x}_b(t), \mathbf{u}_b(t), t] \cdot \mathbf{x}_\delta(t). \quad (5.18)$$

The determination of the dynamic behaviour of the state-variables from the homogeneous variational equation, and its description in terms of time-domain modes, is the first and most important step in any analysis using the LTV small-signal model. Any subsequent analysis of the effect of deviations in instantaneous behaviour and of internally generated noise uses these results: the same time-domain modes are present in the small-signal and noise expressions derived from the nonhomogeneous variational equations (5.16) and (5.17). This is equivalent to the fact that the poles describing the dynamic behaviour of an LTI small-signal circuit are also present in the small-signal transfer and noise transfer functions. Therefore, the rest of this thesis will focus on the description of the dynamic behaviour of a circuit using the time-domain modes of the homogeneous variational equation.

In the sequel of this chapter we will be using the variational equation (5.5) to analyze the behaviour of nonlinear circuits. For reasons of compactness the subscript δ in Equation (5.5) will be omitted, that is we write $\mathbf{x}_\delta = \mathbf{x}$ and $\mathbf{u}_\delta = \mathbf{u}$.

5.3 Theory of linear time-varying systems

In this section we introduce the concepts used in the analysis of the dynamic behaviour of nonlinear circuits with the linear time-varying small-signal model described in the previous sections. In sections 5.4, 5.5 and 5.6 we then apply the LTV small-signal model to analyze the dynamic behaviour of nonlinear circuits. To introduce the concepts used in this analysis we first give a general overview of the theory of linear time-varying systems in this section. The results are stated in time-domain, since Laplace and Fourier transformations cannot be used for

linear time-varying systems. The analysis is *based on the time-domain modes* of a linear time-varying system. We first show that for linear time-invariant systems these modes relate to the familiar Laplace-domain poles. Then the mode concept is generalized for periodic systems and general linear time-varying systems. Most of the material follows the line of the mathematical monograph by Adrianova [2].

The theory of linear time-varying systems deals with systems of the following form:

$$\frac{d}{dt}\mathbf{x}(t) = \mathbf{A}(t) \cdot \mathbf{x}(t) + \mathbf{B}(t) \cdot \mathbf{u}(t) \quad (5.19)$$

where $\mathbf{x}(t) \in \mathcal{C}^n$, $\mathbf{A}(t)$ is a square $n \times n$ matrix, $\mathbf{B}(t)$ is an $n \times m$ matrix and $\mathbf{u}(t)$ is a vector function with values in \mathcal{C}^m . The elements $a_{ij}(t)$ of $\mathbf{A}(t)$, the elements $b_{ik}(t)$ of $\mathbf{B}(t)$ and the coordinates $f_k(t)$ of the vector $\mathbf{x}(t)$ ($i, j = 1, \dots, n$; $k = 1, \dots, m$) are complex functions of the real scalar argument t , continuous in some interval $I \in \mathcal{R}$. In what follows, the latter condition is written as $\mathbf{A} \in C(I)$, $\mathbf{B} \in C(I)$ and $\mathbf{f} \in C(I)$.

The general linear time-varying equation (5.19) maps exactly on the variational equation (5.5) with $\mathbf{A}(t) = \mathbf{A}_x(\mathbf{x}_b(t), \mathbf{u}_b(t), t)$, $\mathbf{B}(t) = \mathbf{A}_u(\mathbf{x}_b(t), \mathbf{u}_b(t), t)$ and $\mathbf{u}(t) = \mathbf{u}_\delta(t)$. However, in the variational equation for an implementable electronic circuit the elements $a_{ij}(t)$ of $\mathbf{A}(t)$, $b_{ik}(t)$ of $\mathbf{B}(t)$ and the coordinates $f_k(t)$ of the vector $\mathbf{f}(t)$ are real functions of t .

The time-domain solution of the linear time-varying system (5.19) contains two main components: the *initial value response* describes the systems response to the initial condition of the state-variables $\mathbf{x}(t_0)$; the *forced response* describes its response to the input vector $\mathbf{u}(t)$. In the following paragraphs we first give the initial value response and forced response for a general linear time-varying system in terms of one of its fundamental matrices, the *matriciant*. Then the significance of this matriciant is explained by examining its structure for a linear system with constant coefficients. We express the matriciant in terms of its eigenvalues and eigenvectors, which determine the modes of this LTI system. Also the link with the familiar frequency domain description of linear time-invariant systems is given. Then we examine the matriciant for periodic systems, which leads us to the Floquet theorem and Floquet exponents, which correspond to the eigenvalues of LTI systems. Next we introduce dynamic eigenvalues and dynamic eigenvectors as a generalized eigenvalue-eigenvector concept for linear time-varying systems. Finally the Lyapunov exponent is introduced as a general measure for the stability of a solution of a nonlinear differential equation.

5.3.1 General solution in terms of the matriciant

We will start with finding the initial value response and forced response of a linear time-varying system. For this we need to find the solution of Equation (5.19)

for an initial condition \mathbf{x}_0 at time t_0 , given an input vector $\mathbf{u}(t)$. We will give a general expression for this solution in terms of one of the fundamental matrices of the linear time-varying system. For any initial condition $(t_0, \mathbf{x}_0) \in I \times \mathcal{C}^n$ this solution exists, is unique and is defined for all $t \in I$.

The system (5.19) is a *linear nonhomogeneous system*. The corresponding *linear homogeneous system* is given by

$$\frac{d}{dt}\mathbf{x}(t) = \mathbf{A}(t) \cdot \mathbf{x}(t) \quad (5.20)$$

It is well known from the theory of differential equations that every solution $\mathbf{x}(t)$ can be written as a linear combination of any set of n linearly independent solutions $\mathbf{x}_1(t), \dots, \mathbf{x}_n(t)$ of system (5.20). Such a set is called a *fundamental system of solutions* and is a basis in the space of its solutions. A matrix $\mathbf{X}(t) = \{\mathbf{x}_1(t), \dots, \mathbf{x}_n(t)\}$ whose columns are the vectors of a basis is called a *fundamental matrix*. We can easily see that such a matrix satisfies the matrix equation

$$\frac{d}{dt}\mathbf{X}(t) = \mathbf{A}(t) \cdot \mathbf{X}(t) \quad (5.21)$$

and, conversely, any nonsingular solution of equation (5.21) is a fundamental matrix of system (5.20). A fundamental matrix $\mathbf{X}(t)$ is said to be *normalized at a point* $t_0 \in I$ if $\mathbf{X}(t_0) = \mathbf{I}_n$, where \mathbf{I}_n is the identity matrix of order n ; then such a matrix is written as $\mathbf{X}(t) = \mathbf{X}(t, t_0) = \Omega_{t_0}^t \mathbf{A}$, which is called the *matriciant*.

Given a fundamental matrix $\mathbf{X}(t)$ of system (5.20) the general solution of the *linear homogeneous system* is

$$\mathbf{x}(t) = \mathbf{X}(t)\mathbf{c}, \quad \text{where} \quad \mathbf{c} \in \mathcal{C}^n \quad (5.22)$$

since any solution $\mathbf{x}(t)$ can be written as a linear combination of the set of n linearly independent solutions which form $\mathbf{X}(t)$. The general solution of the *linear nonhomogeneous system* can be found using the method of variation of parameters and is given by

$$\mathbf{x}(t) = \mathbf{X}(t)\mathbf{c} + \mathbf{X}(t) \int \mathbf{X}^{-1}(t)\mathbf{B}(t)\mathbf{u}(t)dt, \quad t \in I. \quad (5.23)$$

From equation (5.22) we can easily find the solution for the homogeneous system with initial data $(t_0, \mathbf{x}_0) \in I \times \mathcal{C}^n$. It is given by

$$\mathbf{x}(t) = \mathbf{X}(t)\mathbf{X}^{-1}(t_0)\mathbf{x}_0 \triangleq \mathbf{X}(t, t_0)\mathbf{x}_0 = \Omega_{t_0}^t \mathbf{A} \mathbf{x}_0 \quad (5.24)$$

We can write the solution for the nonhomogeneous system as

$$\begin{aligned} \mathbf{x}(t) &= \mathbf{X}(t)\mathbf{X}^{-1}(t_0)\mathbf{x}_0 + \int_{t_0}^t \mathbf{X}(t)\mathbf{X}^{-1}(\tau)\mathbf{B}(\tau)\mathbf{u}(\tau)d\tau \\ &= \Omega_{t_0}^t \mathbf{A} \mathbf{x}_0 + \int_{t_0}^t \Omega_{t_0}^{\tau} \mathbf{A} \mathbf{B}(\tau)\mathbf{u}(\tau)d\tau \end{aligned} \quad (5.25)$$

The matriciant $\Omega_{t_0}^t \mathbf{A} \triangleq \mathbf{X}(t)\mathbf{X}^{-1}(t_0)$, where $t, \tau \in I$, can be considered the *time-varying impulse response* of the state-variables of system (5.19). The first term of (5.25) describes the initial-value response of the state variables and the second term describes the forced response.

To elucidate the concept of fundamental matrix and matriciant let us consider the example of a first-order linear time-invariant system:

$$\frac{d}{dt}x(t) = a \cdot x(t) + b \cdot u(t), \quad x(t_0) = x_0 \quad (5.26)$$

The corresponding homogeneous system is given by

$$\frac{d}{dt}x(t) = a \cdot x(t) \quad (5.27)$$

and a solution of this equation is

$$x(t) = e^{at} \quad (5.28)$$

Since we are dealing with a first-order system the fundamental matrices are scalar functions $\mathbf{X}_{1 \times 1}(t)$ equal to any multiple of e^{at} . We choose $\mathbf{X}_{1 \times 1}(t) = e^{at}$. The corresponding matriciant equals $\Omega_{t_0}^t \mathbf{A} = e^{a(t-t_0)}$.

Therefore, the general solution of the linear homogeneous system is given by

$$x(t) = \mathbf{X}_{1 \times 1}(t) \cdot c = e^{at} \cdot c \quad (5.29)$$

The general solution of the nonhomogeneous system is given by

$$\begin{aligned} x(t) &= e^{at}e^{-at_0}x_0 + \int_{t_0}^t e^{at}e^{-a\tau}b \cdot u(\tau)d\tau \\ &= e^{a(t-t_0)}x_0 + \int_{t_0}^t e^{a(t-\tau)}b \cdot u(\tau)d\tau \end{aligned} \quad (5.30)$$

In this equation e^{at} equals the impulse response of the state-variable, which corresponds via Laplace transform to the familiar system pole at $s = -a$. We easily recognize the first term as the time-domain representation of the initial-value response due to this pole. In the second term we recognize the convolution of the input and the impulse-response, which equals the forced response of an LTI-system.

5.3.2 Linear systems with constant coefficients

In order to explain the significance of the matriciant, we consider a system

$$\frac{d}{dt}\mathbf{x}(t) = \mathbf{A} \cdot \mathbf{x}(t) \quad (5.31)$$

with a constant $n \times n$ matrix \mathbf{A} . In this case the matriciant is given by

$$\Omega_{t_0}^t \mathbf{A} = \mathbf{X}(t, t_0) = e^{\mathbf{A}(t-t_0)}. \quad (5.32)$$

We express this matriciant in terms of the eigenvalues and eigenvectors of \mathbf{A} , which determine the modes of the LTI system. We also give the link to the Laplace-domain description of LTI systems. To simplify the notation we set $t_0 = 0$ in the sequel of this subsection and examine $\Omega_0^t \mathbf{A} = \exp(\mathbf{A}t)$.

Let \mathbf{S} be the matrix transforming \mathbf{A} to its Jordan canonical form. That is, the columns \mathbf{s}_i of \mathbf{S} are the eigenvectors of \mathbf{A} , which satisfy

$$\mathbf{A}\mathbf{s}_i = \lambda_i \mathbf{s}_i \quad (5.33)$$

where the eigenvalues λ_i of \mathbf{A} are the solutions of the characteristic equation

$$\det [\lambda \mathbf{I}_n - \mathbf{A}] = 0 \quad (5.34)$$

The number of independent eigenvectors which satisfy (5.33) determines the multiplicity of the eigenvalue λ_i . An eigenvalue with multiplicity one is called a simple eigenvalue. For brevity let us assume that all eigenvalues are simple ones. The case with multiplicity of eigenvalues greater than one can be found in [2]. Further let us assume that the first m eigenvalues of the matrix \mathbf{A} are real and that the subsequent $(n - m)$ eigenvalues are complex. For a real transition matrix \mathbf{A} (as is the case for the transition matrix of an LTI small-signal model), these complex eigenvalues come in complex conjugate pairs $\lambda_j = \alpha + i\beta$ and $\lambda_{j+1} = \alpha - i\beta$.

Using the matrix \mathbf{S} to transform \mathbf{A} to its Jordan canonical form, the matriciant can be expressed as [2]:

$$\begin{aligned} e^{\mathbf{A}t} &= \mathbf{S}e^{\mathbf{B}t}\mathbf{S}^{-1} \\ &= \mathbf{S} \operatorname{diag} \left[e^{\lambda_1 t}, \dots, e^{\lambda_m t}, e^{\mathbf{B}_2(\lambda_{m+1})t}, \dots, e^{\mathbf{B}_2(\lambda_{n-1})t} \right] \mathbf{S}^{-1} \end{aligned} \quad (5.35)$$

with

$$e^{\mathbf{B}_2(\lambda)t} = \begin{bmatrix} e^{\alpha t} & 0 \\ 0 & e^{\alpha t} \end{bmatrix} \begin{bmatrix} \cos \beta t & \sin \beta t \\ \sin \beta t & \cos \beta t \end{bmatrix} \quad (5.36)$$

The form (5.35) obtained for the matriciant of system (5.31) explicitly demonstrates in time domain that the behaviour of the solutions, as t grows, depends

on the value (and multiplicity, see [2]) of the eigenvalues of the matrix \mathbf{A} . This can be clarified by considering that one of the fundamental matrices of system (5.31) is the matrix

$$\mathbf{X}(t) = \mathbf{S} e^{\mathbf{B}t} \quad (5.37)$$

The first column of this fundamental matrix, corresponding to the real eigenvalue $\lambda_1(t)$, is generated by the entry $e^{\lambda_1 t}$ and defines the mode:

$$\mathbf{s}_1 e^{\lambda_1 t} = \begin{bmatrix} s_{11} \\ \vdots \\ s_{n1} \end{bmatrix} e^{\lambda_1 t}$$

where \mathbf{s}_1 equals the first column of \mathbf{S} . The second column-solution is generated by the entry $e^{\lambda_2 t}$ and defines a mode with the same structure. Finally, the last pair of column-solutions, corresponding to the complex conjugate eigenvalues $\lambda_{n-1} = \alpha_{n-1} + i\beta_{n-1}$ and $\lambda_n = \alpha_{n-1} - i\beta_{n-1}$, are generated by the block $e^{\mathbf{B}_2(\lambda_{n-1})t}$ and define the modes

$$\begin{bmatrix} \mathbf{s}_{n-1} & \mathbf{s}_n \end{bmatrix} e^{\mathbf{B}_{2k-1}(\lambda_{n-1})t} = \begin{bmatrix} s_{1n-1} & s_{1n} \\ \vdots & \vdots \\ s_{nn-1} & s_{nn} \end{bmatrix} \begin{bmatrix} e^{\alpha_{n-1}t} & 0 \\ 0 & e^{\alpha_{n-1}t} \end{bmatrix} \begin{bmatrix} \cos \beta_{n-1}t & \sin \beta_{n-1}t \\ \sin \beta_{n-1}t & \cos \beta_{n-1}t \end{bmatrix}$$

Any solution of (5.31) is a linear combination of these modes. This implies the validity of the following statements. Let λ be an eigenvalue of the matrix \mathbf{A} , then indeed,

1. if $\text{Re}[\lambda] > 0$, then all corresponding solutions exponentially increase as $t \rightarrow \infty$,
2. if $\text{Re}[\lambda] < 0$, then all corresponding solutions exponentially decrease as $t \rightarrow \infty$,
3. if $\text{Re}[\lambda] = 0$, then all the solutions are bounded in the case when λ has multiplicity equal to one, and there are solutions growing as powers of t if λ has multiplicity greater than one (see [2]),
4. if $\text{Im}[\lambda] \neq 0$, then there exists an eigenvalue $\bar{\lambda}$ of the same multiplicity, and the solutions corresponding to these two eigenvalues exhibit oscillatory behaviour.

These properties are of course well-known from the familiar frequency domain description of (5.31). If we apply the unilateral Laplace transform

$$F(s) = \int_0^\infty f(t) e^{-st} dt \quad (5.38)$$

to (5.31) we obtain the equivalent Laplace-domain description

$$s\mathbf{X}(s) - \mathbf{x}(0) = \mathbf{A}\mathbf{X}(s) \quad (5.39)$$

or

$$\mathbf{X}(s) = (s\mathbf{I}_n - \mathbf{A})^{-1} \mathbf{x}(0) \quad (5.40)$$

The behaviour of the solutions as $t \rightarrow \infty$ is determined by the poles p_i of $(s\mathbf{I}_n - \mathbf{A})^{-1}$. These poles follow from

$$\det [p\mathbf{I}_n - \mathbf{A}] = 0 \quad (5.41)$$

and equal the eigenvalues λ_i of \mathbf{A} (compare (5.41) with (5.34)). The solution corresponding to a pole p is stable if $\text{Re}[p] < 0$, and complex poles correspond to solutions exhibiting oscillatory behaviour. Thus for linear time-invariant systems the concepts of eigenvalues and poles are equivalent.

5.3.3 Linear systems with periodic coefficients

As a more general subset of linear time-varying systems we now consider systems of the form

$$\frac{d}{dt} \mathbf{x}(t) = \mathbf{A}(t) \cdot \mathbf{x}(t) \quad (5.42)$$

with

$$\mathbf{A}(t + T) = \mathbf{A}(t) \quad (5.43)$$

in which T is the period. We show that the modes of this type of system are characterized by Floquet exponents and periodic eigenvectors. These Floquet exponents can be considered a generalization of the eigenvalues or poles of an LTI system. We also examine the structure of the matriciant of a periodic LTV system. The Floquet theorem gives this structure in a form similar to the form (5.35) for LTI-systems.

We can prove the following statement (*Floquet theorem* [2]): the matriciant of a periodic LTV system can be represented in the form

$$\Omega_{t_0}^t \mathbf{A} = \Phi(t) e^{\mathbf{B}_T(t-t_0)} \quad (5.44)$$

where

$$\mathbf{B}_T = \frac{1}{T} \text{Ln } \Omega_{t_0}^{t_0+T} \mathbf{A} \quad \text{and} \quad \Phi(t) = \Phi(t + T).$$

From the representation of the matriciant (5.44) it is clear that the dynamics of the solutions are determined by the matrix $\exp(\mathbf{B}_T t)$, which is fundamental for

the system $\dot{\mathbf{x}} = \mathbf{B}_T \mathbf{x}$. The eigenvalues $\beta_1, \beta_2, \dots, \beta_n$ of the matrix \mathbf{B}_T equal the Floquet exponents of system (5.42). As indicated by the presence of the periodic matrix $\Phi(t)$ in (5.44), the eigenvectors are periodic vector-functions. The matrix \mathbf{B}_T represents the overall behaviour of the solutions after each period. From this and from our knowledge about the behaviour of LTI systems the following is immediately clear:

1. if $\text{Re}[\beta] > 0$, then all corresponding solutions exponentially increase as $t \rightarrow \infty$,
2. if $\text{Re}[\beta] < 0$, then all corresponding solutions exponentially decrease as $t \rightarrow \infty$,
3. if $\text{Re}[\beta] = 0$, then all the solutions are bounded in the case when β has multiplicity equal to one, and there are solutions growing as powers of t if β has multiplicity greater than one

For LTI systems these statements about the Floquet exponents are equivalent to the statements about the eigenvalues of \mathbf{A} . For an LTI system we have $\Omega_{t_0}^{t_0+T} \mathbf{A} = \exp[\mathbf{A}(t_0 + T - t_0)] = \exp[\mathbf{A}T]$. The Floquet exponents equal the eigenvalues of \mathbf{B}_T , which is given by

$$\mathbf{B}_T = \frac{1}{T} \text{Ln} \Omega_{t_0}^{t_0+T} \mathbf{A} = \frac{1}{T} \text{Ln} e^{\mathbf{A}T} = \mathbf{A}$$

Thus the Floquet exponents of an LTI system equal the eigenvalues of \mathbf{A} .

5.3.4 Linear systems with arbitrary time-varying coefficients: quasi-static and dynamic eigenvalues and eigenvectors

In Section 5.3.2 we saw that the dynamic behaviour and stability of LTI systems can be described by the eigenvalues and eigenvectors of the state transition matrix \mathbf{A} which determine the modes of these systems. In this subsection we introduce generalizations of these concepts for LTV systems. First we give the straightforward extension to quasi-static eigenvalues and eigenvectors, but these only have significance for a limited set of LTV systems (namely slowly-varying systems). Then we cover dynamic eigenvalues and eigenvectors as introduced by Wu [53]. This generalization is suitable for all LTV systems and enables us to give an expression for the matriciant of an LTV system similar to expression (5.35) for LTI systems and expression (5.44) for periodic LTV systems. We also give the link between dynamic eigenvalues, Floquet exponents of LTV systems and eigenvalues of LTI systems.

Quasi-static eigenvalues and eigenvectors Let us first restate the definition of traditional (time-invariant) eigenvalues and eigenvectors. An eigenvector \mathbf{s} of a constant matrix \mathbf{A} satisfies

$$\mathbf{A} \mathbf{s} = \lambda \mathbf{s} \quad (5.45)$$

where the eigenvalue λ is one of the solutions of the characteristic equation

$$\det [\lambda \mathbf{I}_n - \mathbf{A}] = 0 \quad (5.46)$$

A straightforward extension for LTV systems is obtained by using the same definition of eigenvalues and eigenvectors, replacing the constant matrix \mathbf{A} in (5.45) and (5.46) by the time-varying matrix $\mathbf{A}(t)$ and determining the traditional eigenvalues and eigenvectors *at each point of time separately*. In this approach the time-dependency of the transition matrix is neglected in the determination of eigenvalues and eigenvectors (*'frozen time' approach*) and the time-varying eigenvalues and eigenvectors obtained in this way are called *quasi-static eigenvalues* and *quasi-static eigenvectors*. We denote a quasi-static eigenvalue and eigenvector as $\lambda_{qs}(t)$ and $\mathbf{s}_{qs}(t)$ resp. and they satisfy

$$\mathbf{A}(t) \mathbf{s}_{qs}(t) = \lambda_{qs}(t) \mathbf{s}_{qs}(t) \quad (5.47)$$

where the quasi-static eigenvalue $\lambda_{qs}(t)$ is one of the solutions of the quasi-static characteristic equation

$$\det [\lambda_{qs}(t) \mathbf{I}_n - \mathbf{A}(t)] = 0 \quad (5.48)$$

It is remarked in [4] that this quasi-static approach is justified for slowly-varying systems only.

Dynamic eigenvalues and eigenvectors It is now well known that the quasi-static eigenvalues of the state transition matrix $\mathbf{A}(t)$ do not, in general, determine the stability of LTV systems. It is also known that a time-varying transformation $\mathbf{x}(t) = \mathbf{S}_{qs}(t) \mathbf{y}(t)$ with $\mathbf{S}_{qs}(t)$ formed by the quasi-static eigenvectors of $\mathbf{A}(t)$ will not, in general, result in a simpler form (such as the diagonal or Jordan canonical form) due to the term $\mathbf{S}_{qs}^{-1}(t) \frac{d}{dt} \mathbf{S}_{qs}(t)$ in the transformed state transition matrix (see (A.8)), nor will it preserve the quasi-static eigenvalues.

In [53] Wu introduced the concept of *dynamic eigenvalues* and *dynamic eigenvectors* (he denotes them as "eigenvalues" and "eigenvectors" and also as extended eigenvalues and extended eigenvectors). His definition reduces to the quasi-static one whenever $\mathbf{A}(t)$ is slowly-varying and has slowly-varying eigenvectors and to the conventional one when $\mathbf{A}(t)$ is constant and has constant eigenvectors. We will show that there exists a time-varying transformation

(which is determined by the dynamic eigenvectors and eigenvalues) that will transform $\mathbf{A}(t)$ into a diagonal matrix $\mathbf{\Lambda}(t)$ containing the dynamic eigenvalues of $\mathbf{A}(t)$ and we will give a general expression for the matrix of an LTV system.

We start with the definition of dynamic eigenvalues and eigenvectors [53]. Let $\mathbf{A}(t)$ be a given time-varying $n \times n$ matrix. If there exists a scalar function $\lambda(t)$ and a nonzero differentiable vector function $\mathbf{s}(t)$ such that they satisfy the following condition:

$$\mathbf{A}(t) \mathbf{s}(t) = \lambda(t) \mathbf{s}(t) + \frac{d}{dt} \mathbf{s}(t) \quad \forall t \quad (5.49)$$

then $\lambda(t)$ is said to be a *dynamic eigenvalue* of $\mathbf{A}(t)$ associated with the *dynamic eigenvector* $\mathbf{s}(t)$. If $\mathbf{A}(t)$ has slowly-varying eigenvectors $\mathbf{s}(t)$, then $\frac{d}{dt} \mathbf{s}(t) \ll \lambda(t) \mathbf{s}(t)$ and (5.49) reduces to the definition (5.47) of quasi-static eigenvalues and eigenvectors.

In order to show that the modes of an LTV system are determined by the systems dynamic eigenvalues and eigenvectors, we introduce a *Lyapunov transformation* defined by the dynamic eigenvectors which transforms the state transition matrix $\mathbf{A}(t)$ into a diagonal form and derive a general expression for the matrix of an LTV system. It can be shown [21] that dynamic eigenvalues are invariant under any Lyapunov transformation $\mathbf{x}(t) = \mathbf{L}(t) \mathbf{y}(t)$. The desired diagonal transition matrix $\mathbf{\Lambda}(t)$ is defined by the dynamic eigenvalues $\lambda_i(t)$, i.e.,

$$\mathbf{\Lambda}(t) = \text{diag} [\lambda_1(t), \lambda_2(t), \dots, \lambda_n(t)]. \quad (5.50)$$

Let $\mathbf{s}_i(t)$ be the dynamic eigenvector corresponding to the dynamic eigenvalue $\lambda_i(t)$. Then, by definition (5.49) we have

$$\mathbf{A}(t) \mathbf{s}_i(t) = \lambda_i(t) \mathbf{s}_i(t) + \frac{d}{dt} \mathbf{s}_i(t). \quad (5.51)$$

Let $\mathbf{S}(t)$ be an $n \times n$ matrix formed by the dynamic eigenvectors $\mathbf{s}_i(t)$, i.e.,

$$\mathbf{S}(t) = [\mathbf{s}_1(t), \mathbf{s}_2(t), \dots, \mathbf{s}_n(t)]. \quad (5.52)$$

We obtain from (5.51) and (5.52)

$$\mathbf{A}(t) \mathbf{S}(t) = \mathbf{S}(t) \mathbf{\Lambda}(t) + \frac{d}{dt} \mathbf{S}(t) \quad (5.53)$$

or

$$\frac{d}{dt} \mathbf{S}(t) = \mathbf{A}(t) \mathbf{S}(t) - \mathbf{S}(t) \mathbf{\Lambda}(t) \quad (5.54)$$

Keeping in mind that the derivative of the matrix $\Omega_{t_0}^t \mathbf{A}$ is given by

$$\frac{d}{dt} \Omega_{t_0}^t \mathbf{A} = \mathbf{A}(t) \Omega_{t_0}^t \mathbf{A}$$

we can easily prove that $\mathbf{S}(t)$, a solution of (5.54), is given by

$$\mathbf{S}(t) = \Omega_{t_0}^t \mathbf{A} e^{-\int_{t_0}^t \Lambda(\tau) d\tau} \quad (5.55)$$

It is well known that $\Omega_{t_0}^t \mathbf{A}$ is nonsingular for all t . Hence $\mathbf{S}(t)$ in (5.55) is nonsingular for all t and qualifies as a Lyapunov transformation for $\mathbf{A}(t)$. Note that $\mathbf{S}(t_0)$ equals the unity matrix \mathbf{I}_n , the dynamic eigenvectors are normalized at $t = t_0$. From (5.54) it directly follows that the transformed transition matrix $\mathbf{A}_y(t)$ is given by

$$\mathbf{A}_y(t) = \mathbf{S}^{-1}(t) \mathbf{A}(t) \mathbf{S}(t) - \mathbf{S}^{-1}(t) \frac{d}{dt} \mathbf{S}(t) = \Lambda(t) \quad (5.56)$$

and indeed equals the diagonal matrix $\Lambda(t)$.

From Equation (5.55) we can easily derive the following general expression for the matriciant of an LTV system in terms of its dynamic eigenvalues and eigenvectors:

$$\Omega_{t_0}^t \mathbf{A} = \mathbf{S}(t) e^{\int_{t_0}^t \Lambda(\tau) d\tau} \quad (5.57)$$

In this expression we can recognize the modes

$$\mathbf{m}_i(t) = \mathbf{s}_i(t) e^{\gamma_i(t)}, \quad i = 1, \dots, n, \quad (5.58)$$

where

$$\gamma_i(t) \triangleq \int_{t_0}^t \lambda_i(\tau) d\tau \quad (5.59)$$

and $\mathbf{s}_i(t)$ is the i^{th} column of \mathbf{S} . Thus the modes of an LTV system are determined by its dynamic eigenvalues and dynamic eigenvectors. Any solution $\mathbf{x}(t)$ of an LTV system is a linear combination of these modes:

$$\mathbf{x}(t) = \sum_{i=1}^n c_i \mathbf{m}_i(t) = \sum_{i=1}^n c_i \mathbf{s}_i(t) e^{\gamma_i(t)}. \quad (5.60)$$

Floquet exponents versus dynamic eigenvalues In the special case of periodic LTV systems both the dynamic eigenvalues and the dynamic eigenvectors will be periodic. In order to find the link between dynamic eigenvalues and Floquet exponents of periodic LTV systems we now apply the Floquet theorem (5.44) to Expression (5.57). We find that

$$\Omega_{t_0}^t \mathbf{A} = \Phi(t) e^{\mathbf{B}_T(t-t_0)} \quad (5.61)$$

where

$$\begin{aligned}
\mathbf{B}_T &= \frac{1}{T} \text{Ln} \Omega_{t_0}^{t_0+T} \mathbf{A} \\
&= \frac{1}{T} \text{Ln} \mathbf{S}(t_0 + T) e^{\int_{t_0}^{t_0+T} \Lambda(\tau) d\tau} \\
&= \frac{1}{T} \text{Ln} \mathbf{S}(t_0) e^{\int_{t_0}^{t_0+T} \Lambda(\tau) d\tau} \\
&= \frac{1}{T} \text{Ln} \mathbf{I}_n e^{\int_{t_0}^{t_0+T} \Lambda(\tau) d\tau} \\
&= \frac{1}{T} \int_{t_0}^{t_0+T} \Lambda(\tau) d\tau
\end{aligned}$$

in which the third equality follows from the periodicity of the dynamic eigenvectors and the fourth equality from the normalization of the dynamic eigenvectors at $t = t_0$. The Floquet exponents equal the eigenvalues of the matrix \mathbf{B}_T . Thus the Floquet exponents β_i of a periodic LTV system are equal to the average of the periodic dynamic eigenvalues $\lambda_i(t)$ over one period of time:

$$\beta_i = \frac{1}{T} \int_{t_0}^{t_0+T} \lambda_i(\tau) d\tau. \quad (5.62)$$

LTI poles versus dynamic eigenvalues In the special case of LTI systems the dynamic eigenvalues and eigenvectors will be constant and equal to the traditional eigenvalues and eigenvectors of the constant transition matrix \mathbf{A} . It is well known from conventional linear analysis that the traditional eigenvalues are equal to the LTI poles. Therefore, for LTI systems the dynamic eigenvalues are constant and are equal to the LTI poles.

In the derivation of Expression (5.57) for the matriciant of an LTV system we assumed that both the dynamic eigenvalues and the matriciant were a priori known. It is however in general not trivial to obtain them for a given LTV system. In Sections 5.4 through 5.6 we will give both an analytical and numerical way to obtain the dynamic eigenvalues and eigenvectors and from these the modes of an LTV system.

5.3.5 Lyapunov characteristic exponents

In Sections 5.3.2 and 5.3.3 we saw that the stability of LTI systems and periodic LTV systems is determined by the real part of the eigenvalues of the transition matrix and the real part of the Floquet exponents, respectively. We now establish a stability criterion for general LTV systems based on their dynamic eigenvalues and eigenvectors. For this we use general results obtained by

the method of characteristic exponents due to Lyapunov [2]. In this method the growth rate of solutions is studied in comparison with the exponential function $\exp(\alpha t)$. This growth is determined by *Lyapunov characteristic exponents* α , or in short *Lyapunov exponents*. We apply the method of Lyapunov exponents to the modes (5.58) of a general LTV system. We show that for periodic LTV systems the stability criterion based on Lyapunov exponents is identical to the stability criterion based on Floquet exponents and that for LTI system it is identical to the stability criterion based on poles.

The Lyapunov characteristic exponent determines the growth of the absolute value of a function with respect to the scale of exponential functions $\exp(\alpha t)$. Obviously such an exponential function approaches zero for $t \rightarrow \infty$ if $\alpha < 0$. For an arbitrary function $f(t)$ we can write

$$|f(t)| = e^{\left(\frac{1}{t} \ln|f(t)|\right)t}. \quad (5.63)$$

This clarifies the following definition of the Lyapunov characteristic exponent [2]. Let a complex-valued function $f(t)$ be defined on the interval $[t_0, \infty]$. Then the *Lyapunov characteristic exponent* $\chi[f]$ of the function $f(t)$ is defined as

$$\chi[f] = \overline{\lim}_{t \rightarrow \infty} \frac{1}{t} \ln|f(t)|. \quad (5.64)$$

By substituting the exponential function $\exp(\alpha t)$ in this definition we easily see that its Lyapunov exponent is the number α .

The significance of the Lyapunov exponent of a function $f(t)$ in determining its growth is clarified by the following statement: A function $f(t)$ having the Lyapunov exponent $\alpha \neq \pm\infty$ is such that as $t \rightarrow \infty$ $|f(t)|$ grows slower (or decreases faster) than $\exp[(\alpha + \varepsilon)t]$ and, along a certain sequence of values of t , grows faster (or decreases slower) than $\exp[(\alpha - \varepsilon)t]$ for any $\varepsilon > 0$. That is, $\chi[f] = \alpha \neq \pm\infty$ if and only for any $\varepsilon > 0$ the following two conditions hold simultaneously:

$$1. \quad \lim_{t \rightarrow \infty} \frac{|f(t)|}{e^{(\alpha + \varepsilon)t}} = 0 \quad (5.65)$$

$$2. \quad \overline{\lim}_{t \rightarrow \infty} \frac{|f(t)|}{e^{(\alpha - \varepsilon)t}} = \infty \quad (5.66)$$

The proof of this statement can be found in [2].

We now consider the function $f(t)$ to be a solution of a differential equation. From Condition (5.65) it follows that this solution $f(t)$ is stable if its Lyapunov exponent $\chi[f]$ is negative, since then it decreases faster than any exponential function $\exp[(\chi[f] + \varepsilon)t]$. If we choose $\varepsilon = (|\chi[f]|)/2$ then this exponential function approaches zero for $t \rightarrow \infty$, and the same holds for $|f(t)|$.

To be able to apply the Lyapunov method of characteristic exponents to the solutions of an LTV system expressed in its modes we need two properties of

the characteristic exponents. The mathematical proof for both properties can be found in [2].

1. The Lyapunov exponent of the sum of a finite number of functions $f_i(t)$, $i = 1, \dots, n$, does not exceed the greatest of the Lyapunov exponents of these functions individually and coincides with it if only one function has the greatest exponent. This is to be expected, since for time approaching infinity the linear combination will be dominated by the function with the greatest Lyapunov exponent.
2. The Lyapunov exponent of a finite-dimensional vector-function $\mathbf{f}(t)$ equals the Lyapunov exponent of its norm:

$$\chi[\mathbf{f}] = \overline{\lim}_{t \rightarrow \infty} \frac{1}{t} \ln \|\mathbf{f}(t)\|.$$

Any solution $f(t)$ of an LTV system is a linear combination of the modes (5.58) of this system. Therefore, the LTV system is stable if the Lyapunov exponent of any linear combination of its modes is negative. According to property 1 the Lyapunov exponent of any linear combination of modes does not exceed the greatest Lyapunov exponent of these modes individually. Thus an LTV system is stable if all its modes have a negative Lyapunov exponent.

Stability of LTV systems based on Lyapunov exponents We now apply the definition of the Lyapunov characteristic exponent to the modes (5.58) of an LTV system. These modes are given by $\mathbf{s}_i(t) \exp[\gamma_i(t)]$ and after some manipulations (using property 2 for handling the vector-functions $\mathbf{s}_i(t)$) we get

$$\begin{aligned} \chi_i &= \overline{\lim}_{t \rightarrow \infty} \operatorname{Re} \left[\frac{1}{t} \ln \|\mathbf{s}_i(t)\| + \frac{1}{t} \gamma_i(t) \right] \\ &= \overline{\lim}_{t \rightarrow \infty} \operatorname{Re} \left[\frac{1}{t} \ln \|\mathbf{s}_i(t)\| + \frac{1}{t} \int_{t_0}^t \lambda_i(\tau) d\tau \right] \quad i = 1, \dots, n \end{aligned} \quad (5.67)$$

This clearly gives the relation between the dynamic eigenvalues $\lambda_i(t)$, the dynamic eigenvectors $\mathbf{s}_i(t)$ and the Lyapunov exponents χ_i . The LTV system is stable if the Lyapunov exponents of all its modes are negative.

Floquet exponents versus Lyapunov exponents In the special case of periodic LTV systems both the dynamic eigenvalues and the dynamic eigenvectors are periodic and we can apply some simplifications. Since the dynamic eigenvector is periodic the first term in Expression (5.67) vanishes for time approaching infinity. The second term involves the time-integral of the periodic dynamic eigenvalue and for time approaching infinity the limiting value equals

the time-integral of the dynamic eigenvalue over one period, divided by the period. Thus for periodic LTV systems the Lyapunov exponents are given by

$$\chi_i = \operatorname{Re} \left[\frac{1}{T} \int_{t_0}^{t_0+T} \lambda_i(\tau) d\tau \right] = \operatorname{Re} [\beta_i] \quad (5.68)$$

and they equal the real part of the Floquet exponents β_i (see Equation (5.62)). Thus for periodic LTV systems the stability criterion based on Lyapunov exponents simplifies to the stability criterion based on Floquet exponents.

LTI poles versus Lyapunov exponents For LTI systems both the eigenvalues and eigenvectors are independent of time. The Floquet exponents of an LTI system are equal to the eigenvalues λ_i of the transition matrix \mathbf{A} (as proven in the last paragraph of Section 5.3.3) and the Lyapunov exponents work out to

$$\chi_i = \operatorname{Re} \left[\frac{1}{T} \int_{t_0}^{t_0+T} \lambda_i d\tau \right] = \operatorname{Re} [\lambda_i]. \quad (5.69)$$

For LTI systems the eigenvalues are equivalent to the system poles. Therefore, for LTI systems the stability criterion based on Lyapunov exponents simplifies to the familiar criterion that the system poles should have a negative real part.

5.4 First-order systems and their stability

The dynamic behaviour in the vicinity of a dynamic bias trajectory \mathbf{x}_b of the nonlinear system (5.1) as function of the external sources \mathbf{u}_b can be examined by studying the variational equation (5.5) with $\mathbf{u} = 0$. It is determined by the dynamic eigenvalues and eigenvectors [52, 53] of this variational equation. The stability of a solution can be examined by the method of characteristic exponents due to Lyapunov, see Section 5.3.5. The stability of periodic solutions for periodic sources can be examined by means of Floquet theory [42], see Section 5.3.3. In this section we will introduce these concepts for a first-order variational equation.

5.4.1 The dynamic eigenvalue and eigenvector

If the dynamics of a nonlinear circuit can be described by a first-order nonlinear differential equation, the dynamic eigenvalue is obtained easily. In this case we obtain a first-order variational equation

$$\frac{d}{dt}x(t) = a_x(t)x(t) \quad (5.70)$$

Note that

$$a_x(t) \cdot 1 = a_x(t) \cdot 1 + \frac{d}{dt}1 \quad (5.71)$$

Thus, in agreement with Equation (5.49) [52, 53], the dynamic eigenvalue is simply given by

$$\lambda(t) = a_x(t) \quad (5.72)$$

while the corresponding dynamic eigenvector is given by:

$$s(t) = 1. \quad (5.73)$$

Next, we introduce the quantity

$$\gamma(t) = \int_0^t \lambda(\tau) d\tau \quad (5.74)$$

Multiplication of (5.71) with $\exp[\gamma(t)]$ shows that the time-varying mode $\{1 \cdot \exp[\gamma(t)]\}$ indeed is a solution of the variational equation (5.70), which can also easily be seen by inserting this mode in the variational equation. Thus the normalized fundamental solution of (5.70) is given by

$$x(t, 0) = e^{\gamma(t)} = e^{\int_0^t \lambda(\tau) d\tau} \quad (5.75)$$

5.4.2 Lyapunov and Floquet exponent and stability

The stability of solutions of linear time-varying systems can be determined by the method of characteristic exponents due to Lyapunov (see section 5.3.5). We apply the definition of the characteristic Lyapunov exponent χ to the mode $\exp[\gamma(t)]$ of (5.70). Then

$$\chi = \overline{\lim}_{t \rightarrow \infty} \operatorname{Re} \left[\frac{1}{t} \gamma(t) \right] = \overline{\lim}_{t \rightarrow \infty} \operatorname{Re} \left[\frac{1}{t} \int_0^t \lambda d\tau \right] = \overline{\lim}_{t \rightarrow \infty} \operatorname{Re} \left[\frac{1}{t} \int_0^t a_x(\tau) d\tau \right] \quad (5.76)$$

This clearly gives the relation between the dynamic eigenvalue and the Lyapunov exponent.

The Floquet exponent β for periodic systems follows as a special case of the Lyapunov exponent. For periodic systems the eigenvalue is periodic. Since $\gamma(t)$ is the time-integral of the periodic eigenvalue (see (5.74)), the term $\gamma(t)/t$ can be replaced by the time-integral of the eigenvalue over one period, divided by the period, for time approaching infinity. Therefore, for periodic systems the stability criterion in terms of the Floquet exponent is given by

$$\operatorname{Re}[\beta] = \operatorname{Re} \left[\frac{1}{T} \gamma(T) \right] = \operatorname{Re} \left[\frac{1}{T} \int_0^T \lambda(\tau) d\tau \right] = \operatorname{Re} \left[\frac{1}{T} \int_0^T a_x(\tau) d\tau \right] < 0 \quad (5.77)$$

The periodic solution is stable if the Floquet exponent has a negative real part.

For linear time-invariant (LTI) systems the eigenvalue $\lambda(t)$ is independent of time, so the Floquet exponent β works out to the real part of the eigenvalue, which for LTI systems is equivalent to the system pole. Thus for LTI systems the stability criterion (5.77) simplifies to the familiar criterion that the system pole should have a negative real part.

5.5 Second-order systems and stability

In this section we describe a systematic method to obtain the eigenvalues and eigenvectors for second-order linear time-varying systems, as presented in [21]. It starts with a triangularization of the transition matrix, to be realized by a Lyapunov transformation. To obtain this Lyapunov transformation we need to solve a Riccati equation. As a result the dynamic eigenvalues of [52, 53] are constructed. For the second-order system under consideration, the eigenvectors then follow by inspection. Moreover, the fundamental matrix is obtained. We also present an alternative method to obtain the dynamic eigenvalues, as given by Wu [52]. In this method the Lyapunov transformation is obtained as the limiting value in a series of quasi-static similarity transformations. Finally we show how the Lyapunov and Floquet exponents are obtained from the dynamic eigenvalues and eigenvectors.

5.5.1 Dynamic eigenvalues and eigenvectors using the Riccati equation

We start with the second-order variational state-equation

$$\frac{d}{dt} \begin{bmatrix} x_1 \\ x_2 \end{bmatrix} = \begin{bmatrix} a_{11} & a_{12} \\ a_{21} & a_{22} \end{bmatrix} \begin{bmatrix} x_1 \\ x_2 \end{bmatrix} \Leftrightarrow \frac{d}{dt} \mathbf{x}(t) = \mathbf{A}_x(t) \cdot \mathbf{x}(t) \quad (5.78)$$

in which the elements of \mathbf{A}_x and \mathbf{x} are real functions of the time t . In order to triangularize the state-transition matrix $\mathbf{A}_x(t)$, such that the dynamic eigenvalues appear on the diagonal, we now apply the dynamic similarity transformation

$$\begin{bmatrix} x_1 \\ x_2 \end{bmatrix} = \begin{bmatrix} 1 & 0 \\ l & 1 \end{bmatrix} \begin{bmatrix} y_1 \\ y_2 \end{bmatrix} \Leftrightarrow \mathbf{x}(t) = \mathbf{L}(t) \cdot \mathbf{y}(t) \quad (5.79)$$

to (5.78) in which $l = l(t)$ is a solution of the Riccati equation [5]

$$\frac{d}{dt} l = -a_{12}l^2 - (a_{11} - a_{22})l + a_{21}. \quad (5.80)$$

Then we arrive at the triangularized state-equation

$$\frac{d}{dt} \begin{bmatrix} y_1 \\ y_2 \end{bmatrix} = \begin{bmatrix} \lambda_1 & a_{y12} \\ 0 & \lambda_2 \end{bmatrix} \begin{bmatrix} y_1 \\ y_2 \end{bmatrix} \Leftrightarrow \frac{d}{dt} \mathbf{y}(t) = \mathbf{A}_y(t) \mathbf{y}(t) \quad (5.81)$$

with

$$\begin{cases} \lambda_1(t) = a_{11}(t) + l(t) \cdot a_{12}(t) \\ \lambda_2(t) = -l(t) \cdot a_{12}(t) + a_{22}(t) \end{cases} \quad (5.82)$$

Note that λ_1 and λ_2 in general are not complex conjugated, as is always the case in the time-invariant case.

To come to an expression for the dynamic eigenvalues and eigenvectors, we observe that

$$\text{trace}[\mathbf{A}_y] = a_{y_{11}}(t) + a_{y_{22}}(t) = a_{11}(t) + a_{22}(t) = \text{trace}[\mathbf{A}_x] \quad (5.83)$$

and

$$\mathbf{A}_y(t) \begin{bmatrix} 1 \\ 0 \end{bmatrix} = \lambda_1(t) \begin{bmatrix} 1 \\ 0 \end{bmatrix} + \frac{d}{dt} \begin{bmatrix} 1 \\ 0 \end{bmatrix} \quad (5.84)$$

while, if $m=m(t)$ satisfies

$$\dot{m} = (\lambda_1 - \lambda_2)m + a_{12} \quad (5.85)$$

then

$$\mathbf{A}_y(t) \begin{bmatrix} m(t) \\ 1 \end{bmatrix} = \lambda_2(t) \begin{bmatrix} m(t) \\ 1 \end{bmatrix} + \frac{d}{dt} \begin{bmatrix} m(t) \\ 1 \end{bmatrix} \quad (5.86)$$

In agreement with [52, 53], we now have that $\lambda_1(t)$ and $\lambda_2(t)$ are the dynamic eigenvalues of $\mathbf{A}_x(t)$ and $\mathbf{A}_y(t)$ while $[1 \ 0]^T$ and $[m(t) \ 1]^T$ are the corresponding dynamic eigenvectors of $\mathbf{A}_y(t)$.

Next, we introduce (5.74) for both eigenvalues:

$$\gamma_i(t) = \int_0^t \lambda_i(\tau) d\tau \quad (i = 1, 2) \quad (5.87)$$

Multiplication of (5.84) with $\exp[\gamma_1(t)]$ and of (5.86) with $\exp[\gamma_2(t)]$ shows that

$$\begin{bmatrix} 1 \\ 0 \end{bmatrix} e^{\gamma_1(t)} \quad \text{and} \quad \begin{bmatrix} m(t) \\ 1 \end{bmatrix} e^{\gamma_2(t)} \quad (5.88)$$

are linear independent solutions of (5.81), and with (5.79), the time-varying modes

$$\begin{bmatrix} 1 \\ l(t) \end{bmatrix} e^{\gamma_1(t)} \quad \text{and} \quad \begin{bmatrix} m(t) \\ 1 + m(t) \cdot l(t) \end{bmatrix} e^{\gamma_2(t)} \quad (5.89)$$

are linear independent solutions of (5.78). Note that the function $l = l(t)$ and $m = m(t)$ are solutions of the differential equations (5.80) and (5.85),

respectively, and as a consequence, are not unique. However, the normalized fundamental matrix $\mathbf{X}(t, 0)$ of (5.78) is uniquely given by

$$\mathbf{X}(t, 0) = \begin{bmatrix} 1 & m(t) \\ l(t) & 1 + l(t)m(t) \end{bmatrix} \begin{bmatrix} e^{\gamma_1(t)} & 0 \\ 0 & e^{\gamma_2(t)} \end{bmatrix} \begin{bmatrix} 1 + l(0)m(0) & -m(0) \\ -l(0) & 1 \end{bmatrix} \quad (5.90)$$

We have seen that we need to solve a Riccati equation to obtain a Lyapunov transformation which directly triangularizes the transition matrix of a second-order variational equation. An alternative approach of calculating the dynamic eigenvalue was given by Wu [52]. There the author obtained the dynamic eigenvalues and eigenvectors by an iteration procedure where in each step a quasi-static problem is solved. In this method we do not need to solve a Riccati differential equation to obtain the parameters for a Lyapunov transformation, but we obtain a diagonalized transition matrix as the limiting value in a series of quasi-static similarity transforms. An outline of this procedure is given in Appendix B

5.5.2 Lyapunov and Floquet exponents and stability

We apply the definition (5.64) of the characteristic Lyapunov-exponent χ to the modes (5.89) of the second-order variational equation (5.78). If we write these modes as $\mathbf{s}_i(t) \exp[\gamma_i(t)]$ then

$$\chi_i = \overline{\lim}_{t \rightarrow \infty} \operatorname{Re} \left[\frac{1}{t} \ln \|\mathbf{s}_i(t)\| + \frac{1}{t} \gamma_i(t) \right] \quad (i = 1, 2) \quad (5.91)$$

This again clearly gives the relation between the dynamic eigenvalues and the Lyapunov-exponents.

The Floquet exponents β_i for periodic systems again follow as a special case of the Lyapunov exponents. For periodic systems both the eigenvalues and eigenvectors are periodic. For time approaching infinity the eigenvector term $t^{-1} \ln \|\mathbf{s}_i(t)\|$ in the Lyapunov exponent vanishes. The second term contains $\gamma_i(t)$, which is the time-integral of the periodic eigenvalue (see (5.87)). For time approaching infinity this term can again be replaced by the time-integral of the eigenvalue over one period, divided by the period. Therefore, for periodic systems the stability criterion based on the Floquet exponents is given by:

$$\operatorname{Re} [\beta_i] = \operatorname{Re} \left[\frac{1}{T} \gamma_i(T) \right] = \operatorname{Re} \left[\frac{1}{T} \int_0^T \lambda_i(\tau) d\tau \right] < 0 \quad (i = 1, 2) \quad (5.92)$$

The periodic solution is stable if all Floquet exponents have a negative real part.

For linear time-invariant (LTI) systems the eigenvalues $\lambda_i(t)$ are independent of time, so the Floquet exponents β_i work out to the real part of the eigenvalues,

which for LTI systems are equivalent to the system poles. Thus, as already noted in the first-order case, for LTI systems the stability criterion (5.92) simplifies to the familiar criterion that all system poles should have negative real parts. We can easily show that for linear time-invariant systems the dynamic eigenvalues as defined by Equation (5.82) are indeed constant and complex conjugate, as expected. For LTI systems the Riccati differential equation (5.80) reduces to the algebraic equation

$$0 = -a_{12}l^2 - (a_{11} - a_{22})l + a_{21}, \quad (5.93)$$

which has the following constant solutions:

$$\begin{cases} l_1 = \frac{-(a_{11}-a_{22})}{2a_{12}} + \frac{1}{2a_{12}}\sqrt{(a_{11}-a_{22})^2 + 4a_{12}a_{21}} \\ l_2 = \frac{-(a_{11}-a_{22})}{2a_{12}} - \frac{1}{2a_{12}}\sqrt{(a_{11}-a_{22})^2 + 4a_{12}a_{21}} \end{cases} \quad (5.94)$$

If we use either of these solutions in Equation (5.82), we obtain the following dynamic eigenvalues:

$$\begin{cases} \lambda_1 = \frac{(a_{11}+a_{22})}{2} + \frac{1}{2}\sqrt{(a_{11}-a_{22})^2 + 4a_{12}a_{21}} \\ \lambda_2 = \frac{(a_{11}+a_{22})}{2} - \frac{1}{2}\sqrt{(a_{11}-a_{22})^2 + 4a_{12}a_{21}} \end{cases} \quad (5.95)$$

where the two dynamic eigenvalues switch place depending on the specific choice of l . The eigenvalues are constant, and if complex they are complex conjugate.

5.6 Higher-order systems and stability

The method depicted in section 5.5 can be generalized in order to obtain the dynamic eigenvalues of variational equations of order higher than two. It can be shown that we need to solve $\sum_{k=1}^{n-1} k$ coupled Riccati-equations to obtain the Lyapunov-transformation for triangularization of an n^{th} -order transition matrix. A detailed discussion of this procedure can be found in [22]

An alternative method, in which we obtain the Lyapunov transformation as the limiting value in a series of quasi-static similarity transforms, was already given in appendix B. This method can easily be generalized and might numerically be more convenient for high-order variational equations.

Using either the Riccati-equations method or the iterative method the dynamic eigenvalues of an n^{th} -order variational equation can be found. These dynamic eigenvalues can be used to determine the stability of general LVT systems by calculating the Lyapunov exponents, or to determine the stability of periodic LTV systems by calculating the Floquet exponents, as shown in section 5.5.2 for second-order variational equations.

5.7 Conclusions

The linear time-varying approach was shown to be a good modeling for low-level analysis/synthesis. Using the linear time-varying small-signal model, deviations from the intended large-signal behaviour, due to internally generated noise and in dynamic behaviour can be modeled and the resulting performance degradation can be determined. It can reduce model complexity by only modeling these deviations. It makes explicit use of the knowledge of large-signal behaviour obtained in the high-level synthesis/analysis step, by using it to define the input-signal dependent dynamic bias trajectory. This enables the incorporation of signal-dependent behaviour in the analysis and synthesis of nonlinear circuits.

The linear time-varying approach generalizes the linear small-signal modeling approach (used in conventional linear design methodologies), by describing the behaviour of a nonlinear circuit in the neighbourhood of an (input-signal dependent) *dynamic bias trajectory* rather than a (DC-input dependent) *bias point*. For this, the approach uses a linear time-varying model, in which the input signals and resulting dynamic bias trajectory are implicitly present. The linear time-varying small-signal model is obtained by linearizing the behaviour of the nonlinear circuit in its signal-dependent dynamic bias trajectory. This modeling approach is exact, despite of the (time-varying) linearization involved, because the next point in the linearization is determined by the signal-dependent dynamic bias-trajectory, which incorporates the large-signal behaviour of the nonlinearities in the time-evolution of the state variables. The only limitation is that the influence of deviations on the signal dependent bias-trajectory is neglected. Therefore, circuits in which the behaviour is dominantly changed by small deviations (e.g. chaotic circuits) can not be handled.

The derivation of the linear time-varying small-signal model (also called the variational equation) was given, and also the special case of linear time-invariant small-signal models and linear time-invariant circuits was treated. It was shown how deviations in instantaneous behaviour, internally generated noise and deviation in dynamic behaviour can be incorporated in the LTV small-signal model. The determination of the dynamic behaviour of the state-variables from the homogeneous variational equation, and its description in terms of time-domain modes, is the first and most important step in any analysis using the LTV small-signal model. Any subsequent analysis of the effect of deviations in instantaneous behaviour and of internally generated noise from the nonhomogeneous variational equation uses these results: the same time-domain modes are present in the small-signal and noise expressions derived from the nonhomogeneous variational equation. Therefore, the rest of this thesis will focus on the description of the dynamic behaviour of a circuit using the time-domain modes of the homogeneous variational equation.

For linear systems with constant coefficients these time-domain modes were

shown to be defined by the eigenvalues and eigenvectors of the constant state-transition matrix \mathbf{A} . The solutions are stable if all eigenvalues have a negative real part. This property is well-known from the familiar frequency domain description of LTI systems: the solutions are stable if all poles have negative real part, and these poles equal the eigenvalues of \mathbf{A} . For linear systems with periodic coefficients the modes are defined by periodic eigenvectors and Floquet exponents. The solutions are stable if all Floquet exponents have negative real parts, and the Floquet exponents of an LTI system equal the eigenvalues of \mathbf{A} . For linear systems with arbitrary time-varying coefficients the modes are defined by dynamic eigenvalues and eigenvectors, which can be obtained from a generalized characteristic equation. When the coefficients are slowly-varying, a frozen time approach can be used and quasi-static eigenvalues and eigenvectors are obtained. The solutions of a general LTV system are stable if the Lyapunov exponents of all its modes are negative. This stability criterion based on Lyapunov exponents was shown to simplify to the stability criterion based on Floquet exponents for periodic LTV systems and to the stability criterion based on poles for LTI systems.

In the last sections of this chapter the concept of dynamic eigenvalues and eigenvectors, and stability analysis using Lyapunov and Floquet exponents, was applied to the variational equation for nonlinear circuits exhibiting first-order and second-order dynamic behaviour, respectively. For first-order variational equations the dynamic eigenvalue was obtained easily. For second-order variational equations a method was shown which uses the solution of a Riccati differential equation in order to derive the dynamic eigenvalues. In the following chapters these results are applied to three example nonlinear circuits: a limiter, a dynamic translinear circuit and a class-B amplifier.

6

The linear time-varying approach applied to a negative-feedback class-B output amplifier

In this chapter we apply the linear time-varying approach to the design of an example nonlinear circuit: a negative-feedback amplifier with a class-B output stage [47]. First we discuss the general configuration of a negative-feedback amplifier and motivate the choice of a class-B output stage. Then we analyze the output class-B stage of this amplifier separately. For this we can use a linear time-varying model with first-order dynamic behaviour (“one time-constant”). We give a description of this output stage and deduce the first-order nonlinear differential equation which describes its dynamic behavior. Then we will solve the differential equation for a periodic input signal to obtain the signal-dependent bias trajectory of the stage. We will use the linear time-varying small-signal model to obtain the dynamic eigenvalue of the stage and calculate the Floquet exponent to determine the stability of the periodic solution. Finally the output class-B stage is used in the design of a complete class-B amplifier, and the behaviour of this amplifier is analyzed using a linear time-varying model with second-order dynamics.

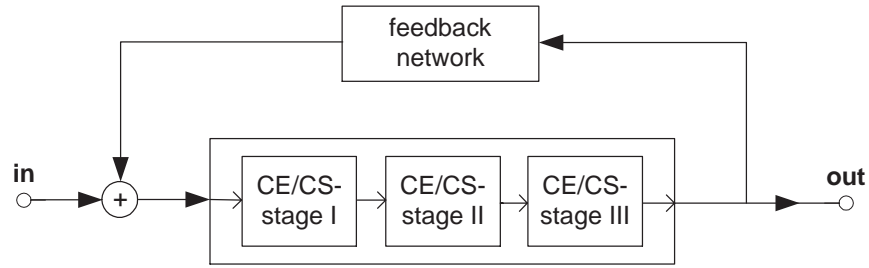


Figure 6.1: Basic configuration of a negative-feedback amplifier

6.1 Negative-feedback amplifiers and class-B output stages

In this chapter the linear time-varying approach is used in the design of an input-output linear negative-feedback amplifier. Though the intended overall transfer is linear, an LTV small-signal model is necessary in order to be able to incorporate the effect of a strongly nonlinear output stage on the dynamic behaviour.

Generally, two main functions can be distinguished in a negative-feedback amplifier (see Figure 6.1). In the forward path of the negative-feedback loop, amplifying stages realize sufficient loopgain. In the feedback path, a feedback network determines the overall transfer. For an intended linear input-output transfer of the negative-feedback amplifier, the feedback network needs to be linear. The amplifying stages in the forward path, however, are intrinsically nonlinear.

In order to contribute maximally to the loopgain for a given bias current consumption, the amplifying stages should be chosen to be CE-stages (or equivalently CS-stages in a CMOS design)[39]. Conventionally, these CE-stages are class-A biased: the bias current is large with respect to the signal current. This enables the use of an LTI-model of the nonlinear CE-stage in the biaspoint, and greatly simplifies the design. This approach has the drawback that only a small part of the current consumed by the amplifier is actually used as signal current. This waist of power is becoming more and more problematic in present-day battery-driven low-power applications. Especially the output-stage, which has to drive the load, often needs to have an unacceptably high bias current when class-A biased. Therefore, most present-day amplifiers use class-AB biased output CE-stages, which have a quiescent current that can be significantly smaller than the maximal output current.

The ultimate low-power choice is the use of a class-B output CE-stage. Such a stage has zero quiescent current and all current consumed is used as signal

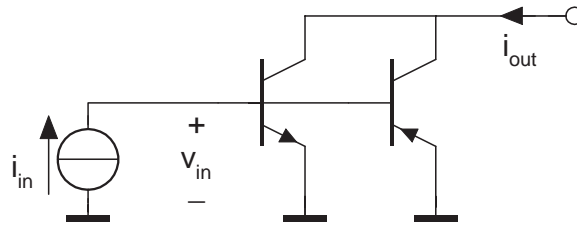


Figure 6.2: Simple push-pull class-B stage (signal diagram)

current. A class-B biased stage, however, is strongly nonlinear. This does not need to be a problem for the overall input-output transfer, since with sufficient loopgain this transfer is determined by the linear feedback network. It does, however, necessitate the incorporation of nonlinear effects in the design of the amplifier. In the next sections we first analyze a simple push-pull class-B output stage separately, using the LTV approach to describe its dynamic behaviour. Then this output stage is applied in a low-power low-voltage negative-feedback amplifier.

6.2 Class-B output stage

The main source of nonlinear dynamic effects in our example, a negative-feedback class-B output amplifier, is the class-B output stage. Therefore, this output stage is first analyzed separately. In the subsequent section the class-B output stage is applied in a low-power negative-feedback amplifier.

6.2.1 Circuit description

The main source of nonlinearity in our example circuit is the simple push-pull class-B output stage. It consists of an NPN and PNP bipolar transistor connected in parallel for the signal, as depicted in figure 6.2. The PNP and NPN transistors are considered to have similar parameters. The stage is excited by the current source i_{in} and we will examine the dynamic behavior of the stage in terms of the output current i_{out} . The transistors are not biased at a quiescent current, so we obtain an exponential-type relation between input voltage v_{in} and output current i_{out} for positive and negative input currents.

For describing the bipolar transistors, we use the relevant part of the Gummel-Poon model [17]. Both transistors are used in the forward region (collector-base junction is reverse biased), such that reverse parameters can be neglected. Second-order effects such as leakage currents, Early effect and high-level injection are also neglected. The transistors are excited by a current source and the

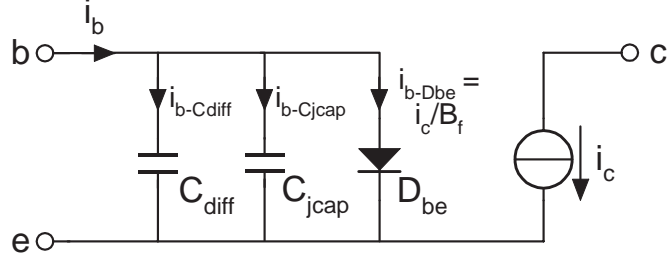


Figure 6.3: Simplified Gummel-Poon model for a single transistor

output current is sensed, so the ohmic resistance in series with base, emitter and collector have no effect.

With these simplifications we end up with a transistor model in which we can distinguish three main effects (see figure 6.3):

1. the instantaneous transfer from intrinsic base-emitter voltage to collector current, which is modeled by the base-emitter diode D_{be} and a controlled current source i_c ;
2. the effect of charge storage in the base-emitter depletion region, which is modeled by the junction capacitor C_{jcap} ;
3. the effect of charge storage in the base region, which is modeled by the diffusion capacitor C_{diff} .

D_{be} , C_{diff} and C_{jcap} all contribute to the base current i_b , whereas the collector current i_c is determined by the controlled current source. This model is used to analyze the instantaneous behaviour and the dynamic behaviour (due to the presence of junction capacitors and diffusion capacitors) of the entire push-pull class-B stage.

Instantaneous behaviour We first analyze the instantaneous behavior of the entire stage. For the instantaneous behaviour, only the base-emitter diodes D_{be} of the NPN and PNP transistor contribute a current i_{b-Dbe} to the total base current, which equals i_{in} . So, we obtain the following relations between output current i_{out} , input voltage v_{in} and instantaneous input current i_{in-Dbe} :

$$i_{out} = I_s \left(e^{\frac{v_{in}}{V_T}} - e^{-\frac{v_{in}}{V_T}} \right) = 2I_s \sinh\left(\frac{v_{in}}{V_T}\right) \quad (6.1)$$

$$i_{in-Dbe} = \frac{I_s}{B_f} \left(e^{\frac{v_{in}}{V_T}} - e^{-\frac{v_{in}}{V_T}} \right) = \frac{i_{out}}{B_f} \quad (6.2)$$

Here I_s is the transport saturation current and B_f the current-gain factor of the transistors (which are assumed to be equal for NPN and PNP transistors) and V_T the thermal voltage.

Diffusion capacitors The diffusion capacitors contribute a current $i_{in-C_{diff}}$ to the total base current which equals

$$i_{in-C_{diff}} = \tau_f \cdot \frac{di_{out}}{dt} \quad (6.3)$$

Here τ_f is the forward transit time of the transistors.

Junction capacitors The junction capacitors contribute a current $i_{in-C_{jcap}}$ to the input current, which can be derived as follows:

$$Q_{jcap} = C_{jcap}(v_{in}) \cdot v_{in} \quad \Leftrightarrow \quad (6.4)$$

$$i_{in-C_{jcap}} = \frac{dQ_{jcap}}{dt} = \left[C_{jcap}(v_{in}) + v_{in} \frac{\partial C_{jcap}(v_{in})}{\partial v_{in}} \right] \frac{dv_{in}}{dt} \quad (6.5)$$

Here $C_{jcap}(v_{in})$ equals the sum of the junction capacitors of both transistors as function of v_{in} . If we approximate the junction capacitors by a constant capacitor C , equal to $C_{jcap}(0)$, and use (6.1) we get

$$i_{in-C_{jcap}} = \frac{C V_T}{\sqrt{i_{out}^2 + 4I_s^2}} \cdot \frac{di_{out}}{dt} \quad (6.6)$$

Total behaviour The total base current i_{in} equals the sum of the instantaneous input current and the currents flowing into the diffusion and junction capacitors. Therefore, we can add equations (6.2), (6.3) and (6.6) to obtain the total input current i_{in} as function of i_{out}

$$i_{in} = \frac{i_{out}}{B_f} + \left(\tau_f + \frac{C V_T}{\sqrt{i_{out}^2 + 4I_s^2}} \right) \cdot \frac{di_{out}}{dt} \quad (6.7)$$

Note that we have used the following notational conventions. DC-variables (e.g. the transport saturation current I_s) are written in capital letters and large-signal variables (e.g. v_{in} , i_{in} and i_{out}) are written in small letters. In large-signal variables the time-dependency is not explicitly included, i.e. $v_{in} = v_{in}(t)$, $i_{in} = i_{in}(t)$ and $i_{out} = i_{out}(t)$.

6.2.2 Model division

The complete behaviour of the class-B push-pull stage is described by the differential equation (6.7). From this differential equation the linear time-varying

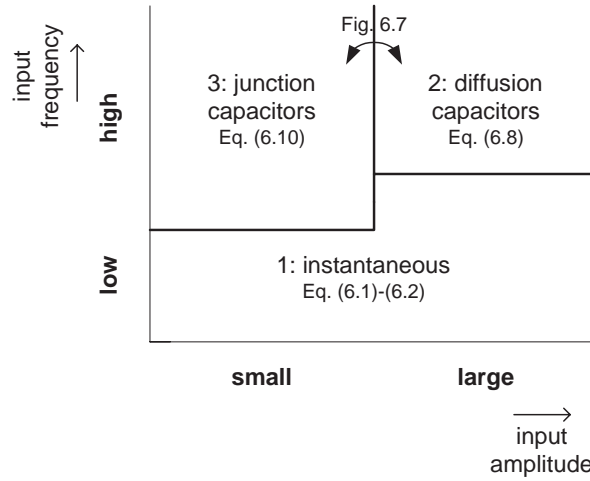


Figure 6.4: Regions of operation of the class-B output stage

model, Equation (6.21), can be derived, as shown later in Section 6.2.4. General results for the dynamic bias-trajectory, dynamic eigenvalue and Floquet exponent can be obtained by numerical evaluations based on these differential equations.

However, to get more insight in the operation of the circuit we try to obtain analytical solutions of equations (6.7) and (6.21). To keep the nonlinear calculus manageable, we consider three regions of operation of the class-B output stage, as shown in Figure 6.4:

1. low frequency input signal;
2. high frequency, large amplitude input signal;
3. high frequency, small amplitude input signal.

For relatively *low frequencies* the stage behaves instantaneously as given by (6.1) and (6.2). For relatively *high frequencies and large amplitudes* of the input current the diffusion capacitors dominate the behaviour and we can ignore the influence of the junction capacitors. For relatively *high frequencies and small amplitudes* the junction capacitors dominate and we can ignore the influence of the diffusion capacitors. The models in the latter two regions are derived in the next section. They are given by equations (6.10) and (6.12), respectively. The boundary amplitude between regions 2 and 3 is also derived and shown in Figure 6.7.

In subsequent sections an approximated dynamic bias trajectory and LTV small-signal model is derived for the three regions. These approximations are

parameter	value
I_s	$18\mu A$
B_f	117
τ_f	$22ps$
$C_{jcap}(0)$	$46fF$

Table 6.1: Transistor parameters of the DIMES-01 process

checked by numerical evaluations (with MATLAB using variable order Runge-Kutta formulas [29]) of the complete nonlinear differential equation (6.7) and of the complete variational equation (6.21). The results are found to be in good agreement.

6.2.3 Dynamic bias trajectory

The first step in analyzing the nonlinear differential equation (6.7) using the linear time-varying approach consists of finding a time-varying bias trajectory as a function of the deterministic part of the input signal (see Section 5.1.1). We choose the sinusoidal input signal $i_{in} = I_A \sin(\omega t)$, which makes it easy to compare the results with frequency-domain LTI results. We rewrite Equation (6.7) into the standard state-space format

$$\frac{di_{out}}{dt} = f(i_{out}, i_{in}, t) = \frac{-\frac{i_{out}}{B_f} + I_A \sin(\omega t)}{\frac{C V_T}{\sqrt{i_{out}^2 + 4I_s^2}} + \tau_f} \quad (6.8)$$

In the following paragraphs an approximated bias trajectory is calculated for the three regions of operation of the class-B stage depicted in Figure 6.4. Further the boundary between region 2 (high frequencies and large amplitudes) and region 3 (high frequencies and small amplitudes) is determined. These approximations are checked by a numerical evaluation (with MATLAB using variable order Runge-Kutta formulas [29]) of the original differential equation (6.8) and the results are in good agreement. The transistor parameters used are summarized in table 6.1, these are the parameters of our in-house DIMES-01 process [38].

Instantaneous behaviour For low frequencies (region 1 in Figure 6.4) the stage behaves instantaneously. We can ignore the influence of both the junction capacitors and diffusion capacitors in Equation (6.8). That is, we can substitute $C = 0$ and $\tau_f = 0$ and obtain

$$i_{out} = B_f \cdot I_A \sin(\omega t) \quad (6.9)$$

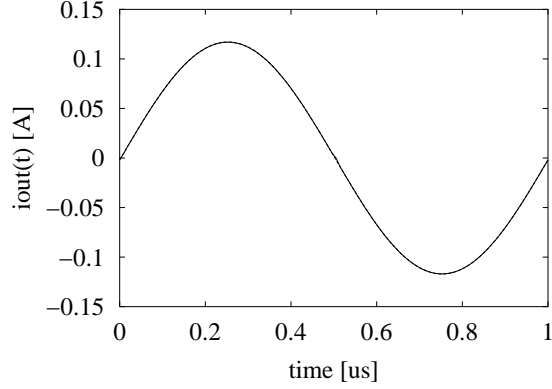


Figure 6.5: Numerically evaluated (solid line) and approximated (dotted line) dynamic bias trajectory $i_{out_b}(t)$ as function of time t for one period of the input signal ($I_A = 1\text{mA}$, $f = 1\text{MHz}$, C_{diff} dominates). The difference can not be seen.

The output current i_{out} simply equals the current gain factor B_f times the input current i_{in} and we needn't analyze this case any further.

Diffusion capacitors If the input current has large amplitude (region 2 in Figure 6.4), we can ignore the influence of the junction capacitors in Equation (6.8). That is, we can substitute $C = 0$ and obtain a linear differential equation for the output current i_{out} :

$$\frac{di_{out}}{dt} = -\frac{i_{out}}{B_f \tau_f} + \frac{I_A \sin(\omega t)}{\tau_f} \quad (6.10)$$

This equation can be solved using standard linear analysis, and we obtain a steady-state dynamic bias trajectory

$$i_{out_b}(t) = \frac{I_A B_f}{\sqrt{1 + \omega^2 B_f^2 \tau_f^2}} \sin[\omega t - \arctan(\omega B_f \tau_f)] \quad (6.11)$$

In this equation we recognize the amplitude and phase of the familiar frequency-domain transfer function for Equation (6.10). In this region of operation the dynamic bias trajectory resulting from the sinusoidal input $I_A \sin(\omega t)$ is again a sinusoid, with amplitude and phase corresponding to a pole at $-\frac{1}{B_f \tau_f}$.

In order to compare the approximated dynamic bias trajectory (6.11) with the dynamic bias trajectory obtained by numerical evaluation of the complete state-space description (6.8), we have plotted both together in Figure 6.5 for an

input frequency $f = 1\text{MHz}$ and input amplitude $I_A = 1\text{mA}$. We can observe that the approximated dynamic bias trajectory (dotted line) is virtually identical to the numerically calculated dynamic bias trajectory (solid line). Only in the zero-transitions of the output signal a small deviation occurs (one has to zoom in order to see this). This is to be expected, since for the zero-crossings the magnitude of i_{out} is small and the influence of the junction capacitors can not be ignored.

Junction capacitors For small amplitudes of the input current (region 3 in Figure 6.4) we can ignore the influence of the diffusion capacitors ($\tau_f = 0$) and we obtain the nonlinear differential equation

$$\frac{di_{out}}{dt} = \left[-\frac{i_{out}}{B_f} + I_A \sin(\omega t) \right] \frac{\sqrt{i_{out}^2 + 4I_s^2}}{C V_T}. \quad (6.12)$$

This equation has no explicit solution. For relatively high frequencies the instantaneous term can be ignored ($i_{out}/B_f \ll I_A \sin(\omega t)$) and we can further simplify the nonlinear differential equation to

$$\frac{di_{out}}{dt} = \frac{I_A \sin(\omega t) \sqrt{i_{out}^2 + 4I_s^2}}{C V_T}. \quad (6.13)$$

We can use the method of separation of variables to solve this differential equation:

$$\begin{aligned} \frac{di_{out}}{\sqrt{i_{out}^2 + 4I_s^2}} &= \frac{I_A \sin(\omega t)}{C V_T} dt && \Leftrightarrow \\ d \operatorname{arcsinh} \left(\frac{i_{out}}{2I_s} \right) &= \frac{I_A \sin(\omega t)}{C V_T} dt && \Leftrightarrow \\ \operatorname{arcsinh} \left(\frac{i_{out}}{2I_s} \right) &= -\frac{I_A \cos(\omega t)}{C V_T \omega} + C_1 && \Leftrightarrow \\ i_{out}(t) &= 2I_s \sinh \left(-\frac{I_A \cos(\omega t)}{C V_T \omega} + C_1 \right) \end{aligned}$$

For high frequencies the integration constant C_1 will equal zero (v_{in} and i_{out} contain no DC-terms), so we obtain the dynamic bias trajectory

$$i_{out_i}(t) = 2I_s \sinh \left(-\frac{I_A \cos(\omega t)}{C V_T \omega} \right) \quad (6.14)$$

A plot of this approximated dynamic bias trajectory, together with the dynamic bias trajectory obtained by numerical evaluation of Equation (6.8), is given in Figure 6.6 for an input frequency $f = 1\text{MHz}$ and input amplitude $I_A = 0.1\mu\text{A}$.

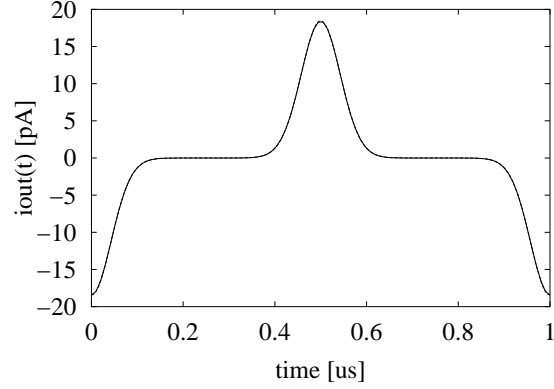


Figure 6.6: Numerically evaluated (solid line) and approximated (dotted line) dynamic bias trajectory $i_{out_b}(t)$ as function of time t for one period of the input signal ($I_A = 0.1\mu\text{A}$, $f = 1\text{MHz}$, C_{jcap} dominates). The difference can not be seen.

Again the approximated dynamic bias trajectory (dotted line) is virtually identical to the numerically calculated one (solid line). The sinh-response to the sinusoidal input signal is clearly visible. Indeed the instantaneous input current $i_{out}/B_f \ll I_A \sin(\omega t)$.

For very small input amplitudes ($I_A \ll 2I_s$) we can apply another simplification: for such amplitudes the nonlinear functions in the differential equation (6.12) can be approximated accurately by a first-order Taylor approximation. This yields the following linear differential equation:

$$\frac{di_{out}}{dt} = -\frac{i_{out}}{\frac{B_f(CV_T + 2I_s\tau_f)}{2I_s}} + \frac{I_A \sin(\omega t)}{\frac{CV_T + 2I_s\tau_f}{2I_s}} \quad (6.15)$$

In this equation (with $2I_s\tau_f \ll CV_T$) we recognize the linear pole $-\frac{2I_s}{B_fCV_T}$. The very small signal amplitudes necessary for this approximation are unsuitable for practical use. However, the linear pole obtained does give a limiting value for the Floquet exponent for very small input amplitudes, as we will shortly see.

Boundary between regions 2 and 3 In order to find the boundary between region 2 and region 3 we need to determine what constitutes a “small” amplitude and what constitutes a “large” amplitude. To this aim we compare the maximum amplitude of the approximated dynamic bias trajectories for diffusion capacitors and junction capacitors found in the previous two paragraphs, as a function of the input frequency and amplitude.

For junction capacitors the maximum amplitude (see Equation (6.14)) is obtained when $\cos(\omega t) = 1$ and is given by:

$$I_{out_{max}-Cjcap}(\omega, I_A) = 2I_s \sinh\left(\frac{I_A}{C V_T \omega}\right) \quad (6.16)$$

Due to the exponential behaviour present in the sinh-response, this maximum amplitude increases very fast as a function of the input amplitude. For instance, for $f = 1\text{MHz}$ we get $C V_T \omega = 7.2 \cdot 10^{-9}$. For the maximum amplitude to increase by a factor of 10 the input amplitude I_A only has to increase by $C V_T \omega \ln(10) = 16.6\text{nA}$.

For diffusion capacitors the maximum amplitude (see Equation (6.11)) is given by:

$$I_{out_{max}-Cdiff}(\omega, I_A) = \frac{I_A B_f}{\sqrt{1 + \omega^2 B_f^2 \tau_f^2}} \quad (6.17)$$

This maximum amplitude is proportional to I_A .

The junction capacitors dominate if the maximum amplitude as given by Equation (6.16) is smaller than the maximum amplitude as given by Equation (6.17). This corresponds to a situation in which virtually all input signal current flows through the junction capacitors. If $I_{out_{max}-Cjcap}(\omega, I_A)$ becomes comparable in size to $I_{out_{max}-Cdiff}(\omega, I_A)$, the diffusion capacitors will start taking most of the input signal current, and they will start dominating the behaviour. Due to the exponential increase of $I_{out_{max}-Cjcap}(\omega, I_A)$ as function of I_A , versus the linear increase of $I_{out_{max}-Cdiff}(\omega, I_A)$, this transition will be quite abrupt.

For the boundary between large and small input amplitudes it is assumed that the two maximum amplitudes are equal. To obtain the boundary amplitude I_{Ab} the following implicit equation needs to be solved:

$$\begin{aligned} I_{out_{max}-Cjcap}(\omega, I_{Ab}) &= I_{out_{max}-Cdiff}(\omega, I_{Ab}) && \Leftrightarrow \\ 2I_s \sinh\left(\frac{I_{Ab}}{C V_T \omega}\right) &= \frac{I_{Ab} B_f}{\sqrt{1 + \omega^2 B_f^2 \tau_f^2}} && (6.18) \end{aligned}$$

For high frequencies $\omega \gg 1/B_f \tau_f$ (that is, frequencies above the diffusion capacitors related pole) we can simplify this boundary condition to:

$$\sinh\left(\frac{1}{C V_T} \frac{I_{Ab}}{\omega}\right) = \frac{1}{2I_s \tau_f} \frac{I_{Ab}}{\omega} \quad \Leftrightarrow \quad (6.19)$$

$$\sinh\left(\frac{1}{C V_T} \cdot k\right) = \frac{1}{2I_s \tau_f} \cdot k \quad (6.20)$$

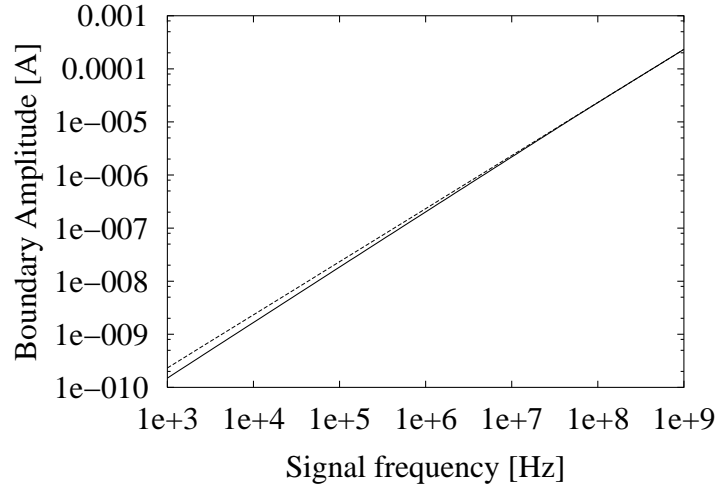


Figure 6.7: Boundary amplitude between junction capacitor and diffusion capacitor domination as function of the input frequency f (dotted line: general solution, solid line: high-frequency approximation)

with $I_{Ab} = k \cdot \omega$. So, for these frequencies we expect the boundary amplitude to be proportional to frequency. For the transistor parameters summarized in Table 6.1 solving the implicit equation (6.20) results in a proportionality constant $k = 3.7 \cdot 10^{-14}$. A plot of this approximated relation between boundary amplitude and frequency is depicted by the solid line in Figure 6.7. A numerical solution of the complete implicit equation (6.18) as a function of the input signal frequency is given by the dotted line in Figure 6.7. Even though the condition for the high frequency approximation equals $f \gg 1/2\pi B_f \tau_f = 62\text{MHz}$, we see that for lower frequencies the boundary amplitude is only slightly higher than predicted by the proportionality constant k . For a signal frequency of 1kHz the deviation is only about 56%.

6.2.4 Linear time-varying small-signal model

As explained in Section 5.4, we can examine the stability of a dynamic bias trajectory of a first-order nonlinear system by determining the eigenvalue of the variational equation (5.70). In the general case we obtain the homogeneous variational equation for the class-B stage of figure 6.2 from its state-space de-

scription (6.8):

$$\frac{di_{out}}{dt} = a_{i_{out_b}}(t) \cdot i_{out} \quad (6.21)$$

with

$$\begin{aligned} a_{i_{out_b}}(t) &= \left. \frac{\partial f(i_{out}, i_{in}, t)}{\partial i_{out}} \right|_{i_{out}=i_{out_b}, i_{in}=I_A \sin(\omega t)} \\ &= \frac{-1}{B_f \left(\frac{C V_T}{\sqrt{i_{out_b}^2 + 4I_s^2}} + \tau_f \right)} \\ &+ \frac{\left(-\frac{i_{out_b}}{B_f} + I_A \sin(\omega t) \right) C V_T i_{out_b}}{\left(\frac{C V_T}{\sqrt{i_{out_b}^2 + 4I_s^2}} + \tau_f \right)^2 (i_{out_b}^2 + 4I_s^2)^{\frac{3}{2}}} \end{aligned} \quad (6.22)$$

The dynamic eigenvalue simply equals $a_{i_{out_b}}(t)$.

For the three regions of operation of the class-B stage, we can simplify the homogeneous variational equation by using the approximated differential equations which we also used to obtain approximated dynamic bias trajectories. In the instantaneous region of operation as given by Equation (6.9), the differential equation degenerates to an algebraic equation and the concept of dynamic eigenvalue and Floquet exponent has no meaning. For the region of operation where the diffusion capacitors dominate (large signal amplitudes) and for the region of operation where the junction capacitors dominate (small signal amplitude) we can derive simplified expressions for the variational equation and dynamic eigenvalue. In the following paragraphs we will give these expressions and compare them to numerically calculated results using the complete state-space description (6.8) and variational equation (6.21)

Dynamic eigenvalue for diffusion-capacitor dominance For large input currents and high frequency the diffusion capacitors dominate and the state-space description can be simplified to the linear equation (6.10). From this approximated state-space description we can derive the following expression for the variational equation:

$$\frac{di_{out}}{dt} = -\frac{1}{B_f \tau_f} \cdot i_{out}. \quad (6.23)$$

This variational equation is again linear and has the constant dynamic eigenvalue $\lambda(t) = -\frac{1}{B_f \tau_f}$, which equals the conventional linear pole of this linear equation.

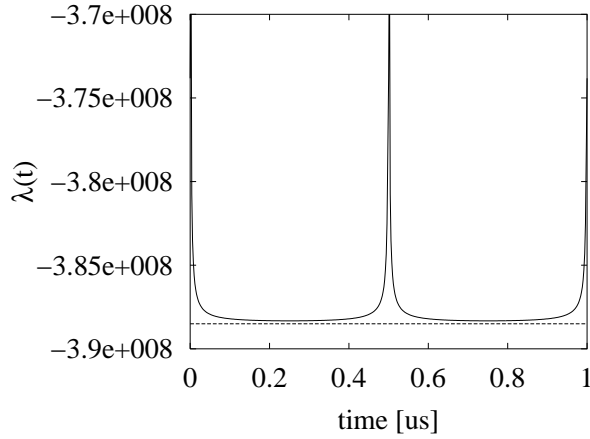


Figure 6.8: Exact (solid line) and approximated (dotted line) dynamic eigenvalue λ as function of time t for one period of the input signal ($I_A = 1\text{mA}$, $f = 1\text{MHz}$, diffusion-capacitor dominance)

In order to compare this approximated result with the complete description in equations (6.8) and (6.21), we use a numerically calculated bias trajectory using Equation (6.8) (with MATLAB using variable order Runge-Kutta formulas [29]). We have used an input signal with an amplitude I_A of 1mA and a frequency f of 1MHz ($\omega = 2\pi f$). The approximated and numerically calculated dynamic bias trajectory for this input signal were shown in Figure 6.5.

The numerically calculated dynamic bias trajectory was used in Equation (6.22) to compute the dynamic eigenvalue for large input currents. The resulting exact dynamic eigenvalue as function of time t for one period of the input signal is shown as the solid line in figure 6.8. We have also plotted the approximated eigenvalue $-\frac{1}{B_f \tau_f} = -3.88 \cdot 10^{-8}$, depicted by the dotted line. We see that during most of the period the eigenvalue is constant and almost equal to the approximated eigenvalue. The dynamic eigenvalue deviates from the linear pole for the zero-crossings of the input signal ($t = 0, 0.5\mu\text{s}$ and $1\mu\text{s}$) only, since for small currents the junction capacitors can no longer be neglected.

Dynamic eigenvalue for junction-capacitor dominance For small input amplitudes the junction capacitors dominate and we can use the simplified state-space description (6.13). From this approximated state-space description we can

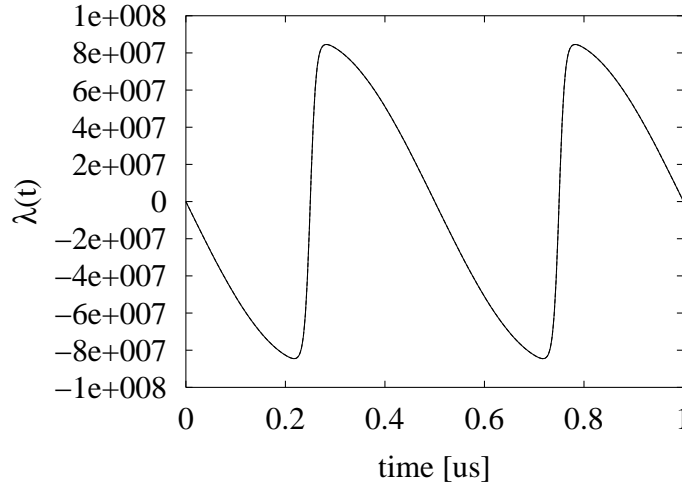


Figure 6.9: Exact (solid line) and approximated (dotted line, indistinguishable) dynamic eigenvalue λ as a function of time t for one period of the input signal ($I_A = 0.1\mu\text{A}$, $f = 1\text{MHz}$, junction-capacitor dominance)

derive the following variational equation:

$$\frac{di_{out}}{dt} = \frac{I_A \sin(\omega t) i_{out_b}}{C V_T \sqrt{i_{out_b}^2 + 4I_s^2}} \cdot i_{out}. \quad (6.24)$$

The dynamic eigenvalue is given by

$$\lambda(t) = \frac{I_A \sin(\omega t) i_{out_b}(t)}{C V_T \sqrt{i_{out_b}(t)^2 + 4I_s^2}} \quad (6.25)$$

Using the approximated dynamic bias trajectory $i_{out_b}(t)$ given by Expression (6.14) we obtain:

$$\lambda(t) = \frac{I_A \sin(\omega t)}{C V_T} \tanh\left(-\frac{I_A \cos(\omega t)}{C V_T \omega}\right) \quad (6.26)$$

As before, we use a numerically calculated bias trajectory using the complete state-space description (6.8) in order to verify this approximated result. For an input amplitude I_A of $.1\mu\text{A}$ and a frequency f of 1MHz we obtain an exact and approximated dynamic bias trajectory as shown in Figure 6.6.

The numerically calculated bias trajectory is inserted in Equation (6.22) to compute the dynamic eigenvalue for small input currents. We obtain an

exact dynamic eigenvalue as shown by the solid line in figure 6.9. This dynamic eigenvalue is indistinguishable from the approximated dynamic eigenvalue given by Equation (6.26) and depicted by the dotted line in figure 6.9. From the figure we see that in this case the dynamic eigenvalue is strongly varying with time. It even has a positive value for almost half of the period.

In this case the dynamic eigenvalue is not easily related to a pole following from linear analysis: using a frozen time approach we would get a pole which is always negative, since it would be determined by the differential input resistance and input capacitance of the stage, which are always positive. We see that for strongly nonlinear systems the dynamic eigenvalue is very different from the classic linear pole.

For very small input amplitudes ($I_A \ll 2I_s$) we can use the linearized state-space description (6.15). This linearized state-space description results in the linear variational equation

$$\frac{di_{out}}{dt} = -\frac{2I_s}{B_f(CV_T + 2I_s\tau_f)} \cdot i_{out}. \quad (6.27)$$

From this linear equation we obtain the constant dynamic eigenvalue or linear pole (with $2I_s\tau_f \ll CV_T$) $-\frac{2I_s}{B_fCV_T} = -2.68 \cdot 10^{-4}$. In the next section we will see again this linear pole as an asymptote of the Floquet exponent for small input amplitudes.

6.2.5 Floquet exponent

As explained in Section 5.4.2 the stability properties of a first-order nonlinear system in the vicinity of a periodic dynamic bias trajectory are characterized by its Floquet exponent β , as given by Equation (5.77). For the class-B stage the Floquet-exponent β equals

$$\beta = \frac{1}{T} \int_0^T \lambda(\tau) d\tau = \frac{1}{T} \int_0^T a_{i_{out_b}}(t)(\tau) d\tau \quad (6.28)$$

in which $a_{i_{out_b}}(t)$ is given by Equation (6.23) and in which $T = 2\pi/\omega$ is the period of the dynamic eigenvalue of the stage.

Floquet exponent for diffusion-capacitor dominance If the numerically calculated dynamic bias trajectory for $I_A = 1\text{mA}$ and $f = 1\text{MHz}$ (large signal amplitude) is used in Equation (6.28), we obtain a Floquet exponent β of $-3.878 \cdot 10^8$. This is almost equal to the linear pole $1/B_f\tau_f$ of $-3.885 \cdot 10^8$ following from the approximated variational equation for diffusion capacitors (6.23). This is to be expected, since the Floquet exponents are identical to system poles for linear systems, and the dynamic eigenvalue for this input signal only deviates from the linear pole in the zero-crossings of the input signal (as shown in Figure 6.8).

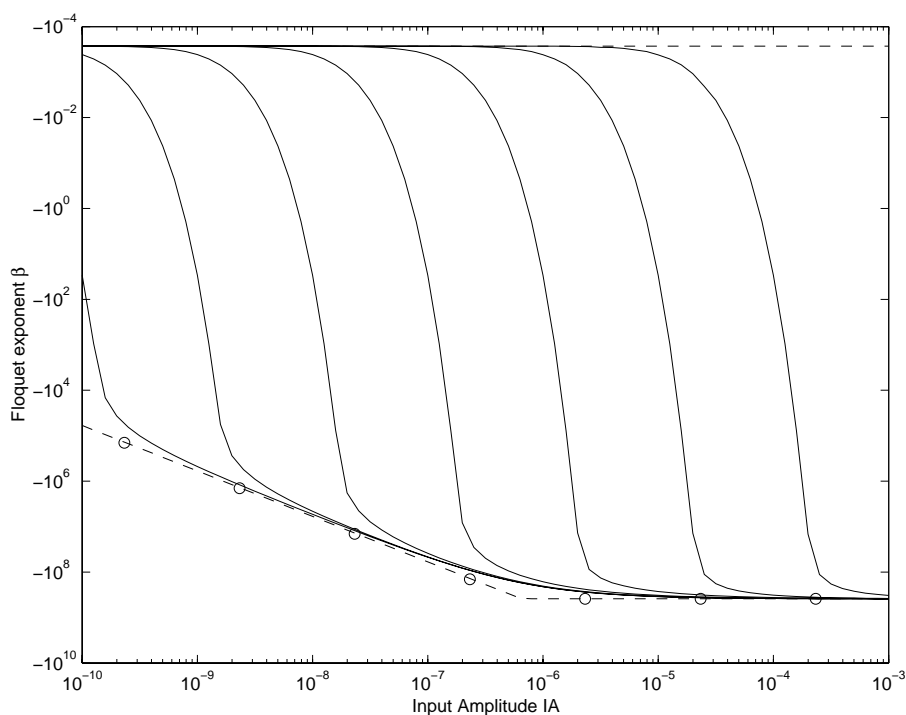


Figure 6.10: Floquet exponent β as function of the amplitude I_A of the input signal ($f = 1\text{kHz}$ to 1GHz , in decades, from left to right)

Floquet exponent for junction-capacitor dominance If we use the numerically calculated dynamic bias trajectory for $I_A = .1\mu\text{A}$ and $f = 1\text{MHz}$ (small signal amplitude) in Equation (6.28), we obtain a Floquet exponent β of -29.7 . Since β is negative we conclude that the dynamic bias trajectory is stable, even though the corresponding dynamic eigenvalue has a positive value for almost half of the period (see Figure 6.9).

For very small input amplitudes ($I_A \ll 2I_s$) we obtained the linear variational equation (6.27). From this linear equation we obtain a Floquet exponent β equal to the (now) constant dynamic eigenvalue $-\frac{2I_s}{B_f C V_T} = -2.68 \cdot 10^{-4}$.

Floquet exponent for a wide operating range In order to characterize the stability properties of the push-pull class-B stage for a wide range of input amplitudes and frequencies, the Floquet exponent was calculated as function of the input amplitude (0.1nA to 1mA) for input frequencies ranging from 1kHz to 1GHz . The results are shown in Figure 6.10.

We see that for increasing input amplitudes the Floquet exponent approaches an asymptote, depicted by the lower dotted line in Figure 6.10. The rightmost horizontal part of this asymptote (for $I_A > 0.5\mu\text{A}$) is given by the linear pole $-1/B_f\tau_f$, as predicted by the diffusion approximation. The leftmost sloping part of this asymptote did not follow from the approximations in the previous sections. The Floquet exponent in this region is determined by the dynamic bias trajectory and dynamic eigenvalue corresponding to the complete nonlinear differential equation for junction capacitors (including the instantaneous part), as given by Equation (6.12). We did not succeed in deriving an analytical solution for this differential equation. The asymptote, however, is seen to be very similar to the transit frequency curve of a bipolar transistor and indeed is quite accurately predicted by the expression

$$\frac{1}{B_f \cdot \frac{V_T}{I_{c_{rms}}} \cdot C} = \frac{1}{B_f \cdot \frac{V_T}{B_f I_A / \sqrt{2}} \cdot C}.$$

In this expression we recognize the LTI input pole of a CE-stage for the region in which the junction capacitor dominates ($1/(B_f r_e C)$), with the collector bias current $I_{c_{bias}}$ given by the current gain factor B_f times the root-mean-square input amplitude $I_A/\sqrt{2}$. Thus the total lower asymptote is given by ω_T/B_f , in which ω_T is the transit-frequency of the bipolar transistors assuming that their collector bias current equals their root-mean-square collector current.

For decreasing input amplitudes the Floquet exponent approaches another asymptote, depicted by the top horizontal dotted line in Figure 6.10. This asymptote is given by the linear pole $-\frac{2I_s}{B_f C V_T} = -2.68 \cdot 10^{-4}$, as predicted by the junction approximation for very small input amplitudes. The Floquet exponent varies fast as a function of input amplitude in the transition region between these two asymptotes. The input amplitude for which the Floquet exponent start deviating from the diffusion approximation is predicted quite accurately by the boundary amplitude given in Figure 6.7, as indicated by the circles in Figure 6.10.

6.3 Application of a class-B output-stage in a negative-feedback amplifier

In this section we apply the class-B stage, that we have studied in detail in the previous section, as output-stage in a negative-feedback amplifier. As discussed in section 6.1, such a class-B output stage is the ultimate low-power choice. Low power is an important design constraint in many fields of application. Especially in the field of the portable communication electronics it is a key issue. Here the application is a completely integrated Long-Wave receiver which is as small as

a Walkman earphone. The radio needs to operate at supply voltages of 1.5 V down to 1 V (power supply is a single battery).

This section deals with the design of the output amplifier of this receiver. Negative feedback is applied to keep the distortion due to the class-B stage at an acceptable level.

The next section gives the specifications of the output amplifier. Section 6.3.2 describes the basic configuration of the amplifier at the level of nullors [6]. The class-B implementation of the nullor is treated in section 6.3.3. The dynamics of the circuit are evaluated by means of the linear time-varying approach in section 6.3.4. Auxiliary circuitry required for the amplifier implementation are presented in section 6.3.5. Finally, measurement results of the built amplifier are given in section 6.3.6.

6.3.1 Specification

Load specifications For the load of the receiver a piezoelectric transducer is chosen [7] for reasons of low power consumption and the relatively ease by which a fully integrated amplifier can be realized.

Ideally, current driving should be used for a piezoelectric element to have the most accurate relation between the signal and the sound [39]. However, here is chosen for voltage driving as in that case the power which can be supplied to the load is maximal over the complete frequency range of interest.

The resulting high pass behavior of the transducer is not a problem in this application.

Source and amplifier specifications The source for the amplifier can be represented by a current source with an impedance of 2 M Ω in parallel with 0.25 pF (the output impedance of the detector driving the output amplifier). The maximum input signal current supplied by the detector is 25 μ A. The power-supply voltage is minimally 1 V and thus the maximum output amplitude can be 0.5 V for a single sided setup. Consequently, the transfer should be 20 k Ω for the given maximum input current. In order to increase the maximum sound pressure further, we chose to use a balanced configuration. Correspondingly, the maximum differential output amplitude equals 1 V.

The intention is to integrate the complete LW-receiver in the bipolar DIMES01 process [38]. Experiments were done with breadboard components of the L422 process of Philips.

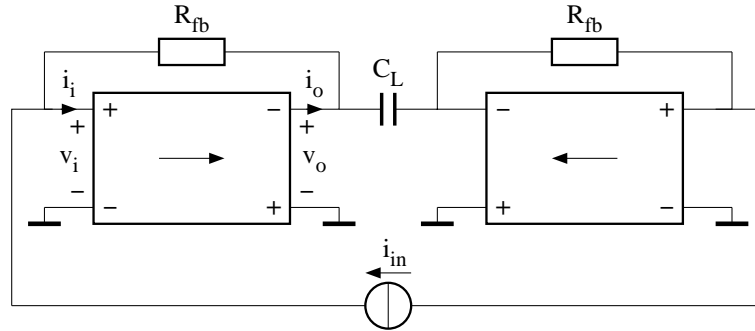
A summary of the specifications is given in table 6.2.

6.3.2 The basic configuration

In figure 6.11, the basic configuration of the balanced transimpedance amplifier is depicted. As both parts are independent of each other it suffices to evaluate

Source impedance	2 M Ω // 0.25 pF
Load impedance	14 nF
Max. output voltage amplitude	1 V
Max. output current amplitude	1 mA
Max. Input current amplitude	25 μ A
Transfer	40 k Ω
Bandwidth	> 7 kHz
Power-supply voltage	1-1.5 V

Table 6.2: Summary of the specifications for the output amplifier.

**Figure 6.11:** The basic configuration of the transimpedance amplifier with load capacitance C_L and feedback resistor R_{fb} .

only one side of the amplifier. In the remainder of this chapter this assumption is used, unless stated otherwise.

The nullors [6] can be seen as ideal amplifying elements, i.e. they have infinite bandwidth and infinite gain. In that case the transfer is set by the feedback resistors (R_{fb}) which thus need to be chosen 20 k Ω each. The nullors should be implemented by realistic devices such that the nullor conditions ($i_i = 0$, $v_i = 0$) are met as closely as required.

6.3.3 Class-B implementation

As a first step in the implementation we chose to use one CE stage as nullor implementation [39], [49]. For low power consumption, we should try to minimize all currents in the circuit which carry no signal information. For this design that means that we chose to use a class-B biased CE stage. To be able to sink and source currents, an NPN and a PNP device connected in parallel are required.

By examining the transfer of the resulting amplifier, it is found that for relatively small input currents the nullor contains a dead zone and the direct

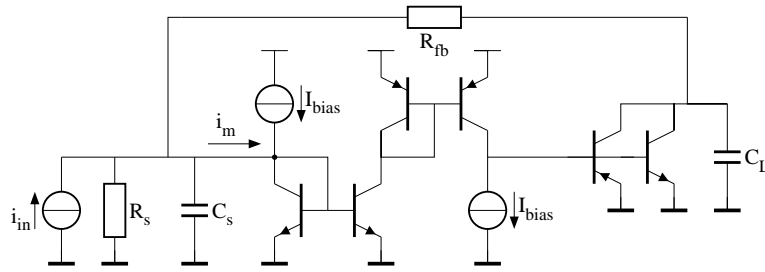


Figure 6.12: The signal diagram of the amplifier extended with two current mirrors for lowering the input impedance of the nullor implementation.

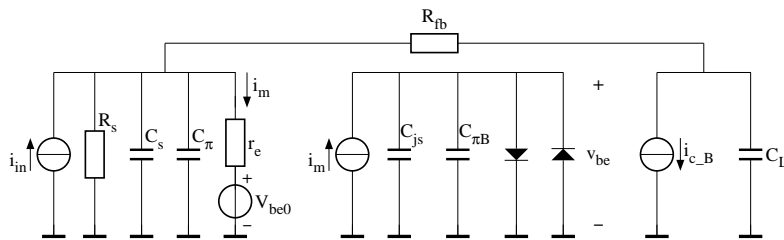


Figure 6.13: Simplified signal diagram of the amplifier, the current mirror is replaced by its LTI model.

transfer dominates. The reason for this phenomenon is that for relatively small signals the input impedance of the class-B stage is a lot higher (transistors are only slightly conducting) than the impedance of the feedback resistor and thus the feedback loop is broken.

To solve this problem, the input impedance of the nullor implementation is lowered by a current follower, preceding the class-B stage. In this design the current follower is implemented by means of a current mirror (see Figure 6.12). A second current mirror is required to maintain a negative loop gain. Both current mirrors are class-A biased, in order to maintain low input impedance for small signal currents. As the signal currents in the current mirror are relatively low, the bias current can be kept as low as $10 \mu\text{A}$. In the figure R_s and C_s are the source resistance and source capacitance, respectively and i_m is the signal flowing into the current mirror.

In figure 6.13 a simplified signal diagram of the circuit is depicted. Since the current mirrors are class-A biased, we can replace them by their LTI-model. The input resistance and capacitance of the first mirror are depicted by r_e (equal to $1/g_m$) and C_π , respectively. The output capacitance of the second mirror is depicted by C_{js} and its output current is represented by the controlled current source i_m . For the class-B output stage LTI-modeling is not possible. In order to

accurately model its dynamic behaviour, its nonlinearity should be incorporated in the signal model.

6.3.4 Stability analysis of the amplifier

The simplified signal diagram of figure 6.13 is used to analyze the dynamic behavior of the negative-feedback class-B output amplifier. The source capacitance and the capacitance of the current mirror can be ignored as the corresponding time constant $\tau \approx r_e(C_s + C_\pi)$ is small compared with the dynamics of the class-B stage and the load.

The input capacitance of the class-B stage, ($C_{\pi B}$) consists of a diffusion and a junction capacitance. The dynamics of the class-B stage are only relevant for relatively small currents, as for relatively high currents the load capacitance dominates the dynamic behaviour. Therefore, it suffices to take only the junction capacitance of the class-B stage into account. The following second-order state-space description models the dynamic behaviour of the amplifier:

$$\frac{dv_{out}(t)}{dt} = \frac{1}{C_L} \cdot \left[\frac{r_e \cdot i_{in}(t) - v_{out}(t)}{R_{fb} + r_e} - 2I_s \cdot \sinh\left(\frac{v_{be2}(t)}{V_T}\right) \right] \quad (6.29)$$

$$\frac{dv_{be2}(t)}{dt} = \frac{1}{C_{\pi B}} \cdot \left[\frac{R_{fb} \cdot i_{in}(t) + v_{out}(t)}{R_{fb} + r_e} - \frac{2I_s}{\beta} \cdot \sinh\left(\frac{v_{be2}(t)}{V_T}\right) \right] \quad (6.30)$$

The sinh-terms are a result of the presence of the class-B stage. The first step in analyzing the nonlinear differential equation (6.29)-(6.30) using the linear time-varying approach consists of finding a dynamic bias trajectory as a function of the deterministic part of the input signal (see section 5.1.1). We choose the sinusoidal input current $i_{in}(t) = I_A \sin(\omega t)$. The dynamic bias trajectory, $v_{out_b}(t), v_{be2_b}(t)$, is found by numerical evaluation of (6.29)-(6.30) for this input signal, using Mathcad [30].

As explained in Section 5.5, we can examine the stability of a dynamic bias trajectory of a second-order nonlinear system by determining the eigenvalues of the variational equation (5.78). For this we need to solve the Riccati differential equation (5.80). In this case, i_{in} is a sinusoid, an explicit solution does not exist. Therefore, the Riccati differential equation is solved numerically using Mathcad [30]. These calculations suffer from singularities in the solution of the Riccati equation. Therefore, the integral transformation as described in Appendix C is applied.

In figure 6.14 the two resulting eigenvalues are depicted for an input amplitude I_A of $10\mu\text{A}$ and an input frequency f of 1 kHz. The Floquet exponents

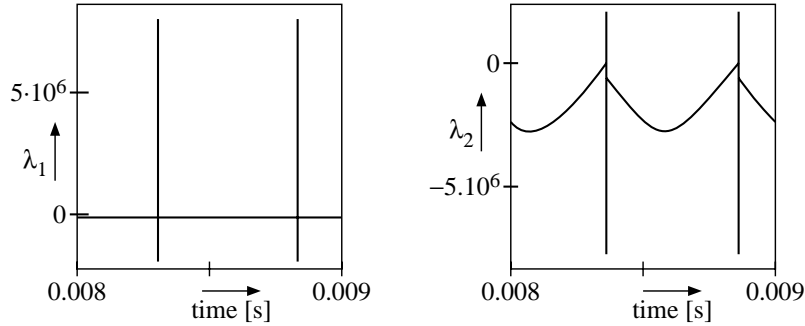


Figure 6.14: The dynamic eigenvalues, λ_1 [Hz] and λ_2 [Hz], as a function of time, for a sinusoidal input signal ($I_A = 10\mu\text{A}$, $f = 1\text{kHz}$).

are found from the eigenvalues by averaging them over one period:

$$\beta_1 = \frac{1}{T} \int_t^{t+T} \lambda_1(\tau) d\tau = -22 \text{ kHz} \quad (6.31)$$

$$\beta_2 = \frac{1}{T} \int_t^{t+T} \lambda_2(\tau) d\tau = -1.6 \text{ MHz} \quad (6.32)$$

The first eigenvalue is due to the dynamics of the load capacitance in combination with the current mirrors, whereas the second eigenvalue is due to the class-B stage. As could be expected, the first dynamic eigenvalue is constant for the main part of the period (the mirrors are class-A biased) whereas the dynamic eigenvalue of the class-B stage varies strongly with the input signal. At the zero crossings of the signal the class-B eigenvalue approaches zero, as a result the systems eigenvalue corresponding to the dynamics of the current mirror approaches zero too and even becomes positive. This is caused by the fact that the loop dynamics become very slow. However, the real part of both Floquet exponents are negative and thus the amplifier is stable for the corresponding input signal.

6.3.5 Implementation of the auxiliary circuitry

For the implementation of the amplifier, auxiliary circuitry is required. The NPN and PNP cannot be connected directly in parallel. At least the emitters have to be at different potentials to be able to sink and source currents. In this design the emitters are connected to the corresponding supply lines, see figure 6.15 (Q_1 - Q_4). For the minimum power-supply voltage of 1V no additional circuitry is required, because in the absence of signal both base-emitter voltages are about 0.5 V and thus hardly any collector current flows, i.e. they are approximately class-B biased. In the case of 1.5 V power-supply voltage,

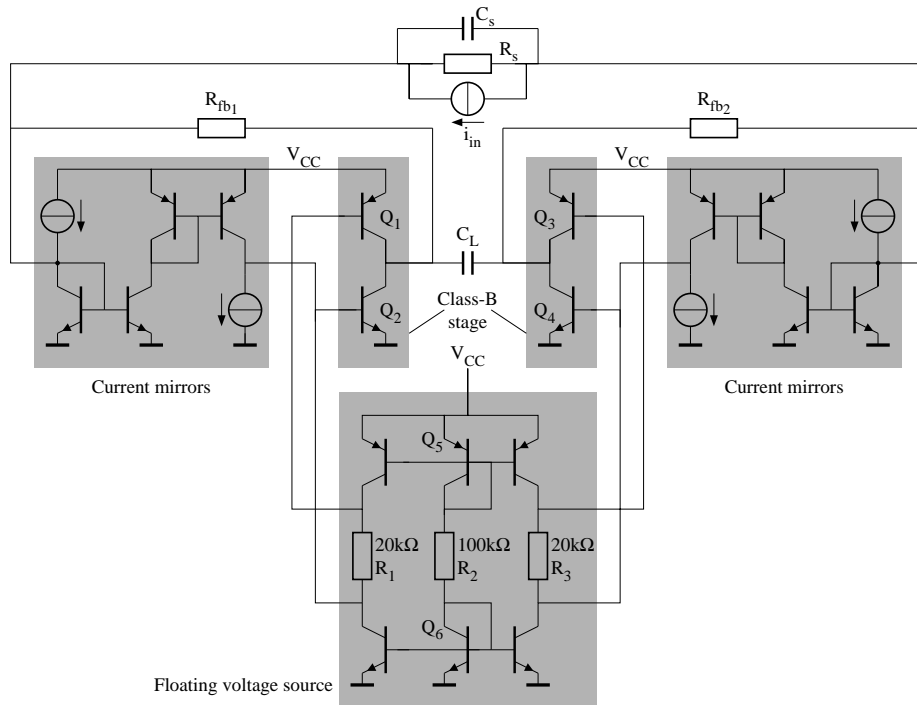


Figure 6.15: The total circuit diagram of the differential amplifier with a class-B output stage.

however, a considerable quiescent current would flow. This can be counteracted by putting a voltage source between both base terminals such that the total available voltage for the sum of the two base-emitter voltages is low enough that both transistors can be assumed to be switched off. This implies that the voltage source needs to be a function of the power-supply voltage. However, it does not need to be a very specific function, since there is not the requirement for a very specific relation between the two collector currents of the transistors, as is the case for class-AB biasing. The complete circuit diagram is depicted in figure 6.15. The level shifts between the N- and P-devices are implemented by the dashed block called "Floating voltage source". With Q_5 , Q_6 and R_2 a supply-voltage-dependent current is generated. This current is mirrored through R_1 and R_3 resulting in the required floating voltage sources. In this case the minimum current through the class-B stage is given by the current flowing through resistor R_2 . The bias currents required for the current mirrors are derived from a conventional PTAT source in a straightforward way (the PTAT source is not depicted here).

6.3.6 Measurement results

The circuit has been built on a PCB with breadboard components of the L422 process of Philips. In figure 6.16 the transfer of the amplifier is depicted as a function of frequency with the amplitude of the input current as a parameter. For the measurement a single sided amplifier was used for reasons of simplifying

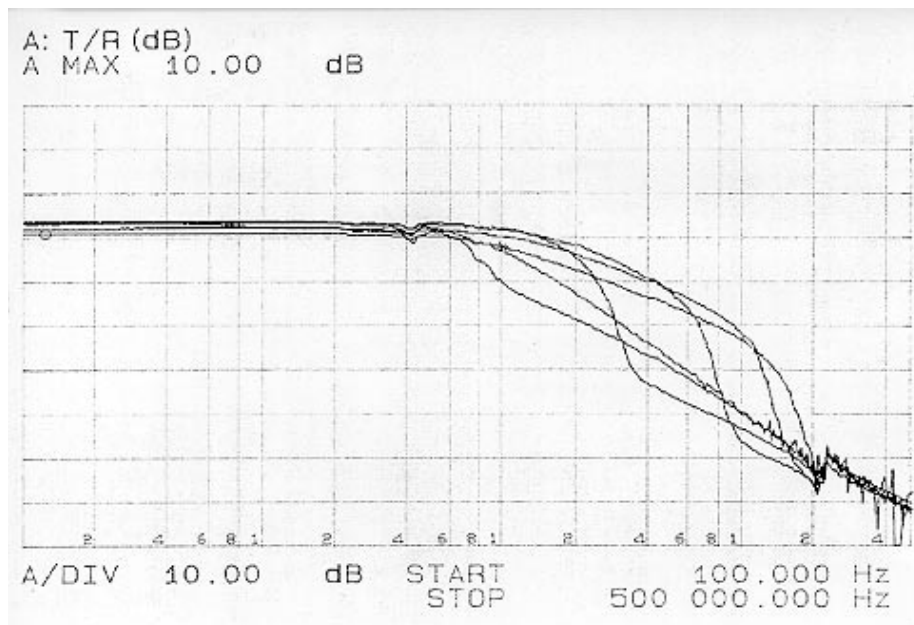


Figure 6.16: The transfer [y-axis 10dB/dev] of the amplifier as a function of the frequency [100 Hz - 1 MHz] with the amplitude of the input current as a parameter [from top to bottom 20, 10, 5, 2, 0.5, 0.1 μA].

the measurement setup. The supply voltage was set to 0.8 V to be able to assume that the class-B stage is completely off at zero crossings of the signal. At a supply voltage of 1.2 V the quiescent current through the class-B stage is about 30 μA . This is a consequence of the implementation of the floating voltage source. For higher supply voltages the voltage available for the series connection of the two class-B base-emitter junctions is relatively large, i.e. a considerable current, in terms of class-B biasing, flows.

The bandwidth of the transfer is about 20 kHz for the larger input currents. This bandwidth is comparable to the Floquet exponent which was calculated. For increasing input frequency, the transfer first decreases very fast and then levels out to a 20dB/decade slope. This can be explained with reference to the results obtained for the class-B stage separately. If the junction capacitors

Max. output current amplitude	1 mA
Max. output voltage amp. @ $V_{sup}=1.2$ V	0.5 V
Power supply voltage	0.8 V - 1.5 V
DC-current consumption	40 μ A - 110 μ A
Transfer	20 k Ω
Bandwidth(i_{in})	7 kHz - 18 kHz
Distortion @ maximum signal	$\approx 3\%$
Distortion @ signal < 10 μ A	< 1%

Table 6.3: The summarized measurement results for a single-sided amplifier.

dominate the behaviour of the class-B stage, the output amplitude and the Floquet exponent of the class-B stage decrease rapidly as a function of frequency. As a consequence, the loopgain and overall transfer decrease rapidly, until the direct transfer (open-loop transfer) of the amplifier starts dominating.

In the transfer a dip at 4 kHz can be seen. This results from the impedance of the piezoelectric transducer [7], the same holds for the peak at about 200 kHz.

Distortion measurements were performed at a supply voltage of 1.2 V. At the maximum output signal (amplitude = 0.5 V, single sided), the distortion is about 3 %. For lower amplitudes the distortion is below 1 %.

In table 6.3 the results are summarized for the single sided amplifier.

6.4 Conclusions

In this chapter we applied the linear time-varying approach to the design of a negative-feedback amplifier with class-B output stage. Though the intended transfer is linear, an LTV small-signal model is necessary in order to be able to incorporate the effect of the strongly nonlinear class-B output stage on the dynamic behaviour.

The class-B output stage was chosen because it is the ultimate low-power choice: all current consumed by this stage is used as signal current. A class-B biased stage, however, is strongly nonlinear. This does not need to be a problem for the overall input-output transfer, since with sufficient loopgain this transfer is determined by the linear feedback network. It does, however, necessitate the incorporation of nonlinear effects in the design of the amplifier.

Since the main source of nonlinear effect in the negative-feedback class-B output amplifier is the class-B output stage, we first analyzed this push-pull class-B output stage separately. We considered three regions of operation of the class-B stage. For relatively low frequencies the stage behaves instantaneously. For relatively high frequencies and large signal amplitudes, the dynamic behaviour is dominated by the diffusion capacitor. For relatively high frequencies

and small signal amplitudes, the dynamic behaviour is dominated by the junction capacitors.

By the division in three regions of operation, we were able to find some explicit expressions for the dynamic bias trajectory, dynamic eigenvalue and Floquet exponent of the class-B stage. The approximated results were compared with exact results, obtained using numerical evaluation of the complete nonlinear differential equation and corresponding variational equation, and the results were found to be in good agreement. We were able to generate a plot of the Floquet exponent versus the input signal amplitude, for various input signal frequencies, in which we were able to give explicit expressions for the asymptotes. This enables a fast evaluation of the dynamic behaviour of the class-B stage.

The push-pull class-B output stage was applied in a low-voltage low-power balanced transimpedance amplifier, designed and evaluated for a piezoelectric transducer (14 nF).

For examining the dynamic behavior, the linear time-varying approach was used. From this model the dynamic eigenvalues and the corresponding Floquet exponents were calculated.

The measured bandwidth of the built amplifier was comparable with the calculated Floquet exponents. An intuitive explanation of the transfer characteristics versus frequency could be given, using the knowledge of the class-B stage dynamic behaviour.

The realized amplifier functions properly for power-supply voltages in the range of 0.8 V to 1.5 V. The corresponding DC current consumption varies from 40 μA to 110 μA . This variation is mainly a result of the implementation of the level shift between the two sides of the class-B stage. The minimum of 40 μA is consumed by the current mirrors. Implementing the current follower by means of a CB-stage can reduce this by a factor of two. Adding an additional class-B stage can even reduce its current consumption to a few μAs .

The linear time-varying approach applied to dynamic translinear circuits

In this chapter we apply the linear time-varying approach to analyze the dynamic behaviour of dynamic translinear circuits. Dynamic translinear (DTL) circuits, also known as log-domain or exponential state-space circuits, constitute a class of circuits in which a nonlinear relation, being the exponent input-output relation of the bipolar transistor (or the MOS transistor in its weak inversion regime), is used as primitive for synthesis [1], [31], [43]. These circuits are based on the so-called "dynamic translinear principle" [34], a generalization of the well-known "static translinear principle" (TL) [18]. Whereas conventional TL circuits can be used to implement various linear and nonlinear *instantaneous* input-output relations, DTL circuits implement a wide variety of *dynamic* input-output relations, described by differential equations. Both linear differential equations, e.g. filters [14], [40], [44], and nonlinear differential equations, e.g. oscillators [41], [45], adaptive filters [15], PLL's [46],[48] and RMS-DC converters [16], [34] can be realized.

High-level synthesis/analysis methods are available for DTL circuits [9], [12], [13], [32], [40]. These current design approaches for DTL circuits generally only incorporate the ideal behaviour of the transistor. If parasitic parameters are considered at all, only instantaneous parasitic effects are included, e.g. finite current gain factors for the employed transistors [28]. By lack of a suitable modelling method, the effect of parasitic capacitances has not yet been rigorously incorporated. The same holds for the nonlinear analysis of noise in DTL circuits. Methods that account for the nonlinear and nonstationary properties of noise

in DTL circuits [33], to date are still based on the ideal dynamic translinear relations and do not cover parasitic effects.

DTL synthesis and analysis are based on the nonlinear input-output relation of the transistor. Therefore, the system behaviour in the presence of parasitics is often defined by nonlinear differential equations, even if the ideal overall transfer function is linear. In this chapter we use the LTV approach for handling these nonlinear differential equations for the low-level analysis/synthesis of two example DTL circuits: a first-order DTL filter [25] and a DTL oscillator [8].

First we give, in Section 7.1, a short overview of the underlying principles of both static and dynamic translinear circuits. Then, in Section 7.2, a linear first-order DTL filter (described by a linear first-order differential equation) is introduced by applying DTL synthesis. The linear time-varying approach is applied to analyze its dynamic behaviour in the presence of parasitic capacitances. The quasi-static approach and LTI-approach are also applied, in order to compare the quasi-static eigenvalue and LTI pole with the dynamic eigenvalue and show their limitations. In Section 7.3 a DTL oscillator (described by a nonlinear second-order differential equation) is introduced by applying DTL synthesis and the LTV approach is used to describe its dynamic behaviour. This example is chosen because the nonlinearity in the differential equation describing this circuit is not a consequence of parasitic effects, but rather a conscious design choice. The quasi-static and LTI approach can not be applied to this circuit, due to its inherent nonlinearity. However, the results of the LTV approach are found to match the stability properties reported in [10], which were obtained using an alternative method. Finally, in Section 7.4, the results are summarized and conclusions are drawn.

7.1 Static and dynamic translinear circuits

Translinear (TL) circuits can be divided into two major groups: static [18] and dynamic [32] translinear circuits. The first group can be used to realize a wide variety of linear and nonlinear instantaneous input-output relations. Differential equations, both linear and nonlinear, can be implemented by the second group. In this section we review the underlying principle of both static and dynamic translinear circuits.

7.1.1 The static translinear principle

The bipolar transistor (and analogously the MOS transistor in its weak inversion regime) has a well-defined exponential relation between the base-emitter voltage and the collector current over a large range of currents. This relationship has been adopted as a primitive for the synthesis of electronic circuits. The input-output relation of the bipolar transistor in its forward regime of operation can

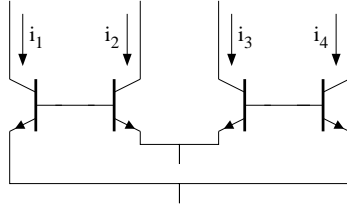


Figure 7.1: A four transistor translinear loop

be written as

$$i_c = I_s \left(e^{\frac{v_{be}}{V_T}} - 1 \right) \Leftrightarrow v_{be} = V_T \ln \left(\frac{i_c}{I_s} + 1 \right) \quad (7.1)$$

in which i_c , I_s , v_{be} , V_T are the collector current, the saturation current, the base-emitter voltage and the thermal voltage kT/q , respectively. Here the -1 and $+1$ terms, respectively, can be neglected in the forward regime of operation.

The TL principle applies to loops with an even number of base-emitter voltages. The number of devices with a clockwise orientation equals the number of counter-clockwise oriented devices. An example of a loop with four base-emitter voltages is given in Figure 7.1. If we assume the transistors to have equal emitter areas and the devices to operate at the same temperature (i.e. we assume equal saturation currents and thermal voltages), then the following relation results:

$$i_1 \cdot i_3 = i_2 \cdot i_4 \quad (7.2)$$

where i_1 , i_2 , i_3 and i_4 are the collector currents of the respective transistors. This generic equation is the basis for a wide variety of instantaneous input-output relations, which are theoretically temperature and process independent.

7.1.2 The dynamic translinear principle

In order to implement differential equations the static translinear principle can be extended by adding capacitors in the TL loop [32]. The DTL principle can be explained with reference to the circuit shown in Figure 7.2. The circuit is described in terms of the collector current i_c and the capacitance current i_{cap} , flowing through the capacitance C . An expression for i_{cap} can be derived with the help of Equation (7.1):

$$i_{cap} = C \cdot V_T \cdot \frac{di_c}{i_c} \quad (7.3)$$

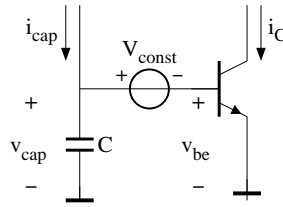


Figure 7.2: Basic structure of DTL circuits

Equation (7.3) shows that i_{cap} is a nonlinear function of i_c and its time derivative di_c/dt . Slightly rewritten we obtain:

$$C \cdot V_T \cdot \frac{di_c}{dt} = i_{cap} \cdot i_c. \quad (7.4)$$

This equation is representative for the DTL principle: *a time derivative of a current can be mapped onto a product of currents*. This allows us to map a differential equation onto a multivariable polynomial of currents.

7.2 The linear time-varying approach applied to a first-order dynamic translinear filter

In this section we introduce a linear first-order DTL filter by applying DTL synthesis. The circuit topology is extended in order to eliminate the influence of most of the parasitic capacitors. Only one dominant parasitic capacitor remains. We apply the linear time-varying approach to analyze the dynamic behaviour of the DTL filter in the presence of this remaining parasitic capacitor [25]. For this we derive a first-order variational equation, and determine its dynamic eigenvalue and Floquet exponent, using the theory described in Section 5.4. The quasi-static approach (see Section 5.3.4) and LTI approach (see Section 5.1.2) are also applied in order to compare the quasi-static eigenvalue and LTI pole with the dynamic eigenvalue. This comparison clearly shows the limitations of the quasi-static and LTI approach.

7.2.1 DTL synthesis and circuit description

A linear first-order filter can be described by the following dimensionless linear differential equation:

$$\frac{dy}{d\tau} + y = x \quad (7.5)$$

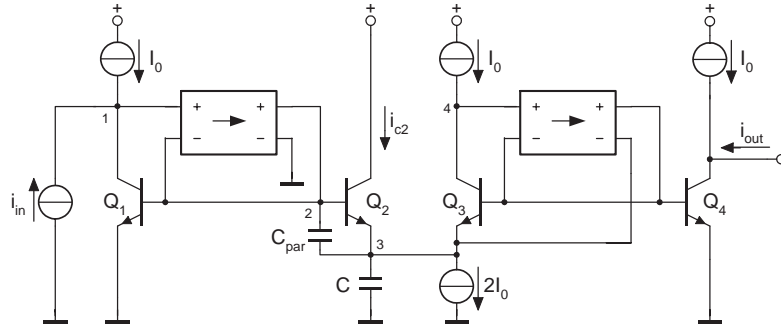


Figure 7.4: Modified linear first-order DTL filter

to supply the base-currents of the four transistors in the translinear loop we add two nullors [6]. These are ideal network elements that adjust their output current and voltage in order to nullify their input voltage and current (they can be visualized as ideal OPAMPs). In this way the influence of most of the parasitic capacitances and of finite current gain of the transistors can be made negligible. The resulting circuit is shown in Figure 7.4. Only the influence of C_{par} (the base-emitter capacitance of transistor Q_2) can not be counteracted by proper circuit design. Therefore, its influence on the circuit HF behaviour is further analyzed.

7.2.2 The linear time-invariant and quasi-static approach

We first analyze the DTL filter in Figure 7.4 by using a linear time-invariant small-signal model. Then we apply the quasi-static approach, by assuming that the bias point and as a consequence also the parameters of the small-signal model are instantaneously signal dependent.

The LTI approach

In the LTI approach (see Section 5.1.2) we assume the signals to be small compared to the DC bias currents. The circuit is linearized in its DC bias point by replacing the transistors with simplified hybrid- π models. After applying the nullor conditions we obtain the LTI small-signal model of Figure 7.5. In this figure i_{in} and i_{out} are the input and output current (which are assumed to be small), i_{c1} and i_{c2} are the small-signal collector currents of transistors Q_1 and Q_2 , g_{m1} , g_{m2} and g_{m4} are the transconductance of transistors Q_1 , Q_2 and Q_4 , C is the external capacitor and C_{par} is the base-emitter capacitance of transistor Q_2 .

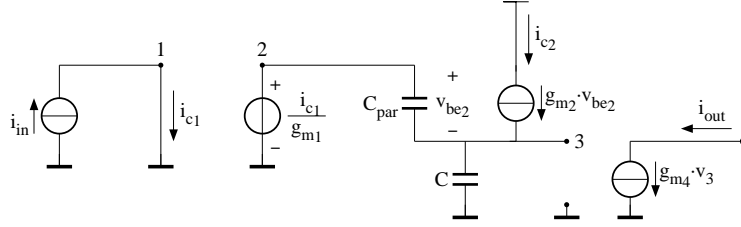


Figure 7.5: LTI small-signal model of the modified DTL filter

The input-output relation in the Laplace domain is given by:

$$\frac{I_{out}(s)}{I_{in}(s)} = \frac{g_{m4}}{g_{m1}} \cdot \frac{1 + s \frac{C_{par}}{g_{m2}}}{1 + s \frac{C + C_{par}}{g_{m2}}} \quad (7.9)$$

The pole of the system equals:

$$p = -\frac{g_{m2}}{C + C_{par}} = -\frac{I_0}{V_T(C + C_{par})} \triangleq -\frac{I_0}{\alpha + \beta} \quad (7.10)$$

where $\alpha = V_T C$ and $\beta = V_T C_{par}$. Note that the cut-off frequency is reduced due to the parasitic capacitor (compare with (7.8)) and that a zero appears at $z = -I_0/\beta$. The LTI approach gives us a first idea for the circuit behaviour, but it can not be applied for large input signals.

The quasi-static approach

We drop the assumption that the signals should be small compared with the bias currents, but suppose the signals to be slowly varying. Then we can apply the quasi-static approach (see Section 5.3.4) by substituting the bias point of the LTI small-signal model by a signal dependent bias trajectory. We obtain

$$\frac{I_{out}(s)}{I_{in}(s)} = \frac{g_{m4}[i_{out}(t) + I_0]}{g_{m1}[i_{in}(t) + I_0]} \cdot \frac{1 + s \frac{C_{par}}{g_{m2}[i_{c2}(t)]}}{1 + s \frac{C + C_{par}}{g_{m2}[i_{c2}(t)]}} \quad (7.11)$$

Since the parameter C_{par} is a junction capacitor it is virtually current independent. The time-varying quasi-static eigenvalue $\lambda_{qs}(t)$ or, equivalently, the time-varying pole $p(t)$ of the system equals:

$$\lambda_{qs}(t) = p(t) = -\frac{i_{c2}(t)}{\alpha + \beta} \quad (7.12)$$

Note that this pole varies with time if the large-signal current $i_{c2}(t)$ varies with time. This is the case even if $\beta = 0$, which corresponds to a parasitic capacitor C_{par} equal to zero.

7.2.3 The linear time-varying approach

If the slowly varying condition is dropped then the QS approach is not applicable. In that case only the LTV approach is a consistent generalization of the LTI small-signal model. We will now apply the LTV approach to the first-order DTL filter under consideration.

The state-space description

We use the Ebers-Moll large-signal model of the bipolar transistor to find the nonlinear differential equation describing the circuit behaviour. By applying Kirchhoffs current law at node 3 of Figure 7.4 and using the translinear loop equation we obtain:

$$-i_{c2} - \beta \frac{di_{c2}}{i_{c2}} + \alpha \frac{di_{out}}{i_{out} + I_0} + 2I_0 - I_0 = 0 \quad (7.13)$$

$$i_{c2} \cdot (i_{out} + I_0) = (i_{in} + I_0) \cdot I_0 \quad (7.14)$$

By substituting Equation (7.14) into Equation (7.13) and choosing i_{out} as the state-variable we arrive at the following state-space description:

$$\frac{dx}{dt} = f(x, u) \quad x = i_{out} \quad u = i_{in} \quad (7.15)$$

$$f(x, u) = \frac{1}{\alpha + \beta} \left[\left(\frac{\beta \dot{u}}{u + I_0} - I_0 \right) \cdot x + u I_0 + \frac{\beta \dot{u} I_0}{u + I_0} \right]$$

which is a linear time-varying differential equation.

The dynamic bias trajectory

In order to find the dynamic bias trajectory we need to specify the input signal. We choose the following sinusoidal input signal:

$$u_b = I_0 \xi \sin(\omega_s t) \quad (7.16)$$

where I_0 is the bias current, ξ is the modulation depth ($\xi \in [0, 1]$) and ω_s is the radial frequency.

The dynamic bias trajectory $x_b(t)$ equals the solution of the state-space description (7.15) for the chosen input signal $u_b = I_0 \xi \sin(\omega_s t)$. This is a first-order linear time-varying differential equation and in this special case we can

find the following analytical expression for the dynamic bias trajectory:

$$x_b(t) = [1 + \xi \sin(\omega_s t)]^{\frac{\beta}{\alpha+\beta}} e^{-\frac{I_0}{\alpha+\beta} t} I_0 \times \left\{ I_0 + \frac{I_0}{\alpha + \beta} \int_0^t \left[I_0 \xi \sin(\omega_s \tau) + \frac{\beta \omega_s \xi \cos(\omega_s \tau)}{1 + \xi \sin(\omega_s \tau)} \right] \times [1 + \xi \sin(\omega_s \tau)]^{-\frac{\beta}{\alpha+\beta}} e^{\frac{I_0}{\alpha+\beta} \tau} d\tau \right\} \quad (7.17)$$

where we have chosen the initial condition $x_b(0) = I_0$ since for an input current equal to zero at $t = 0$ the output current equals $i_{out}(0) = x_b(0) = I_0$.

The linear time-varying small-signal model

The homogeneous variational equation is obtained by inserting equations (7.15) and (7.17) in equations (5.1) and (5.70). This yields:

$$\frac{dx_\delta}{dt} = a_x(t) \cdot x_\delta = \frac{1}{\alpha + \beta} \left[\beta \frac{\omega_s \xi \cos(\omega_s t)}{1 + \xi \sin(\omega_s t)} - I_0 \right] \cdot x_\delta \quad (7.18)$$

Using Equation (5.72) the dynamic eigenvalue $\lambda(t)$ is given by:

$$\lambda(t) = \frac{1}{\alpha + \beta} \left[\beta \frac{\omega_s \xi \cos(\omega_s t)}{1 + \xi \sin(\omega_s t)} - I_0 \right] \quad (7.19)$$

To show the significance of the dynamic eigenvalue we consider two special cases. If $\beta \rightarrow 0$, that is, if the parasitic capacitance C_{par} becomes negligible, then the dynamic eigenvalue approaches the constant pole $p = -I_0/(C V_T)$ of the ideal overall transfer function (compare with (7.8)). This occurs even if the time-variations of the input-signal are on the same order of magnitude as the ideal time-constant of the system.

If $\omega_s \rightarrow \infty$, the modulus of the dynamic eigenvalue goes to infinity. Physically this can be explained by a signal bypass, caused by the parasitic capacitor C_{par} . This signal bypass causes the input-output transfer to become constant above a certain frequency. A constant (frequency independent) transfer corresponds to the dynamic eigenvalue approaching infinity (since there is no "zero" to obtain a similar effect). Note that in the LTI small-signal model of the circuit this behaviour occurs in the frequency range above the pole and zero.

The Floquet exponent

The Floquet exponent is obtained by substituting (7.19) into (5.77):

$$\beta = \frac{1}{T} \int_0^T \lambda(\tau) d\tau = -\frac{I_0}{\alpha + \beta} \quad (7.20)$$

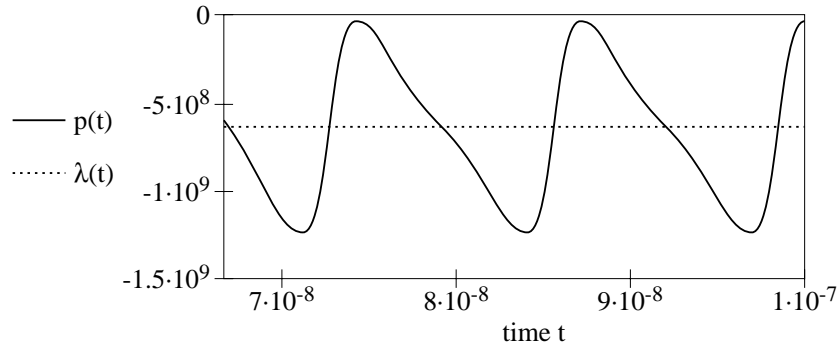


Figure 7.6: Dynamic eigenvalue $\lambda(t)$ (dotted) and quasi-static pole $p(t)$ as a function of time t ($f_s = 80\text{MHz}$, $C_{par} = 0.01\text{pF}$)

Thus for any sinusoidal input source the dynamic bias trajectory is stable, since for any input frequency or amplitude β is negative. Note that the Floquet exponent equals the pole of the LTI small-signal model (see Equation (7.10)).

7.2.4 Comparison between the quasi-static and linear time-varying approach

The example worked out shows that the dynamic eigenvalue converges to the ideal linear pole if the parasitic capacitor vanishes. This convergence takes place independently of the time-variations of the input signal in comparison to the internal dynamics of the system. Thus the dynamic eigenvalue reflects the fact that in this situation the overall dynamic behaviour is determined by the ideal linear differential equation, which is a required property when designing the dynamic behaviour. The quasi-static pole does not have this property and is only a good model if we deal with slowly-varying signals.

We illustrate the difference between the two approaches through some numerical examples of the linear first-order DTL-filter. Suppose that an ideal cut-off frequency of 100MHz is specified. We choose the intended capacitor to be $C = 5\text{pF}$, which implies that $I_0 = 81.7\mu\text{A}$ (see Equation (7.8)).

First we apply a sinusoid to the input with a frequency of $f_s = 80\text{MHz}$. We choose a modulation depth ξ of 0.97, which ensures that the circuit operates in its nonlinear region. Thus the input amplitude equals $79.25\mu\text{A}$. The dynamic eigenvalue and the quasi-static pole are plotted for a parasitic capacitor C_{par} of 0.01pF in Figure 7.6 and of 5pF in Figure 7.7. Figure 7.6 shows that for a very small parasitic capacitor the dynamic eigenvalue is almost time-invariant and converges to the ideal linear pole. The quasi-static pole does not converge. Figure 7.7 shows that for $C_{par} = 5\text{pF}$ the dynamic eigenvalue even becomes

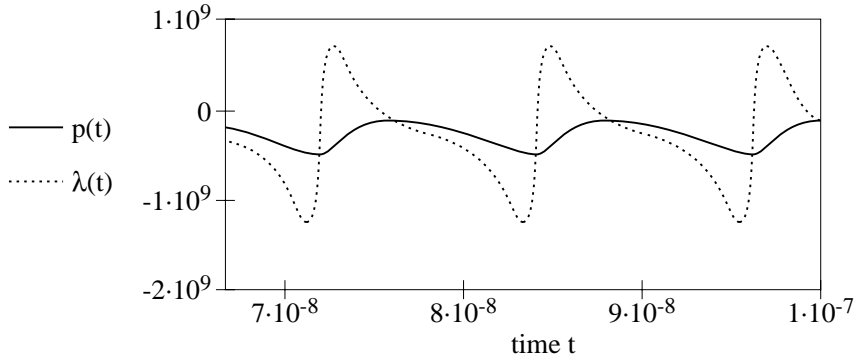


Figure 7.7: Dynamic eigenvalue $\lambda(t)$ (dotted) and quasi-static pole $p(t)$ as a function of time t ($f_s = 80\text{MHz}$, $C_{par} = 5\text{pF}$)

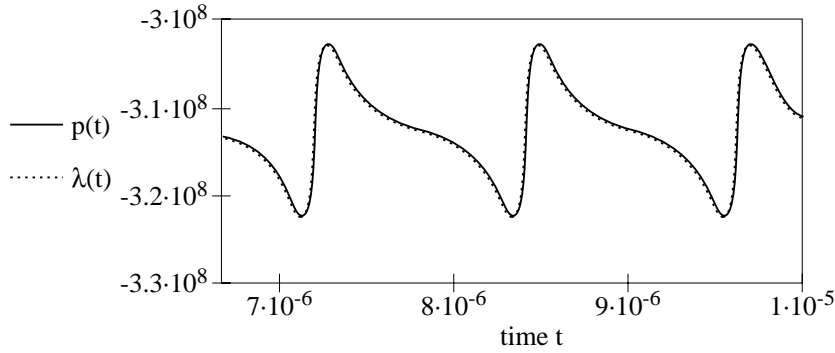


Figure 7.8: Dynamic eigenvalue $\lambda(t)$ (dotted) and quasi-static pole $p(t)$ as a function of time t ($f_s = 800\text{kHz}$, $C_{par} = 5\text{pF}$)

positive. The Floquet exponent however is negative, thus the system is stable.

In Figure 7.8 the frequency of the input signal is chosen to be $f_s = 800\text{kHz}$, the input amplitude remains $79.25\mu\text{A}$ and $C_{par} = 5\text{pF}$. Then we deal with a slowly-varying system and we see that the quasi-static pole is equal to the dynamic eigenvalue.

7.3 The linear time-varying approach applied to a dynamic translinear oscillator

In this section we apply the LTV approach to describe the dynamic behaviour of the DTL oscillator introduced in [45], as reported before in [8]. This example

is chosen because the nonlinearity in the differential equation describing this circuit is not a consequence of parasitic effects, but rather a conscious design choice. Neither the quasi-static nor the LTI approach can be applied to analyze this oscillator. Its operation is based on an instantaneous control action, and as a consequence it is neither a slowly varying nor a linear system.

First the DTL oscillator is introduced by applying DTL synthesis. Second the LTV approach is applied to describe the dynamic behaviour of this second-order system. For this we use the theory described in Section 5.5 and the transformation of the Riccati differential equation described in Appendix C. The resulting Floquet exponents are found to match the results reported in [10].

7.3.1 DTL synthesis of a second-order oscillator

The design of the second-order DTL oscillator starts with a dimensionless differential equation that describes the oscillator behaviour in the time domain [45]. A possible choice for the differential equation is:

$$\frac{d^2x}{d\tau^2} + p f(x) \frac{dx}{d\tau} + p^2 x = 0 \quad (7.21)$$

where x is the oscillating signal, p is a positive control parameter that is related to the oscillating frequency, $f(x)$ determines the damping and undamping behaviour of the oscillator and τ is the dimensionless time of the oscillator. We choose $f(x)$ to be an even-symmetric function of x because then the even harmonics of the oscillating signal are suppressed.

We make the dimensions of the resulting differential equation suitable for a dynamic translinear realization. The signal x and parameter p are transformed into the currents i_{osc} and i_F , while the dimensionless time τ is transformed into the time t with dimension [s]. For this we apply the following transformations:

$$p = \frac{i_F}{i_{osc}}, \quad x = \frac{i_{osc}}{I_0}, \quad \frac{d}{d\tau} = \frac{C V_T}{I_0} \frac{d}{dt} \quad (7.22)$$

where I_0 is a DC bias current that determines the absolute current swings, C is an intended capacitor and V_T is the thermal voltage.

Applying the transformations the following differential equation results:

$$C^2 V_T^2 \frac{d^2}{dt^2} i_{osc} + C V_T i_F f(i_{osc}, i_F) \frac{d}{dt} i_{osc} + i_F^2 i_{osc} = 0 \quad (7.23)$$

If we choose i_F to be a constant current I_F , we can use the substitution $f(i_{osc}, I_F) \frac{d}{dt} i_{osc} = \frac{d}{dt} F(i_{osc}, I_F)$. This yields:

$$C^2 V_T^2 \frac{d^2}{dt^2} i_{osc} + C V_T I_F \frac{d}{dt} F(i_{osc}, I_F) + I_F^2 i_{osc} = 0 \quad (7.24)$$

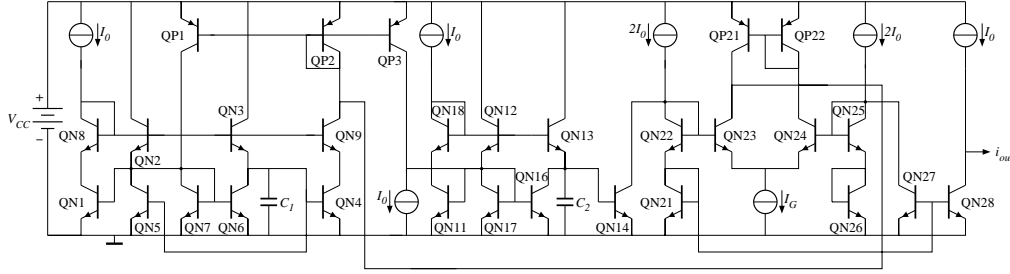


Figure 7.9: Circuit implementation of a DTL oscillator [45]

It follows from our choice for the function $f(x)$ that the function $F(i_{osc}, I_F)$ is odd-symmetric. It is chosen so that it can be easily implemented with translinear techniques. A suitable choice for $F(i_{osc}, I_F)$ is [45]:

$$F(i_{osc}, I_F) = 2 i_{osc} - \frac{2 G i_{osc} I_F^2}{i_{osc}^2 + I_F^2} \quad (7.25)$$

where G is a constant that must be larger than one. For the derivative $\frac{d}{dt}F(i_{osc}, I_F)$ we can deduce:

$$\begin{aligned} \frac{d}{dt}F(i_{osc}, I_F) &= \frac{dF(i_{osc}, I_F)}{di_{osc}} \cdot \frac{di_{osc}}{dt} \\ &= \left\{ 2 - 2 G I_F^2 \left[\frac{I_F^2 - i_{osc}^2}{(I_F^2 + i_{osc}^2)^2} \right] \right\} \frac{di_{osc}}{dt} \end{aligned} \quad (7.26)$$

Finally the nonlinear differential equation that describes the DTL oscillator is given by:

$$\begin{aligned} C^2 V_T^2 \frac{d^2}{dt^2} i_{osc} + C V_T I_F 2 \left\{ 1 - G I_F^2 \left[\frac{I_F^2 - i_{osc}^2}{(I_F^2 + i_{osc}^2)^2} \right] \right\} \frac{di_{osc}}{dt} \\ + I_F^2 i_{osc} = 0 \end{aligned} \quad (7.27)$$

This nonlinear differential equation can be mapped on the DTL circuit depicted in Figure 7.9 [45].

If we assume that the oscillator current is approximately sinusoidal, that is $i_{osc}(t) \approx \hat{i}_{osc} \sin(\omega_{osc} t + \theta)$, than substitution into the differential equation (7.23) gives an estimate for the oscillating frequency and amplitude. We obtain [45]:

$$\omega_{osc} \approx \frac{I_F}{C V_T} \quad (7.28)$$

and

$$\int_0^T f(i_{osc}(\tau), I_F) di_{osc}(\tau) \approx 0 \quad (7.29)$$

in which $T = \frac{2\pi}{\omega_{osc}}$. From Equation (7.29) we can obtain the following estimate for the amplitude of the oscillator output, again under the assumption of a sinusoidal oscillation:

$$\hat{i}_{osc} \approx I_F \sqrt{G - 1} \quad (7.30)$$

7.3.2 The linear time-varying approach

We now use the LTV approach to model the dynamic behaviour of the DTL oscillator in its dynamic bias-trajectory.

The state-space description Rewriting the differential equation (7.27), the oscillator can be described by the following state-space system:

$$\frac{d}{dt} \begin{bmatrix} x_1 \\ x_2 \end{bmatrix} = \begin{bmatrix} f_1(x_1, x_2) \\ f_2(x_1, x_2) \end{bmatrix} \quad (7.31)$$

with

$$\begin{aligned} f_1(x_1, x_2) &= x_2 - \omega x_1 \\ f_2(x_1, x_2) &= 2G I_F^2 \omega \left[\frac{I_F^2 - x_1^2}{(I_F^2 + x_1^2)^2} \right] (x_2 - \omega x_1) - \omega x_2 \end{aligned}$$

In this state-space description the state-space variables x_1 and x_2 correspond to i_{osc} and $\frac{d}{dt}i_{osc}$, respectively, and ω equals:

$$\omega = \frac{I_F}{C V_T} \quad (7.32)$$

The dynamic bias trajectory We consider the state variables to consist of the sum:

$$\begin{cases} x_1 = x_{1b} + x_{1\delta} \\ x_2 = x_{2b} + x_{2\delta} \end{cases} \quad (7.33)$$

where x_{1b} and x_{2b} are the dynamic bias trajectories of the state-space variables and $x_{1\delta}$ and $x_{2\delta}$ are relatively small variations on x_{1b} and x_{2b} , respectively. Since an oscillator generates its dynamic bias trajectory (limit cycle) autonomously,

we do not need to specify an input signal. The dynamic bias trajectory is given by the solution of the state-space description (7.31) for $x_{1\delta} = x_{2\delta} = 0$:

$$\frac{d}{dt} \begin{bmatrix} x_{1b} \\ x_{2b} \end{bmatrix} = \begin{bmatrix} f_1(x_{1b}, x_{2b}) \\ f_2(x_{1b}, x_{2b}) \end{bmatrix} \quad (7.34)$$

An analytical solution for this differential equation can not be obtained. It must be solved numerically, an example of which is presented later in Figure 7.10.

The variational equation The variational equation (5.78) is obtained from the state-space description of the oscillator (7.31) as

$$\frac{d}{dt} \begin{bmatrix} x_{1\delta} \\ x_{2\delta} \end{bmatrix} = \begin{bmatrix} a_{11}(t) & a_{12}(t) \\ a_{21}(t) & a_{22}(t) \end{bmatrix} \begin{bmatrix} x_{1\delta} \\ x_{2\delta} \end{bmatrix} \quad (7.35)$$

in which

$$\begin{aligned} a_{11}(t) &= \frac{\partial f_1}{\partial x_1}(x_{1b}, x_{2b}) = -\omega \\ a_{12}(t) &= \frac{\partial f_1}{\partial x_2}(x_{1b}, x_{2b}) = 1 \\ a_{21}(t) &= \frac{\partial f_2}{\partial x_1}(x_{1b}, x_{2b}) \\ &= 2G\omega^2 I_F^2 \left[\frac{-x_{1b}^4 + 6I_F^2 x_{1b}^2 - I_F^4}{(x_{1b}^2 + I_F^2)^3} \right] \\ &\quad + 2G\omega I_F^2 x_{2b} \left[\frac{2x_{1b}^3 - 6I_F^2 x_{1b}}{(x_{1b}^2 + I_F^2)^3} \right] \\ a_{22}(t) &= \frac{\partial f_2}{\partial x_2}(x_{1b}, x_{2b}) \\ &= 2G\omega I_F^2 \left[\frac{I_F^2 - x_{1b}^2}{(x_{1b}^2 + I_F^2)^2} \right] - \omega \end{aligned}$$

Note that the elements a_{11} , a_{12} , a_{21} and a_{22} are time-dependent since they are functions of the dynamic bias trajectory (x_{1b}, x_{2b}) .

The dynamic eigenvalues In order to calculate the dynamic eigenvalues, the Riccati differential equation must be solved (see Section 5.5.1). Substitution of

a_{11} , a_{12} , a_{21} and a_{22} in the Riccati equation (5.80) yields:

$$\begin{aligned} \frac{d}{dt} l(t) &= -l^2(t) - 2G\omega I_F^2 \left[\frac{I_F^2 - x_{1b}^2}{(x_{1b}^2 + I_F^2)^2} \right] \cdot l(t) \\ &+ 2G\omega^2 I_F^2 \left[\frac{-x_{1b}^4 + 6I_F^2 x_{1b}^2 - I_F^4}{(x_{1b}^2 + I_F^2)^3} \right] \\ &+ 2G\omega I_F^2 x_{2b} \left[\frac{2x_{1b}^3 - 6I_F^2 x_{1b}}{(x_{1b}^2 + I_F^2)^3} \right] \end{aligned} \quad (7.36)$$

This is a time-varying quadratic differential equation in the unknown $l = l(t)$. Its solution contains singularities and is found via the transformation (C.2), repeated below:

$$u(t) = e^{\int_0^t a_{12}(\tau) l(\tau) d\tau} \iff a_{12}(t) l(t) = \frac{\frac{d}{dt} u(t)}{u(t)}. \quad (7.37)$$

This transformation is more elaborately described in Appendix C. Application of this transformation gives the solution of the Riccati differential equation in terms of the new transformation variables $u(t)$ and $q(t) = \frac{d}{dt} u(t)$, as given by Equation (C.5). Substitution of this solution in Expression (5.82) for the dynamic eigenvalues, and using Expression (7.35) for the DTL oscillator variational equation, gives the following dynamic eigenvalues:

$$\begin{aligned} \lambda_1(t) &= \frac{q(t)}{u(t)} - \omega \quad \text{and} \\ \lambda_2(t) &= -\frac{q(t)}{u(t)} + 2G\omega I_F^2 \left[\frac{I_F^2 - x_{1b}^2}{(x_{1b}^2 + I_F^2)^2} \right] - \omega \end{aligned} \quad (7.38)$$

Here $u(t)$ and $q(t)$ are the solutions of the state-space system (C.4), which can be added to the DTL-oscillator state-space description (7.31) and solved simultaneously.

The Floquet exponents The Floquet exponents β_1 and β_2 are obtained by substituting (7.35) in (C.7):

$$\begin{aligned} \beta_1 &= \frac{1}{T} \ln(u)|_{t'}^{t'+T} - \omega \quad \text{and} \\ \beta_2 &= -\frac{1}{T} \ln(u)|_{t'}^{t'+T} + \frac{1}{T} \int_0^T 2G\omega I_F^2 \left[\frac{I_F^2 - x_{1b}^2}{(x_{1b}^2 + I_F^2)^2} \right] d\tau - \omega \end{aligned} \quad (7.39)$$

Any oscillator is characterized by having a stable limit cycle and thus a constant oscillation amplitude in steady state. As a consequence, one Floquet exponent

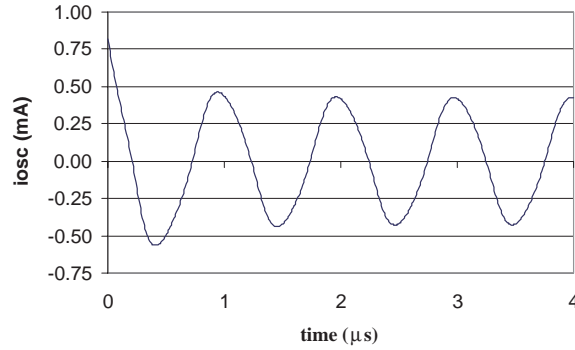


Figure 7.10: Oscillator output as a function of time for $C_1 = C_2 = 5\text{nF}$, $I_F = 817\mu\text{A}$ and $G = 1.2$

should equal zero and the other Floquet exponent should have a negative real part. In the following paragraph this statement is checked by a numerical example, and the Floquet exponents obtained are compared with the results reported in [10].

Numerical example Suppose an oscillating frequency of 1MHz is specified. We choose the capacitors to be $C = 5\text{nF}$. It follows from Equation (7.28) that $I_F = 817\mu\text{A}$. The oscillating output signal $i_{osc} = x_{1b}$ is plotted for $G = 1.2$ in Figure 7.10. Notice that the estimation of the amplitude according to Equation (7.30) ($\hat{I}_{osc} = 365\mu\text{A}$) corresponds to the simulated value. The dynamic eigenvalues follow from Expression (7.38). The real parts are plotted in Figures 7.11 and 7.12. The imaginary parts of both dynamic eigenvalues are equal to zero. Notice that both dynamic eigenvalues contain periodic singularities. Possibly this behaviour occurs because two "coupled dynamic eigenvalues" are considered separately. The same would occur in an LTI system with a pair of complex poles, when one pole is considered separately.

Using Equation (7.39), the Floquet exponents can be calculated directly from the solution of the transformed Riccati differential equation. We obtain the following result: $\beta_1 = 0$ and $\beta_2 = -2.07 \cdot 10^6$. These values correspond to the properties of a stable limit cycle and they match the Floquet multipliers reported in [10], i.e. $\rho_1 = 1$ and $\rho_2 = 0.126$ (the Floquet exponents equal the logarithm of the Floquet multipliers divided by the period T [19]).

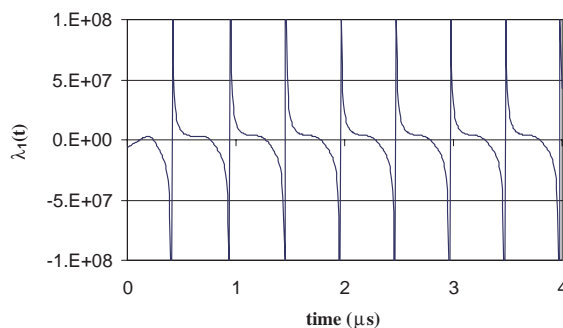


Figure 7.11: Real part of the dynamic eigenvalue $\lambda_1(t)$ of the DTL oscillator as a function of time

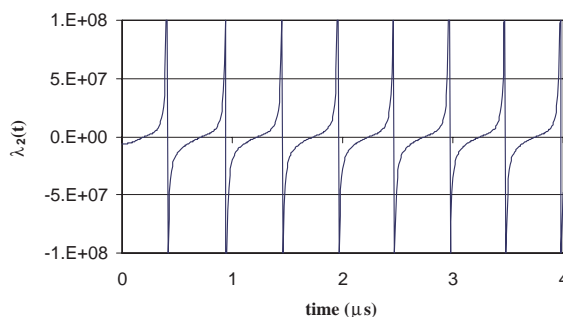


Figure 7.12: Real part of the dynamic eigenvalue $\lambda_2(t)$ of the DTL oscillator as a function of time

7.4 Conclusions

In this chapter we applied the linear time-varying approach to analyze the dynamic behaviour of dynamic translinear circuits. Dynamic translinear circuits use the exponential input-output relation of the transistor and as a primitive for the synthesis of electronic circuits. They can implement a wide variety of dynamic functions, described by differential equations, both linear and nonlinear.

High-level synthesis/analysis methods are available for DTL circuits. These are based on the static and dynamic translinear principle. These principles were reviewed in the first section of this chapter. The current design approaches for DTL circuits generally only incorporate the ideal behaviour of the transistor. If

parasitic parameters are considered at all, only instantaneous parasitic effects are included, e.g. finite current gain factors for the transistors employed. By lack of a suitable modeling method, the effect of parasitic capacitances has not yet been rigorously incorporated.

DTL synthesis and analysis are based on the nonlinear input-output relation of the transistor. Therefore, the system behaviour in the presence of parasitics is often defined by nonlinear differential equations, even if the ideal overall transfer function is linear. In this chapter we used the LTV approach for handling these nonlinear differential equations for the low-level analysis/synthesis of two example DTL circuits: a first-order DTL filter and a DTL oscillator.

Through the example of a first-order linear DTL filter it has been shown that the linear time-varying approach is a useful method for analyzing DTL circuits in the presence of parasitics. The linear first-order DTL filter was introduced by applying DTL synthesis. The circuit topology was extended in order to eliminate the influence of most of the parasitic capacitors. Only one dominant parasitic capacitor remained. We applied the linear time-varying approach to analyze the dynamic behaviour of the DTL filter in the presence of this remaining parasitic capacitor and compared the results with the quasi-static and LTI approach. The dynamic eigenvalue of the DTL filter was shown to converge to the designed ideal linear pole if the parasitics vanish, which is a required property. The time-varying pole of the quasi-static approach does not have this property. If the DTL filter is operating under slowly-varying conditions the quasi-static pole was shown to be equal to the dynamic eigenvalue.

The second example, a DTL oscillator, was chosen because the nonlinearity in the differential equation describing this circuit is not a consequence of parasitic effects, but rather a conscious design choice. Neither the quasi-static nor the LTI approach can be applied to analyze this oscillator. Its operation is based on an instantaneous control action, and as a consequence it is neither a slowly varying nor a linear system. Therefore, only the linear time-varying approach is applicable. The DTL oscillator was introduced by applying DTL synthesis. Then the LTV approach was applied to describe the dynamic behaviour of this second-order system. The dynamic eigenvalues, which contain periodic singularities, were derived using the transformation method given in Appendix C. The Floquet exponents were derived from these dynamic eigenvalues; they correspond to the properties of a stable limit cycle and they match the Floquet multipliers reported in [10]. This confirms the consistency of the method used.

The linear time-varying approach applied to a limiting differential pair

In the previous chapters we described how the dynamic behaviour of a class-B stage and of dynamic translinear circuits can be analyzed using the linear time-varying approach. This chapter covers the analysis of the dynamic behaviour of another example nonlinear circuit, namely the familiar differential pair, driven to limiting. The differential pair is one of the most commonly used amplifier input stages in circuit design. When biased in class A, that is, when the input voltage is kept sufficiently small, an LTI model can be applied for designing and analyzing this amplifier stage. However, when driven with a sufficiently large input signal, the differential pair starts behaving as a simple voltage-to-current limiter, and the LTI modeling approach breaks down. In this chapter we use the linear time-varying approach for analyzing a simple implementation of a limiting differential pair, built with bipolar transistors.

In the first section of this chapter we give a description of this circuit and its large-signal model. In the second section we derive the linear time-varying model and analyze the first-order and second-order dynamic behaviour. We end with some conclusions.

8.1 Circuit description

One of the most simple implementations of a voltage-to-current limiter is the familiar differential pair, driven to limiting by a sufficiently large input signal. An implementation using bipolar transistors is shown in Figure 8.1.

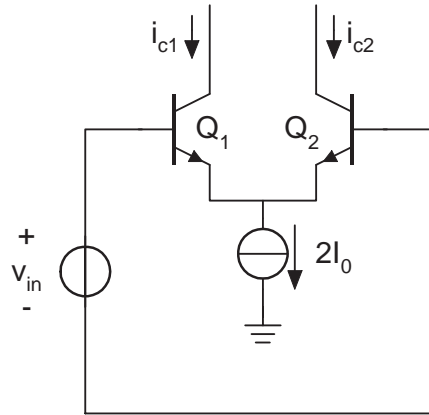


Figure 8.1: A simple voltage-to-current limiter: the differential pair

The ideal operation of this configuration is depicted in Figure 8.2 and explained as follows. If the bipolar transistors are assumed to be ideal memoryless switches, then for positive input voltages transistor Q_1 is conducting with a collector current i_{c1} equal to the complete tail current $2I_0$ and with base-emitter voltage $v_{be1} = 0$. Transistor Q_2 is cut off with zero collector current i_{c2} , base-emitter voltage v_{be2} equal to $-v_{in}$ and zero base-current i_{b2} . For negative input voltages $i_{c1} = 0$, $v_{be1} = v_{in}$, $i_{b1} = 0$, $i_{c2} = 2I_0$ and $v_{be2} = 0$. Thus, ideally, the total output current $i_{c1} - i_{c2}$ equals $2I_0$ for $v_{in} > 0$ and $-2I_0$ for $v_{in} < 0$, the transition between these two situations is instantaneous and the input current is zero in all cases. Evidently, the bipolar transistors are not ideal switches, they have finite input resistance, finite output resistance and finite speed. The consequence of these limitations is investigated using the linear time-varying approach.

The first step in applying the linear time-varying approach is obtaining a nonlinear large-signal description of this circuit. We use the relevant part of the Gummel-Poon model for the bipolar transistors [17]. Both transistors are used in the forward region (collector-base junction is reverse biased) and we neglect second-order effects such as leakage currents, Early effect and high-level injection. Since the output current of the circuit is sensed (it implements a voltage-to-current limiter) we neglect ohmic resistances in series with the collector. As a result of the voltage drive the ohmic resistances in series with base and emitter can not be neglected. The emitter resistance R_E , however, (which is usually very small anyway) can in first order be modeled by an equivalent resistance $(B_f + 1) \cdot R_E$ in series with the base resistance R_B , where B_f is the forward current-gain factor of the transistor. Therefore, we include R_b in our large-signal model, which models $R_B + (B_f + 1) \cdot R_E$.

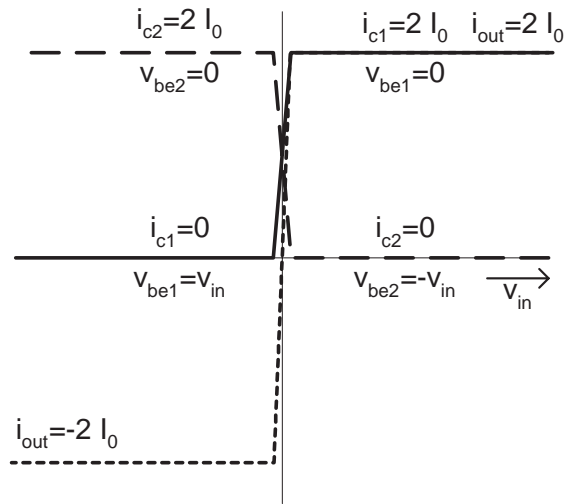


Figure 8.2: Ideal operation of a voltage-to-current limiter (solid line: Q_1 , lines: Q_2 , dots: $i_{out} = i_{c1} - i_{c2}$)

With these simplifications we end up with a transistor model in which we can distinguish four main effects (see figure 8.3):

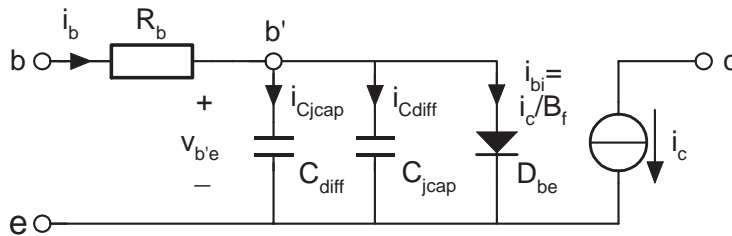


Figure 8.3: Simplified Gummel-Poon model for the bipolar transistor

1. the instantaneous transfer from intrinsic base-emitter voltage to collector current is modeled by the base-emitter diode D_{be} and a controlled current source i_c ;
2. the effect of charge storage in the base-emitter depletion region is modeled by the junction capacitor C_{jcap} ;

3. the effect of charge storage in the base region is modeled by the diffusion capacitor C_{diff} ;
4. the base resistance and equivalent emitter resistance are modeled by R_b .

D_{be} , C_{diff} and C_{jcap} all contribute to the base current i_b and the emitter current i_e , whereas the collector current i_c is determined by the controlled current source only.

For the instantaneous transfer from intrinsic base-emitter voltage $v_{b'e}$ to collector current i_c and the resulting instantaneous base current i_{b_i} we have the familiar relations

$$i_c = I_s \left(e^{\frac{v_{b'e}}{V_T}} - 1 \right) \quad (8.1)$$

$$i_{b_i} = \frac{i_c}{B_f} = \frac{I_s}{B_f} \left(e^{\frac{v_{b'e}}{V_T}} - 1 \right) \quad (8.2)$$

Here, I_s is the transport saturation current and B_f is the forward current-gain factor of the transistor and V_T is the thermal voltage.

The diffusion capacitor contributes a current $i_{C_{diff}}$ to the base and emitter currents which equals

$$i_{C_{diff}} = \tau_f \cdot \frac{di_c}{dt} = \frac{\tau_f I_s}{V_T} e^{\frac{v_{b'e}}{V_T}} \cdot \frac{dv_{b'e}}{dt} \quad (8.3)$$

Here τ_f is the forward transit time of the transistor.

The junction capacitor contributes a current $i_{C_{jcap}}$ to the base and emitter currents, which can be derived as follows:

$$Q_{jcap} = C_{jcap}(v_{b'e}) \cdot v_{b'e} \quad \Leftrightarrow \quad (8.4)$$

$$i_{C_{jcap}} = \frac{dQ_{jcap}}{dt} = \left[C_{jcap}(v_{b'e}) + v_{b'e} \frac{\partial C_{jcap}(v_{b'e})}{\partial v_{b'e}} \right] \frac{dv_{b'e}}{dt} \quad (8.5)$$

If we approximate the junction capacitors by a constant capacitor C_{jcap} equal to $C_{jcap}(0)$ we get

$$i_{C_{jcap}} = C_{jcap} \cdot \frac{dv_{b'e}}{dt} \quad (8.6)$$

The total base-current equals the sum of the instantaneous base current (8.2) and the capacitance currents in equations (8.3) and (8.6):

$$i_b = \frac{I_s}{B_f} \left(e^{\frac{v_{b'e}}{V_T}} - 1 \right) + \frac{\tau_f I_s}{V_T} e^{\frac{v_{b'e}}{V_T}} \cdot \frac{dv_{b'e}}{dt} + C_{jcap} \cdot \frac{dv_{b'e}}{dt} \quad (8.7)$$

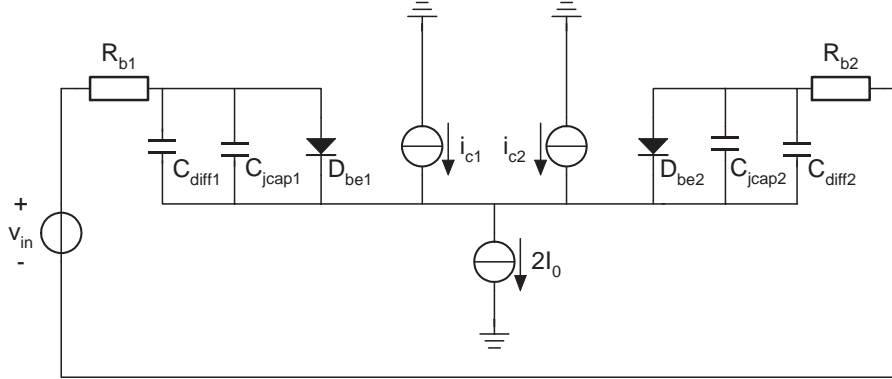


Figure 8.4: Large-signal model for the differential pair

If we use the simplified model for the bipolar transistor in the differential pair of Figure 8.1, we obtain the large-signal model as shown in Figure 8.4. By applying the Kirchhoff voltage law to the loop formed by the input voltage source v_{in} and the two base-emitter junctions and the Kirchhoff current law to the common emitter node we obtain the following set of equations:

$$\begin{cases} v_{in} = R_{b1}i_{b1} + v_{b'e1} - v_{b'e2} - R_{b2}i_{b2} \\ 2I_0 = i_{b1} + i_{c1} + i_{c2} + i_{b2} \end{cases} \quad (8.8)$$

in which $2I_0$ is the tail current of the limiter. Using equations (8.1) and (8.7) this can be written as

$$\begin{cases} v_{in} = R_{b1} \left[\frac{I_{s1}}{B_{f1}} \left(e^{\frac{v_{b'e1}}{V_T}} - 1 \right) + \left(\frac{\tau_{f1}I_{s1}}{V_T} e^{\frac{v_{b'e1}}{V_T}} + C_{jcap1} \right) \frac{dv_{b'e1}}{dt} \right] \\ \quad - R_{b2} \left[\frac{I_{s2}}{B_{f2}} \left(e^{\frac{v_{b'e2}}{V_T}} - 1 \right) + \left(\frac{\tau_{f2}I_{s2}}{V_T} e^{\frac{v_{b'e2}}{V_T}} + C_{jcap2} \right) \frac{dv_{b'e2}}{dt} \right] \\ \quad + v_{b'e1} - v_{b'e2} \\ 2I_0 = \frac{1 + B_{f1}}{B_{f1}} I_{s1} \left(e^{\frac{v_{b'e1}}{V_T}} - 1 \right) + \left(\frac{\tau_{f1}I_{s1}}{V_T} e^{\frac{v_{b'e1}}{V_T}} + C_{jcap1} \right) \frac{dv_{b'e1}}{dt} \\ \quad + \frac{1 + B_{f2}}{B_{f2}} I_{s2} \left(e^{\frac{v_{b'e2}}{V_T}} - 1 \right) + \left(\frac{\tau_{f2}I_{s2}}{V_T} e^{\frac{v_{b'e2}}{V_T}} + C_{jcap2} \right) \frac{dv_{b'e2}}{dt} \end{cases} \quad (8.9)$$

Note that we have used the notational conventions introduced in Chapter 6. DC-variables (e.g. the DC-current I_0) are written in capital letters and large-signal variables (e.g. v_{in} , $v_{b'e1}$ and $v_{b'e2}$) are written in small letters. In large-signal variables the time-dependency is not explicitly included, i.e. $v_{in} = v_{in}(t)$,

$v_{b'e1} = v_{b'e1}(t)$ and $v_{b'e2} = v_{b'e2}(t)$. The set of equations (8.9) describes the large-signal behaviour of the differential pair of Figure 8.1.

In the next sections we analyze the dynamic behaviour of the differential pair of Figure 8.1 using the large-signal model as given in Figure 8.4 and described by the set of equations (8.9). We will use the capacitance voltages, i.e. the intrinsic base-emitter voltages $v_{b'e1}$ and $v_{b'e2}$, as state variables. First we derive a linear time-varying model of the differential pair neglecting the influence of the base-resistances R_{b1} and R_{b2} . This assumption enables a first-order analysis using only one state variable, since then the input voltage source v_{in} and the capacitor voltages $v_{b'e1}$ and $v_{b'e2}$ form a closed loop. Second we drop this assumption and derive a second-order linear time-varying model of the differential pair using the large-signal description including R_{b1} and R_{b2} .

8.2 First-order dynamic behaviour

If we neglect the influence of the base-resistances R_{b1} and R_{b2} then the first equation of equation set (8.9) reduces to

$$v_{in} = v_{b'e1} - v_{b'e2} \quad (8.10)$$

Thus, due to the closed loop of the input voltage and the two intrinsic base-emitter voltages, we can eliminate one of the state variables from the set of equations (8.9) and end up with a model with first-order dynamics only. If we assume that both transistors have identical parameters and choose $v_{b'e1}$ as a state variable we obtain the following large-signal expression:

$$\frac{dv_{b'e1}}{dt} = f(v_{b'e1}, v_{in}) \quad (8.11)$$

with

$$f(v_{b'e1}, v_{in}) = \frac{2I_0 + 2\frac{B_f+1}{B_f}I_s - \frac{B_f+1}{B_f}I_s e^{\frac{v_{b'e1}}{V_T}} \left(1 + e^{-\frac{v_{in}}{V_T}}\right) + \left(\frac{\tau_f I_s}{V_T} e^{\frac{v_{b'e1}}{V_T}} e^{-\frac{v_{in}}{V_T}} + C_{jcap}\right) \frac{dv_{in}}{dt}}{\frac{\tau_f I_s}{V_T} e^{\frac{v_{b'e1}}{V_T}} \left(1 + e^{-\frac{v_{in}}{V_T}}\right) + 2 C_{jcap}}$$

Alternatively we can choose $v_{b'e2}$ as a state variable. Then we obtain:

$$\frac{dv_{b'e2}}{dt} = f'(v_{b'e2}, v_{in}) \quad (8.12)$$

parameter	value
I_s	$18\mu A$
B_f	117
τ_f	$22ps$
$C_{jcap}(0)$	$46fF$

Table 8.1: Transistor parameters of the DIMES-01 process

with

$$f'(v_{b'e2}, v_{in}) = \frac{2I_0 + 2\frac{B_f+1}{B_f}I_s - \frac{B_f+1}{B_f}I_s e^{\frac{v_{b'e2}}{V_T}} \left(1 + e^{\frac{v_{in}}{V_T}}\right) - \left(\frac{\tau_f I_s}{V_T} e^{\frac{v_{b'e2}}{V_T}} e^{\frac{v_{in}}{V_T}} + C_{jcap}\right) \frac{dv_{in}}{dt}}{\frac{\tau_f I_s}{V_T} e^{\frac{v_{b'e2}}{V_T}} \left(1 + e^{\frac{v_{in}}{V_T}}\right) + 2 C_{jcap}}$$

Notice that both large-signal descriptions are very similar. Apart from the opposite sign in places where v_{in} is present, they are identical, i.e. $f'(v_{b'e2}, v_{in}) = f(v_{b'e2}, -v_{in})$. This is a result of the anti-symmetric function both transistors have in the circuit: apart from the fact that the input voltage has an opposite-sign effect on the base-emitter voltages of the transistors, they behave similarly.

8.2.1 Dynamic bias-trajectory

The first step in describing the dynamic behaviour using the LTV approach is the calculation of the dynamic bias trajectory of the state variables $v_{b'e1_b}$ and $v_{b'e2_b}$ as a function of the input signal v_{in_b} . As argued in Chapter 6, we choose a sinusoidal input signal:

$$v_{in_b}(t) = V_A \sin(\omega t) = V_A \sin(2\pi f t) \quad (8.13)$$

The dynamic bias-trajectory is computed numerically for a range of input amplitudes V_A , input frequencies f and tail currents $2I_0$ (with MATLAB using variable order Runge-Kutta formulas [29]) for both choices of state-equations (8.11) and (8.12). The transistor parameters used are summarized in Table 8.1; these are the parameters of our in-house DIMES-01 process [38].

In Figure 8.5 we show the dynamic bias-trajectories of $v_{b'e1_b}$ and $v_{b'e2_b}$ for an input amplitude V_A of $0.5V$, a frequency f of $1MHz$ and a tail current $2I_0$ of $0.2\mu A$. As expected from the anti-symmetry of the circuit, $v_{b'e2_b}$ is a time-shifted copy of $v_{b'e1_b}$, with this time-shift equal to half a period of the input signal. It can be noticed that the base-emitter voltage of the transistor which is conducting ($v_{b'e1_b}$ for $v_{in} > 0$ and $v_{b'e2_b}$ for $v_{in} < 0$) is not constant. This is caused by an extra current generated at the emitter node as a result of the

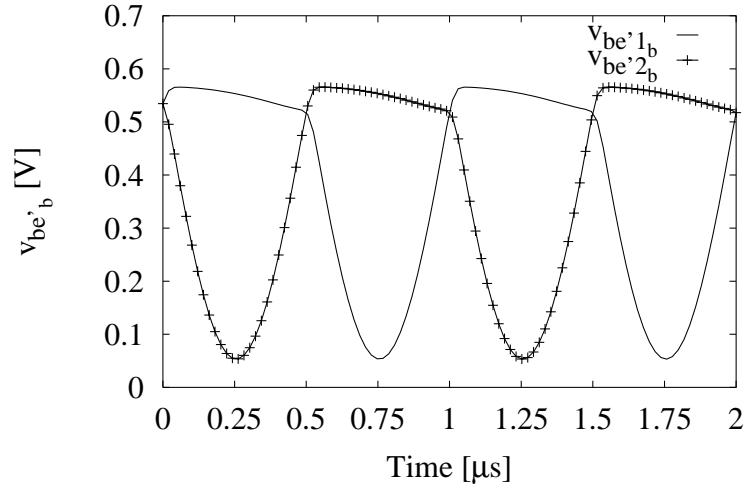


Figure 8.5: Dynamic bias-trajectory of $v_{b'e1}$ and $v_{b'e2}$ for two periods of the input signal ($V_A = 0.5V$, $f = 1MHz$ and $I_0 = 0.1\mu A$)

charging and discharging of the junction capacitor of the transistor which is in cut off. This current acts as “extra tail current” for the transistor which is conducting.

8.2.2 Dynamic eigenvalue

The second step in the LTV-approach for a first-order system is the modeling of the dynamic behaviour in the neighbourhood of the dynamic bias-trajectory. This is done by determining the dynamic eigenvalue of the homogeneous variational equation (5.70). For the first-order model of the limiter we obtain the homogeneous variational equation from Equation (8.11):

$$\frac{dv_{b'e1\delta}}{dt} = a_{v_{b'e1}}(t) \cdot v_{b'e1\delta} \quad (8.14)$$

with

$$\begin{aligned}
a_{v_{b'e1}}(t) &= \left. \frac{\partial f(v_{b'e1}, v_{in})}{\partial v_{b'e1}} \right|_{v_{b'e1}=v_{b'e1b}, v_{in}=v_{inb}} = \\
&= \frac{-\frac{B_f+1}{B_f} \frac{I_s}{V_T} e^{\frac{v_{b'e1b}}{V_T}} \left(1 + e^{-\frac{v_{inb}}{V_T}}\right) + \frac{\tau_f I_s}{V_T^2} e^{\frac{v_{b'e1b}}{V_T}} e^{-\frac{v_{inb}}{V_T}} \frac{dv_{inb}}{dt}}{\frac{\tau_f I_s}{V_T} e^{\frac{v_{b'e1b}}{V_T}} \left(1 + e^{-\frac{v_{inb}}{V_T}}\right) + 2 C_{jcap}} \\
&= \frac{\frac{\tau_f I_s}{V_T^2} e^{\frac{v_{b'e1b}}{V_T}} \left(1 + e^{-\frac{v_{inb}}{V_T}}\right) f(v_{b'e1}, v_{in})}{\frac{\tau_f I_s}{V_T} e^{\frac{v_{b'e1b}}{V_T}} \left(1 + e^{-\frac{v_{inb}}{V_T}}\right) + 2 C_{jcap}}
\end{aligned}$$

With the alternative choice of $v_{b'e2}$ as state variable, the homogeneous variational equation is derived from (8.12). Then we obtain

$$\frac{dv_{b'e2\delta}}{dt} = a_{v_{b'e2}}(t) \cdot v_{b'e2\delta} \quad (8.15)$$

with

$$\begin{aligned}
a_{v_{b'e2}}(t) &= \left. \frac{\partial f'(v_{b'e2}, v_{in})}{\partial v_{b'e2}} \right|_{v_{b'e2}=v_{b'e2b}, v_{in}=v_{inb}} = \\
&= \frac{-\frac{B_f+1}{B_f} \frac{I_s}{V_T} e^{\frac{v_{b'e2b}}{V_T}} \left(1 + e^{\frac{v_{inb}}{V_T}}\right) - \frac{\tau_f I_s}{V_T^2} e^{\frac{v_{b'e2b}}{V_T}} e^{\frac{v_{inb}}{V_T}} \frac{dv_{inb}}{dt}}{\frac{\tau_f I_s}{V_T} e^{\frac{v_{b'e2b}}{V_T}} \left(1 + e^{\frac{v_{inb}}{V_T}}\right) + 2 C_{jcap}} \\
&= \frac{\frac{\tau_f I_s}{V_T^2} e^{\frac{v_{b'e2b}}{V_T}} \left(1 + e^{\frac{v_{inb}}{V_T}}\right) f'(v_{b'e2}, v_{in})}{\frac{\tau_f I_s}{V_T} e^{\frac{v_{b'e2b}}{V_T}} \left(1 + e^{\frac{v_{inb}}{V_T}}\right) + 2 C_{jcap}}
\end{aligned}$$

In both cases the dynamic eigenvalues $\lambda_{v_{b'e1}}(t)$ and $\lambda_{v_{b'e2}}(t)$ are simply given by $a_{v_{b'e1}}(t)$ and $a_{v_{b'e2}}(t)$ respectively.

In Figure 8.6 we show the dynamic eigenvalues $\lambda_{v_{b'e1}}(t)$ and $\lambda_{v_{b'e2}}(t)$, again for the dynamic bias-trajectories $v_{b'e1b}$ and $v_{b'e2b}$ corresponding to an input amplitude of $0.5V$, an input frequency $1MHz$ and a tail current of $0.2\mu A$. In this figure we see that for either choice of state variable $v_{b'e1}$ or $v_{b'e2}$ the corresponding dynamic eigenvalue is identical. Using the fact that the two alternative state variables form a closed loop with the input voltage (Equation 8.10) it can be proven that this identity holds for any choice of input signal: as a result of the

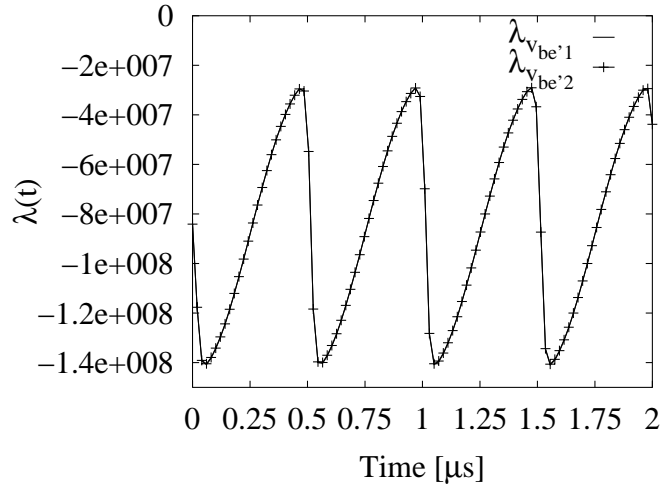


Figure 8.6: Dynamic eigenvalues $\lambda_{v_{be'1}}(t)$ and $\lambda_{v_{be'2}}(t)$ for two periods of the input signal ($V_A = 0.5V$, $f = 1MHz$ and $I_0 = 0.1\mu A$)

instantaneous relation (8.10) between the two intrinsic base-emitter voltages any disturbance in one base-emitter voltage corresponds to an equal disturbance in the other base-emitter voltage. Thus when studying the dynamic behaviour it does not matter which of the two intrinsic base-emitter voltages we choose as state variable. Note that in general the dynamic eigenvalue of a first-order system does depend on the choice of state variable, though the Floquet exponent derived from it is unique.

8.2.3 Floquet exponent

In the case of a periodic input signal v_{in} , the last step in describing the dynamic behaviour using the LTV approach consists of determining the Floquet exponent as a measure of stability. In the case of a first-order system it is found by calculating the time-average of the dynamic eigenvalue over one period of the system behaviour. The Floquet exponent was calculated for signal amplitudes V_A of $1mV$ (corresponding to a differential pair operating in its linear region) and $0.5V$ (corresponding to a differential pair operating nonlinearly as a limiter). These calculations were done for a range of signal frequencies f (Figure 8.7) and tail currents $2I_0$ (Figures 8.9 through 8.11), with $v_{be'1}$ as state variable and using Expression (8.14) for the dynamic eigenvalue. As shown in the previous paragraph, for this specific circuit the alternative choice of $v_{be'2}$ as state variable

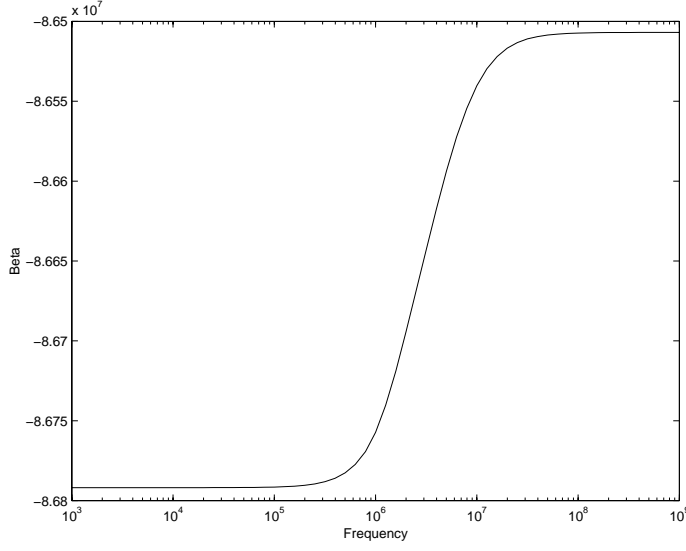


Figure 8.7: Floquet exponent as a function of the signal frequency ($V_A = 0.5V$, $I_0 = 0.1\mu A$)

results in an identical dynamic eigenvalue. Therefore, this choice is not further explored.

In Figure 8.7 the Floquet exponent β is shown as a function of the signal frequency for $V_A = 0.5V$ and $I_0 = 0.1\mu A$. The Floquet exponent is almost constant (note the very small scale difference on the y-axis). For low signal frequencies it is equal to the transit frequency of the transistors for a bias-current $I_0 = 0.1\mu A$. For higher frequencies we see a slight deviation, an effect of the nonlinear behaviour of the limiter. Note that using the LTI-model we do not find a pole at all. As depicted in Figure 8.8a., the transfer from the input voltage to either of the base-emitter voltages equals:

$$\frac{V_{be}(s)}{V_{in}(s)} = \frac{R_\pi/(1 + sR_\pi C_\pi)}{2R_\pi/(1 + sR_\pi C_\pi)} = \frac{1}{2} \quad (8.16)$$

The pole due to the input $R_\pi C_\pi$ time-constant cancels due to a zero at the same location and a frequency independent transfer from input voltage v_{in} to either of the base-emitter voltages v_{be} and to the collector currents $g_m \cdot v_{be}$ results. Of course, this latter result is physically not very realistic: for high frequencies we at least expect to see the effect of the finite speed of the transistor (diffusion capacitance). The Floquet exponent from the LTV-approach does show this finite speed. Though the topology of the input network is identical, as depicted in Figure 8.8b., the Floquet exponent does not vanish ($R_1(t) \neq R_2(t)$) and

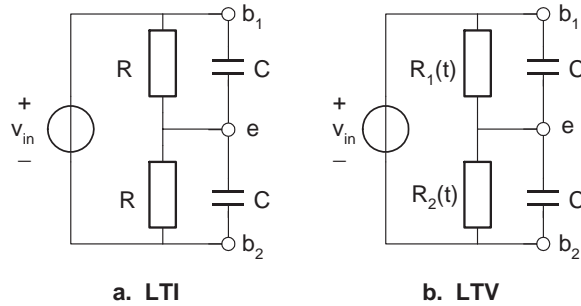


Figure 8.8: Input part of the differential pair model without base-resistance: a. LTI-model, b. LTV-model

shows that the speed is limited by the transit frequency.

In Figure 8.9 the Floquet exponent β is shown as a function of the tail current of the limiter for $V_A = 1mV$ and $f = 1MHz$. This curve is identical to a plot of the transit frequency of the transistors used as a function of their bias-current I_0 (half the tail current). In Figure 8.10 again the Floquet exponent is plotted as a function of the tail current, but now for an input amplitude V_A of $0.5V$. For this input amplitude the differential pair is really operating as a limiter. Despite the fact that for almost the entire period of the input signal either one or the other transistor in the limiter is turned off, the curve still is almost equal to the transit-frequency curves of the transistors (note that the x-axis has a different range). The relative difference with the transit-frequency curve is shown in Figure 8.11. We can conclude that in this first-order analysis the nonlinearity of the limiter has no significant effect on the stability analysis, and that the conventional LTI pole provides a good estimate for the Floquet exponent.

8.3 Second-order dynamics

In the previous section we neglected the influence of the base-resistances R_{b1} and R_{b2} , enabling the use of a first-order linear time-varying model. Now we drop this assumption and derive a second-order linear time-varying model including the base-resistances.

If we include the base-resistances we have to use the complete large-signal description of the limiter as given by the set of equations (8.9). Choosing the capacitance-voltages $v_{b'e1}$ and $v_{b'e2}$ as state variables and assuming identical transistor parameters (i.e. $R_{b1} = R_{b2} = R_b$) we obtain the following large-

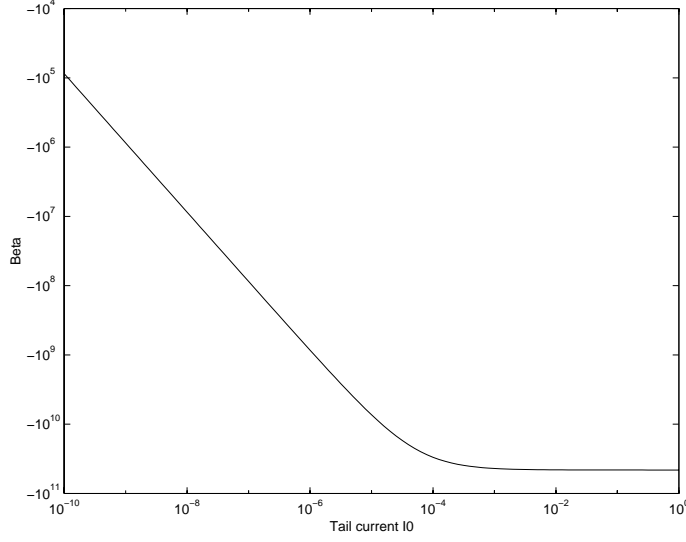


Figure 8.9: Floquet exponent as a function of tail current ($V_A = 1mV$, $f = 1MHz$)

signal state-space equation:

$$\frac{d}{dt} \begin{bmatrix} v_{b'e1} \\ v_{b'e2} \end{bmatrix} = \begin{bmatrix} f_1(v_{b'e1}, v_{b'e2}, v_{in}) \\ f_2(v_{b'e1}, v_{b'e2}, v_{in}) \end{bmatrix} \Leftrightarrow \frac{d}{dt} \mathbf{v} = \mathbf{f}(\mathbf{v}, v_{in}) \quad (8.17)$$

with

$$f_1(v_{b'e1}, v_{b'e2}, v_{in}) = \frac{-\frac{B_f+2}{B_f} R_b I_s e^{\frac{v_{b'e1}}{V_T}} - v_{b'e1} - R_b I_s e^{\frac{v_{b'e2}}{V_T}} + v_{b'e2} + 2R_b \left(I_0 + \frac{B_f+1}{B_f} I_s \right) + v_{in}}{2R_b \left(C_{jcap} + \frac{\tau_f I_s}{V_T} e^{\frac{v_{b'e1}}{V_T}} \right)}$$

and

$$f_2(v_{b'e1}, v_{b'e2}, v_{in}) = \frac{-\frac{B_f+2}{B_f} R_b I_s e^{\frac{v_{b'e2}}{V_T}} - v_{b'e2} - R_b I_s e^{\frac{v_{b'e1}}{V_T}} + v_{b'e1} + 2R_b \left(I_0 + \frac{B_f+1}{B_f} I_s \right) - v_{in}}{2R_b \left(C_{jcap} + \frac{\tau_f I_s}{V_T} e^{\frac{v_{b'e2}}{V_T}} \right)}$$

Notice that the anti-symmetric mode of operation of the two transistors in the circuit is reflected in the two nonlinear functions of the second-order state-space description: $f_2(v_{b'e1}, v_{b'e2}, v_{in}) = f_1(v_{b'e2}, v_{b'e1}, -v_{in})$.

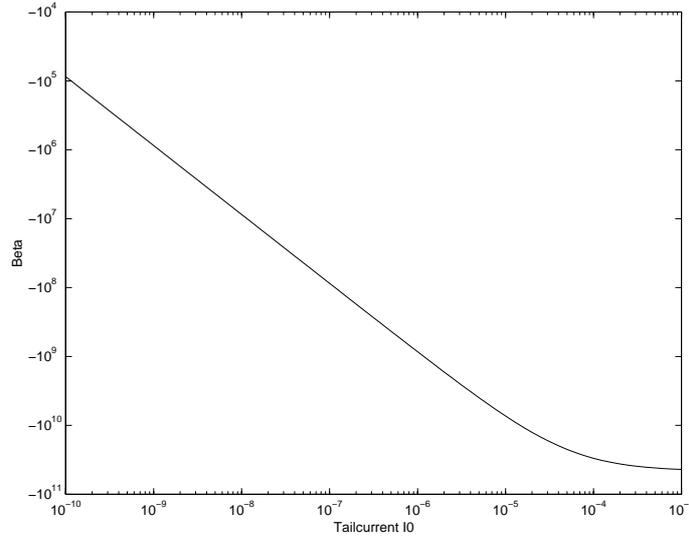


Figure 8.10: Floquet exponent as a function of tail current ($V_A = 0.5V$, $f = 1MHz$)

8.3.1 Dynamic bias-trajectory

The first step in obtaining a second-order LTV model is the determination of the dynamic bias trajectory of the state variables $v_{b'e1_b}$ and $v_{b'e2_b}$ as a function of a specific input signal v_{in_b} . This dynamic bias-trajectory is found by solving the state-space equation (8.17) for this input signal. Again we take a sinusoid as an obvious first choice of input-signal:

$$v_{in_b}(t) = V_A \sin(\omega t) = V_A \sin(2\pi f t) \quad (8.18)$$

The dynamic bias-trajectory was computed numerically for an input amplitude V_A of $0.5V$, an input frequency f of $1GHz$ and a tail current $2I_0$ of $0.2mA$ with MATLAB using variable order Runge-Kutta formulas [29] (these large values for frequency and tail current were chosen for numerical reasons). The transistor parameters used are summarized in Table 8.1. In Figure 8.12 we show the resulting dynamic bias-trajectory of $v_{b'e1_b}$ and $v_{b'e2_b}$. As expected from the anti-symmetry of the circuit, $v_{b'e2_b}$ is a time-shifted copy of $v_{b'e1_b}$, with this time-shift equal to half a period of the input signal.

8.3.2 Dynamic eigenvalues and eigenvectors

As the next step in the LTV approach for a second-order system we model the dynamic behaviour in the vicinity of the dynamic bias trajectory by determining the dynamic eigenvalues and eigenvectors of the second-order homogeneous

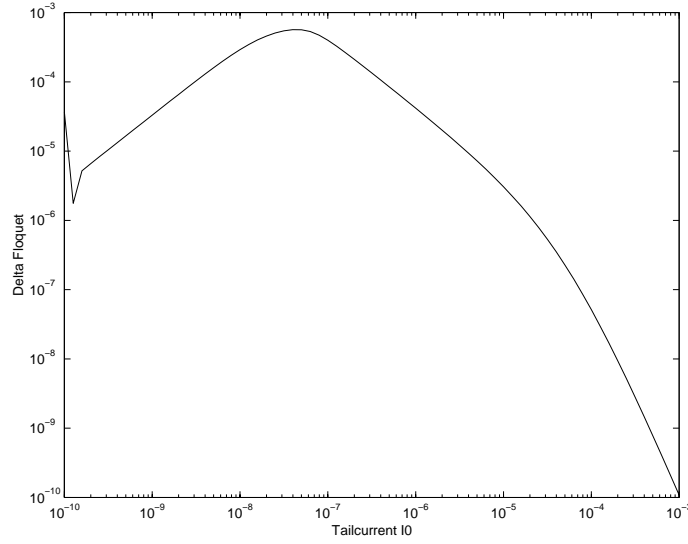


Figure 8.11: Relative difference $(\beta_1 - \beta_2)/\beta_1$ between Floquet exponents as a function of tail current, input amplitude = 1mV (β_1) and 500mV (β_2)

variational equation, as outlined in Section 5.5. This homogeneous variational equation is given by

$$\frac{d}{dt} \begin{bmatrix} v_{b'e1\delta} \\ v_{b'e2\delta} \end{bmatrix} = \begin{bmatrix} a_{11}(t) & a_{12}(t) \\ a_{21}(t) & a_{22}(t) \end{bmatrix} \begin{bmatrix} v_{b'e1\delta} \\ v_{b'e2\delta} \end{bmatrix} \Leftrightarrow \frac{d}{dt} \mathbf{v}_\delta = \mathbf{A}_v(t) \mathbf{v}_\delta \quad (8.19)$$

in which $\mathbf{A}_v(t)$ is the Jacobian of $\mathbf{f}(\mathbf{v}, v_{in})$ with respect to the state-space vector \mathbf{v} in its dynamic bias trajectory. Thus the elements of $\mathbf{A}_v(t)$ are defined as

$$a_{nm}(t) = \left. \frac{\partial f_n(v_{b'e1}, v_{b'e2}, v_{in})}{\partial v_{b'em}} \right|_{v_{b'e1}=v_{b'e1_b}, v_{b'e2}=v_{b'e2_b}, v_{in}=v_{in_b}}$$

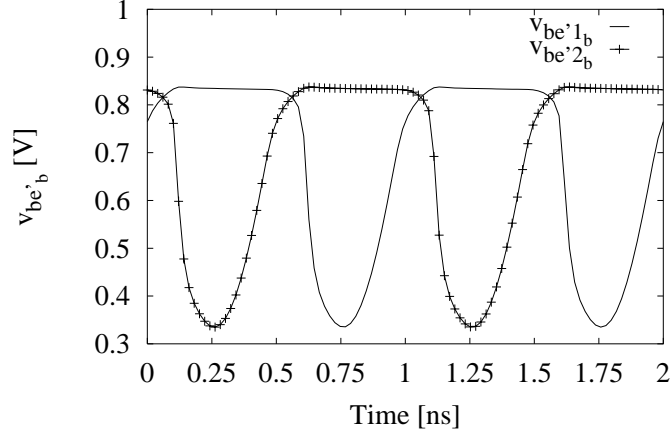


Figure 8.12: Dynamic bias-trajectory of $v_{b'e1_b}$ and $v_{b'e2_b}$ for two periods of the input signal ($V_A = 0.5V$, $f = 1GHz$ and $I_0 = 0.1mA$)

and from the large-signal state-space equation (8.17) they are found as

$$a_{11}(t) = \frac{-\frac{B_f+2}{B_f} R_b \frac{I_s}{V_T} e^{\frac{v_{b'e1_b}}{V_T}} - 1}{2R_b \left(C_{jcap} + \frac{\tau_f I_s}{V_T} e^{\frac{v_{b'e1_b}}{V_T}} \right)} - \frac{\frac{\tau_f I_s}{V_T^2} e^{\frac{v_{b'e1_b}}{V_T}} f_1(v_{b'e1_b}, v_{b'e2_b}, v_{in_b})}{\left(C_{jcap} + \frac{\tau_f I_s}{V_T} e^{\frac{v_{b'e1_b}}{V_T}} \right)},$$

$$a_{12}(t) = \frac{-R_b \frac{I_s}{V_T} e^{\frac{v_{b'e2_b}}{V_T}} + 1}{2R_b \left(C_{jcap} + \frac{\tau_f I_s}{V_T} e^{\frac{v_{b'e1_b}}{V_T}} \right)},$$

$$a_{21}(t) = \frac{-R_b \frac{I_s}{V_T} e^{\frac{v_{b'e1_b}}{V_T}} + 1}{2R_b \left(C_{jcap} + \frac{\tau_f I_s}{V_T} e^{\frac{v_{b'e2_b}}{V_T}} \right)},$$

and

$$a_{22}(t) = \frac{-\frac{B_f+2}{B_f} R_b \frac{I_s}{V_T} e^{\frac{v_{b'e2_b}}{V_T}} - 1}{2R_b \left(C_{jcap} + \frac{\tau_f I_s}{V_T} e^{\frac{v_{b'e2_b}}{V_T}} \right)} - \frac{\frac{\tau_f I_s}{V_T^2} e^{\frac{v_{b'e2_b}}{V_T}} f_2(v_{b'e1_b}, v_{b'e2_b}, v_{in_b})}{\left(C_{jcap} + \frac{\tau_f I_s}{V_T} e^{\frac{v_{b'e2_b}}{V_T}} \right)}.$$

The dynamic eigenvalues and eigenvectors of this second-order variational equation are obtained by the procedure outlined in Section 5.5.

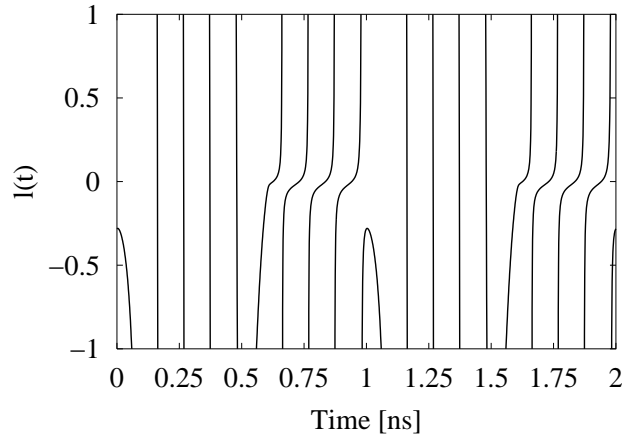


Figure 8.13: Solution of the Riccati equation $l(t)$ for two periods of the input signal ($V_A = 0.5V$, $f = 1GHz$ and $I_0 = 1mA$)

As explained in Section 5.5, in some cases the solution of the Riccati equation can contain singularities. In such cases the Riccati-equation cannot be solved directly. However, the solution of the Riccati-equation can be found by transforming this quadratic nonlinear differential equation into a second-order linear time-varying differential equation, as outlined in Appendix C. This method was used to find the transformation variables $l(t)$ and $m(t)$, and from these the dynamic eigenvalues and eigenvectors, for the second-order homogeneous variational equation (8.19).

In figures 8.13 through 8.15 we show the first transformation variable $l(t)$, the dynamic eigenvalues $\lambda_1(t)$ and $\lambda_2(t)$ and the second transformation variable $m(t)$, for the dynamic bias-trajectory corresponding to an input amplitude of $0.5V$, a frequency $1GHz$ and a tail current of $0.2mA$. We see that the dynamic eigenvalues contain singularities (resulting from singularities in the solution of the Riccati equation $l(t)$). Moreover, the second transformation variable $m(t)$ increases exponentially with time.

The singularities in the solution of the Riccati equation can be explained intuitively with reference to the qualitative analysis of solutions of the Riccati equation in [3]. There we see that the complex solution of a Riccati-equation with constant coefficients, and thus constant equilibrium points, has periodic singularities if the equilibrium points are complex conjugated and if the initial condition of the Riccati-equation is on the real axis. If the equilibrium points are real, then the solutions converge to the largest equilibrium point and thus to the real axis. In our limiter example, the equilibrium points of the Riccati

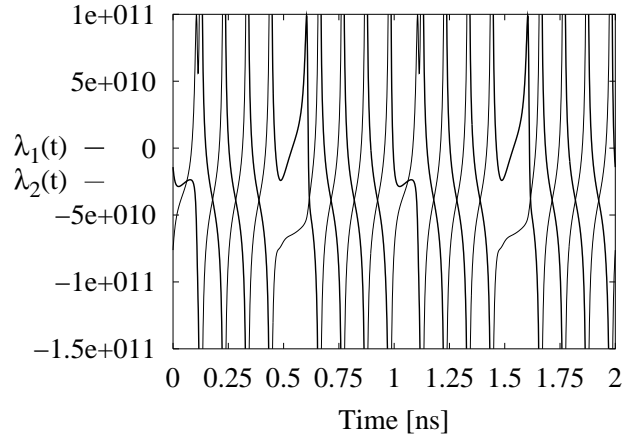


Figure 8.14: Dynamic eigenvalues $\lambda_1(t)$ and $\lambda_2(t)$ for two periods of the input signal ($V_A = 0.5V$, $f = 1GHz$ and $I_0 = 1mA$)

equation are functions of time (through the time-dependency of the coefficients of the Riccati-equation). They are real in some parts of the period and complex in the other parts of the period. During the part that the equilibrium points are real, $l(t)$ will converge to the real axis. If the equilibrium points become complex again, then $l(t)$ will have a real initial condition and will contain singularities. The singularities appear to be caused by the separate determination of closely coupled dynamic eigenvalues. A method should be found which is similar to the LTI-handling of complex poles.

Floquet exponents In the case of a periodic input signal v_{in} the last step in the LTV approach consists of determining the Floquet exponent as a measure of stability. However, in Section 5.5 it was proven that the Floquet exponents of a second-order system can only be determined directly from the dynamic eigenvalues if the dynamic eigenvectors are periodic. In Figure 8.15 we can see that for the second-order LTV model of the limiter the second transformation variable $m(t)$ increases exponentially with time. Therefore, the second dynamic eigenvector is not periodic and we cannot determine the Floquet exponents from the dynamic eigenvalues alone.

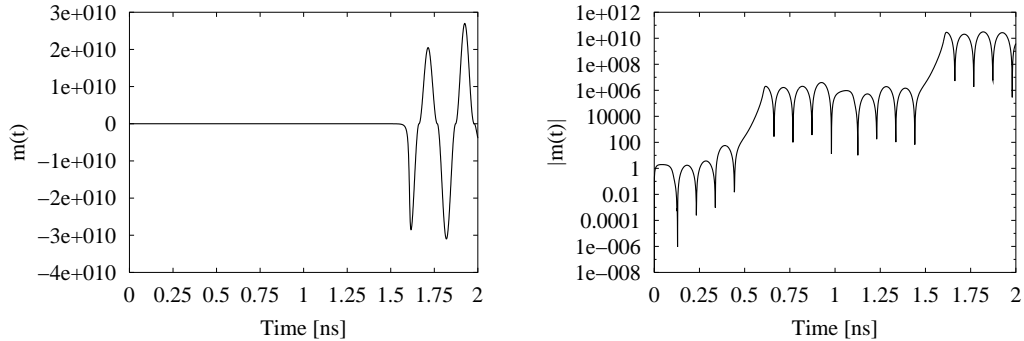


Figure 8.15: Second transformation variable $m(t)$ for two periods of the input signal, normal and logarithmic plot ($V_A = 0.5V$, $f = 1GHz$ and $I_0 = 1mA$)

8.4 Conclusions

In this chapter we applied the linear time-varying approach to a simple implementation of a voltage-to-current limiter, namely the familiar differential pair.

We derived a nonlinear large-signal model of the differential pair, using the relevant part of the Gummel-Poon model for modeling the bipolar transistors. First we ignored the base-resistances, which resulted in a first-order nonlinear model for the limiter. The dynamic bias trajectory for a sinusoidal input signal was determined, and from this the dynamic eigenvalue and Floquet exponent was calculated.

We found that the Floquet exponent is equal to the transit frequency of the transistor for the specific tail bias-current. This is quite different from the LTI-model of the differential pair without base-resistances, for which the pole cancels with a zero and which predicts a frequency independent transfer. The latter result is physically not very realistic. We expect to see at least the finite speed of the transistors used due to the base transition time, and the Floquet exponent obtained with the LTV approach does have this property.

We also found that even for a limiter which is completely switching the Floquet exponent still almost equals the transit-frequency curve of the transistors. We can conclude that in this first-order analysis the nonlinearity of the limiter has no significant effect on the stability analysis and that the LTI-pole provides a good estimate of the Floquet exponent.

When the base-resistances are not neglected, a second-order state-space model of the limiter results. Again a dynamic bias trajectory and dynamic eigenvalues were derived. In order to obtain the dynamic eigenvalues, a Riccati quadratic differential equation has to be solved. The solution turned out to have

singularities, and the transformation method elaborated in appendix C had to be used. Using this method the dynamic eigenvalues were obtained.

The second transformation variable $m(t)$, which defines the dynamic eigenvector, turned out to increase exponentially with time. Therefore, a Floquet exponent could not be determined.

A topic of future research should be to find a method for deriving the dynamic eigenvalues which does not result in singularities. The singularities appear to be caused by the separate determination of closely coupled dynamic eigenvalues. A method should be found which is similar to the LTI-handling of complex poles.

Another problem was the non-periodicity of the second transformation variable $m(t)$. A method should be found which keeps this second transformation variable normalized, such that it only changes the orientation of the dynamic eigenvectors, and not the modulus.

Conclusions

A general approach to the design of nonlinear circuits has been presented, which handles the nonlinear design complexity by dividing the design process in two main steps. The first step of the presented general approach consists of a high-level synthesis/analysis step, in which a topology implementing the wanted (nonlinear) function is found. We concluded that an expansion in basic functions, chosen to fit the nonlinear building blocks used, appears to be the best option for implementing this step.

In the second step of the design approach, a low-level analysis/synthesis step, the quality of the topologies is investigated and the effect of non-idealities on the instantaneous behaviour, noise behaviour and dynamic behaviour is determined. The linear time-varying small-signal model—or, if the signals are sufficiently small, the linear time-invariant small-signal model—has been chosen for this second step, since it can decrease complexity by letting the model be dependent on the input signals and only modeling the effect of small deviations, and since it can give insight to the designer.

The linear time-varying (LTV) approach generalizes the conventional linear time-invariant small-signal modeling approach by describing the behaviour of a nonlinear circuit in the neighbourhood of an (input-signal dependent) dynamic bias trajectory rather than a (DC-input dependent) bias point. The LTV small-signal model, obtained by linearizing the behaviour of the nonlinear circuit in its signal-dependent dynamic bias trajectory, is exact in the trajectory, despite of the (time-varying) linearization involved: the next point in the linearization is determined by the signal-dependent dynamic bias trajectory, which incorporates the large-signal behaviour of the nonlinearities in the time evolution of the state variables.

Deviations in instantaneous behaviour, internally generated noise and deviation in dynamic behaviour can be incorporated in the LTV small-signal model.

The determination of the dynamic behaviour of the state-variables from the homogeneous variational equation, and its description in terms of time-domain modes, is the first and most important step in any analysis using the LTV small-signal model. Any subsequent analysis of the effect of deviations in amplitude behaviour and of internally generated noise from the nonhomogeneous variational equation uses these results: the same time-domain modes are present in the small-signal and noise expressions derived from the nonhomogeneous variational equation. Therefore, this thesis focuses on the description of the dynamic behaviour of a circuit using the time-domain modes of the homogeneous variational equation.

For linear systems with arbitrary time-varying coefficients the modes are defined by dynamic eigenvalues and eigenvectors, which can be obtained from a generalized characteristic equation. When the coefficients are slowly-varying, a frozen time approach can be used and quasi-static eigenvalues and eigenvectors are obtained. The solutions of a general LTV system are stable if the Lyapunov exponents of all its modes are negative. This stability criterion based on Lyapunov exponents was shown to simplify to the stability criterion based on Floquet exponents for periodic LTV systems and to the familiar stability criterion based on poles for LTI systems.

For second-order variational equations a method was shown which uses the solution of a Riccati differential equation in order to derive the dynamic eigenvalues. A transformation method was given in order to obtain this solution, even if it contains singularities.

The linear time-varying approach was applied in the design of three classes of circuits. First, we applied the linear time-varying approach to the design of a negative-feedback amplifier with class-B output stage. By considering three regions of operation of the class-B stage (relatively low frequencies with instantaneous behaviour; relatively high frequencies and large input amplitudes with behaviour dominated by diffusion capacitors; relatively high frequencies and small signal amplitudes with behaviour dominated by junction capacitors), we were able to find some explicit expressions for the dynamic bias trajectory, dynamic eigenvalue and Floquet exponent of the class-B stage. We were able to generate a plot of the Floquet exponent versus the input signal amplitude, for various input signal frequencies, in which we were able to give explicit expressions for the asymptotes. This enables a fast evaluation of the dynamic behaviour of the class-B stage. The push-pull class-B output stage was applied in a low-voltage low-power balanced transimpedance amplifier, and the linear time-varying approach was used for examining the dynamic behavior. The measured bandwidth of the built amplifier was in correspondence with the calculated Floquet exponents. An intuitive explanation of the transfer characteristics could be given, using the knowledge of the class-B stage dynamic behaviour.

Second, we applied the linear time-varying approach to analyze the dynamic

behaviour of dynamic translinear (DTL) circuits in the presence of parasitics. DTL synthesis and analysis are based on the nonlinear input-output relation of the transistor. Therefore, the system behaviour in the presence of parasitics is often defined by nonlinear differential equations, even if the ideal overall transfer function is linear. We used the LTV approach for handling these nonlinear differential equations for the low-level analysis/synthesis of two example DTL circuits: a first-order DTL filter and a DTL oscillator. Through the example of a first-order linear DTL filter it has been shown that the linear time-varying approach is a useful method for analyzing DTL circuits in the presence of parasitics. We applied the linear time-varying approach to analyze the dynamic behaviour of the DTL filter in the presence of parasitic capacitors and compared the results with the quasi-static and LTI approach. The dynamic eigenvalue of the DTL filter was shown to converge to the designed ideal linear pole if the parasitics vanish, which is a required property. The time-varying pole of the quasi-static approach does not have this property. If the DTL filter is operating under slowly-varying conditions the quasi-static pole was shown to be equal to the dynamic eigenvalue. The example of a DTL oscillator was chosen because the nonlinearity in the differential equation describing this circuit is not a consequence of parasitic effects, but rather a conscious design choice. Neither the quasi-static nor the LTI approach can be applied to analyze this oscillator since its operation is based on an instantaneous control action. The dynamic eigenvalues, which contain periodic singularities, were derived using a transformation method. The Floquet exponents were derived from these dynamic eigenvalues; they correspond to the properties of a stable limit cycle. This confirms the consistency of the method used.

Third, we applied the linear time-varying approach to the familiar differential pair, which when driven with a sufficiently large input signal is a simple implementation of a voltage-to-current limiter. When the base-resistances are ignored, a first-order nonlinear model for the limiting differential pair results, and we found that the Floquet exponent is equal to the transit frequency of the transistor for the specific tail bias-current. This is quite different from the LTI-model of the differential pair without base-resistances, for which the pole cancels out and which predicts a frequency independent transfer. The latter result is physically not very realistic. We expect to see at least the finite speed of the transistors used, and the Floquet exponent obtained with the LTV approach does have this property. We also found that even for a differential pair which is completely switching the Floquet exponent still almost equals the transit-frequency curve of the transistors. We can conclude that in this first-order analysis the nonlinearity of the limiting differential pair has no significant effect on the stability analysis and that the LTI-pole provides a good estimate of the Floquet exponent. When the base-resistances are not neglected, a second-order state-space model of the limiting differential pair results. In order to

obtain the dynamic eigenvalues, the transformation method elaborated in appendix C had to be used, since the solution of the Riccati equation contained singularities. The second transformation variable $m(t)$, which defines the dynamic eigenvector, turned out to increase exponentially with time. Therefore, a Floquet exponent could not be determined.

Through the design examples treated the LTV approach has been shown to be a good modeling candidate for low-level analysis/synthesis. Especially the explicit asymptotes and expressions for the Floquet exponent of the class-B stage and of the dynamic translinear filter would be very useful in nonlinear circuit design. A topic of future research should be to find a method for deriving the dynamic eigenvalues which does not result in singularities. The singularities appear to be caused by the separate determination of closely coupled dynamic eigenvalues. A method should be found which is similar to the LTI-handling of complex poles. Another open problem was the non-periodicity of the second transformation variable $m(t)$ for a periodic variational equation. A method should be found which keeps this second transformation variable normalized, such that it only changes the orientation of the dynamic eigenvectors, and not the modulus.

A

Lyapunov transformations

In Section 5.3.4 we introduced the concepts of dynamic eigenvalues and dynamic eigenvectors of LTV systems. For this we need the notion of time-varying transformations of LTV systems. Lyapunov transformations are a subset of these. First we review time-invariant transformations of LTI systems and then generalize this concept to time-varying transformation. Finally the properties of Lyapunov transformations are discussed.

The analysis of the dynamic behaviour of LTI systems in section 5.3.2 was based on a similarity relation using the constant matrix \mathbf{S} which expresses the transition matrix \mathbf{A} in its Jordan canonical form (see Equation (5.35)). Using this relation we found an expression for the modes of an LTI system.

Equivalently this matrix \mathbf{S} can be considered to define the time-invariant transformation

$$\mathbf{x}(t) = \mathbf{S} \cdot \mathbf{y}(t) \quad (\text{A.1})$$

which transforms the system

$$\frac{d}{dt}\mathbf{x}(t) = \mathbf{A} \cdot \mathbf{x}(t) \quad (\text{A.2})$$

into the system

$$\frac{d}{dt}\mathbf{y}(t) = \mathbf{A}_y \cdot \mathbf{Y}(t) \quad (\text{A.3})$$

Combining Equations (A.1) and (A.2) it is easily shown that the new transition matrix \mathbf{A}_y is given by

$$\mathbf{A}_y = \mathbf{S}^{-1} \mathbf{A} \mathbf{S} \quad (\text{A.4})$$

The relation (A.4) between the matrices \mathbf{A} and \mathbf{A}_y is called *static similarity*. That is, both matrices have the same eigenvalues. Since \mathbf{S} contains the eigenvectors of \mathbf{A} , the transformed state transition matrix \mathbf{A}_y equals the Jordan canonical form (5.35) of \mathbf{A} . If a simple mode of the transformed system is given by $\mathbf{i}_k \cdot \exp(\lambda_k t)$ (where \mathbf{i}_k is the n^{th} -order unit vector with $i_k[k] = 1$) then the corresponding mode of the original system is given by $\mathbf{s}_k \cdot \exp(\lambda_k t)$.

Let us now consider the LTV system

$$\frac{d}{dt}\mathbf{x}(t) = \mathbf{A}(t) \cdot \mathbf{x}(t) \quad (\text{A.5})$$

where

$$\mathbf{x}(t) \in \mathcal{C}^n, \quad \mathbf{A}(t) \in C[t_0, \infty), \quad \sup_{t \geq 0} \|\mathbf{A}(t)\| \leq M$$

and a time-varying transformation defined by the nonsingular and continuously differentiable for $t \geq 0$ matrix $\mathbf{T}(t)$

$$\mathbf{x}(t) = \mathbf{T}(t) \cdot \mathbf{y}(t) \quad (\text{A.6})$$

This transformation transforms (A.5) into the system

$$\frac{d}{dt}\mathbf{y}(t) = \mathbf{A}_y(t) \cdot \mathbf{y}(t) \quad (\text{A.7})$$

Inserting (A.6) into (A.5) we find for the transition matrix of the transformed system

$$\mathbf{A}_y(t) = \mathbf{T}^{-1}(t)\mathbf{A}(t)\mathbf{T}(t) - \mathbf{T}^{-1}(t)\frac{d}{dt}\mathbf{T}(t) \quad (\text{A.8})$$

The relation (A.8) between the matrices $\mathbf{A}(t)$ and $\mathbf{A}_y(t)$ is called *kinematic similarity*. In section 5.3.4 we saw that this means that $\mathbf{A}(t)$ and $\mathbf{A}_y(t)$ have the same dynamic eigenvalues. Note that in relation (A.8) the time-derivative of the transformation matrix $\mathbf{T}(t)$ is present. For constant $\mathbf{T}(t) \triangleq \mathbf{T}$ this time-derivative equals zero and we again find a static similarity between $\mathbf{A}(t)$ and $\mathbf{A}_y(t)$.

Lyapunov transformations are a subset of kinematic similarity transformations which ensure that system (A.5) remains in the class of systems with bounded coefficients. For this it is necessary to strengthen the conditions on the matrix $\mathbf{T}(t)$. The time-varying transformation

$$\mathbf{x}(t) = \mathbf{L}(t) \cdot \mathbf{y}(t) \quad (\text{A.9})$$

is called a *Lyapunov transformation* if

1. $\mathbf{L}(t) \in C^1[t_0, \infty)$,

2. $\mathbf{L}(t)$, $\mathbf{L}^{-1}(t)$, $\frac{d}{dt}\mathbf{L}(t)$ are bounded for $t \geq t_0$.

The most important property of Lyapunov transformations is that they do not change dynamic eigenvalues (see section 5.3.4) and Lyapunov exponents (see section 5.3.5). In sections 5.5 and 5.6 we use Lyapunov transformations to transform an LTV-system to an upper-triangular or diagonal form, which enables the determination of these dynamic eigenvalues and Lyapunov exponents.

B

Dynamic eigenvalues using quasi-static similarity-transforms

In section 5.5.1 we saw that we need to solve a Riccati differential equation to obtain a Lyapunov transformation which directly triangularizes the transition matrix of a second-order variational equation. An alternative approach of calculating the dynamic eigenvalue was given by Wu [52]. There the author obtained the dynamic eigenvalues and eigenvectors by an iteration procedure where in each step a quasi-static problem is solved. In this method we do not need to solve a Riccati differential equation to obtain the parameters for a Lyapunov transformation, but we obtain a diagonalized transition matrix as the limiting matrix in a series of quasi-static similarity transforms.

Consider the second-order variational state-space equation

$$\frac{d}{dt}\mathbf{x}(t) = \mathbf{A}(t) \cdot \mathbf{x}(t) \quad (\text{B.1})$$

We aim to find a Lyapunov transformation

$$\mathbf{x}(t) = \mathbf{L}(t) \cdot \mathbf{y}(t) \quad (\text{B.2})$$

such that the transformed transition matrix $\mathbf{A}_y(t)$ is diagonal:

$$\begin{aligned} \mathbf{A}_y(t) &= \mathbf{L}^{-1}(t) \cdot \mathbf{A}(t) \cdot \mathbf{L}(t) - \mathbf{L}^{-1}(t) \cdot \dot{\mathbf{L}}(t) \\ &= \Lambda(t) \end{aligned} \quad (\text{B.3})$$

As a first approximation we compute the quasi-static eigenvalues and eigenvectors of $\mathbf{A}(t)$ and use these to define a quasi-static similarity transformation.

That is, we 'freeze' the time-dependency of the elements of $\mathbf{A}(t)$ and compute eigenvalues and eigenvectors with time as a parameter. We use the obtained quasi-static similarity transformation $\mathbf{T}_{(0)}(t)$ as a first approximation $\mathbf{L}_{(0)}(t)$ of the desired Lyapunov transformation $\mathbf{L}(t)$.

In general the resulting transformed transition matrix $\mathbf{A}_{y^{(1)}}(t)$ will not be diagonal, due to the term containing $\dot{\mathbf{T}}_{(0)}(t)$ in (B.3). For linear time-invariant systems however this term vanishes, since in this case $\mathbf{T}_{(0)}(t)$ is a constant matrix, and we obtain the correct Lyapunov transformation in one step. For linear time-variant systems we iterate by applying the same quasi-static approximation to the new transition matrix $\mathbf{A}_{y^{(j)}}(t)$ (with $j = 1 \cdots k$) until the transition matrix is diagonal in step k . The correct Lyapunov transformation is equal to the product of the quasi-static similarity transformations.

Thus we get the following algorithm.

Step 1 Let $j = 0$ and let $\mathbf{A}_{y^{(j)}}(t) = \mathbf{A}_x(t)$.

Step 2 Compute the quasi-static eigenvalues and eigenvectors of $\mathbf{A}_{y^{(j)}}(t)$ and use these to compose the transformation matrix $\mathbf{T}_{(j)}(t)$ such that

$$\mathbf{A}_{y^{(j)}}(t) = \mathbf{T}_{(j)}(t) \cdot \Lambda_{(j)}(t) \cdot \mathbf{T}_{(j)}^{-1}(t) \quad (\text{B.4})$$

Step 3 Use this transformation matrix to perform the Lyapunov transformation

$$\begin{aligned} \mathbf{y}_{(j)}(t) &= \mathbf{L}_{(j)}(t) \cdot \mathbf{y}_{(j+1)}(t) \\ &= \mathbf{T}_{(j)}(t) \cdot \mathbf{y}_{(j+1)}(t) \end{aligned} \quad (\text{B.5})$$

to obtain the new transition matrix

$$\begin{aligned} \mathbf{A}_{y^{(j+1)}}(t) &= \mathbf{T}_{(j)}^{-1}(t) \cdot \mathbf{A}_{(j)}(t) \cdot \mathbf{T}_{(j)}(t) - \mathbf{T}_{(j)}^{-1}(t) \cdot \dot{\mathbf{T}}_{(j)}(t) \\ &= \Lambda_{(j)}(t) - \mathbf{T}_{(j)}^{-1}(t) \cdot \dot{\mathbf{T}}_{(j)}(t) \end{aligned} \quad (\text{B.6})$$

$$= \Lambda_{(j)}(t) - \mathbf{E}_{(j)}(t) \quad (\text{B.7})$$

Step 4 If $\mathbf{E}_{(j)}(t) = \mathbf{0}$ we have found the desired diagonal transition matrix $\mathbf{A}_y(t)$ of equation (B.3)

$$\mathbf{A}_y(t) = \mathbf{A}_{y^{(j+1)}}(t) = \Lambda_{(j)}(t) = \Lambda(t) \quad (\text{B.8})$$

and the diagonalizing Lyapunov transformation is given by

$$\mathbf{L}(t) = \mathbf{T}_{(0)}(t) \cdots \mathbf{T}_{(j)}(t) \quad (\text{B.9})$$

If $\mathbf{E}_{(j)}(t) \neq \mathbf{0}$, then $\mathbf{A}_{y^{(j+1)}}(t)$ is not diagonal, let $j = j + 1$ and go back to **Step 2**.

The dynamic eigenvalues are equal to the diagonal elements of the diagonalized transition matrix $\Lambda(t)$, and using this algorithm we can obtain them without the need to solve a Riccati differential equation.

C

Transformation of the Riccati differential equation

In section 5.5.1 we described a systematic method to obtain the dynamic eigenvalues and eigenvectors for the second-order variational equation (5.78). It starts with a triangularization of the transition matrix of the variational equation, such that the dynamic eigenvalues are easily obtained as the main diagonal elements of the triangularized transition matrix. In order to find the dynamic similarity transformation (5.79) which triangularizes the transition matrix, we need to solve the Riccati differential equation (5.80), which is repeated below:

$$\frac{d}{dt} l(t) = -a_{12}(t) l^2(t) - [a_{11}(t) - a_{22}(t)] l(t) + a_{21}(t). \quad (\text{C.1})$$

In general this equation has no analytical solution. Even numerical calculation is difficult as singularities (finite escape times) may be involved. In order to facilitate the calculations, we here introduce an integral transformation, which transforms the quadratic Riccati differential equation into a second-order linear time-varying differential equation.

We introduce the new variable $u(t)$ as

$$u(t) = e^{\int_0^t a_{12}(\tau) l(\tau) d\tau} \iff a_{12}(t) l(t) = \frac{\frac{d}{dt} u(t)}{u(t)}. \quad (\text{C.2})$$

By applying (C.2), the Riccati differential equation (C.1) is transformed into the following second-order linear time-varying differential equation:

$$\begin{aligned} -a_{12}(t) \frac{d^2}{dt^2} u(t) + \left\{ \frac{d}{dt} a_{12}(t) - a_{12}(t) [a_{11}(t) - a_{22}(t)] \right\} \frac{d}{dt} u(t) \\ + a_{12}^2(t) a_{21}(t) u(t) = 0 \end{aligned} \quad (\text{C.3})$$

This transformed Riccati differential equation can on turn be written in the state-space formulation

$$\begin{cases} \frac{d}{dt} u(t) = q(t) \\ \frac{d}{dt} q(t) = \left[\frac{\frac{d}{dt} a_{12}(t) - a_{12}(t)[a_{11}(t) - a_{22}(t)]}{a_{12}(t)} \right] q(t) + a_{12}(t) a_{21}(t) u(t) \end{cases} \quad (\text{C.4})$$

This new set of differential equations does not necessarily have to be solved as a separate step, following the determination of the dynamic bias trajectory by evaluation of the original nonlinear state-space description. Rather the transformed Riccati state-space description (C.4) can be explicitly written in terms of the parameters of the original nonlinear system (5.1). Then the new state-space equations (C.4) can be added to this original nonlinear state-space system (5.1): a fourth-order state-space system results. This fourth-order system is evaluated in order to simultaneously find both the dynamic bias trajectory $[x_{b1}(t), x_{b2}(t)]$ and the transformation state variables $[u(t), q(t)]$, respectively. The solution of the Riccati equation $l(t)$ is given by

$$l(t) = \frac{1}{a_{12}(t)} \frac{q(t)}{u(t)} \quad (\text{C.5})$$

while the dynamic eigenvalues follow from Equation (5.82).

If the dynamic eigenvalues and eigenvectors are periodic (as is the case for most of the examples in this thesis), we can use Equation (5.92) to determine the Floquet exponents. In order to calculate these exponents directly from the solution of the transformed Riccati equation, we rewrite Equation (C.2) as

$$\int^t a_{12}(\tau) l(\tau) d\tau = \ln[u(t)] \quad (\text{C.6})$$

Then, substitution of Equation (C.6) in Expression (5.82) for the dynamic eigenvalues, and using Equation (5.92) to derive the Floquet exponents yields

$$\begin{cases} \beta_1 = \frac{1}{T} \ln(u)|_{t'}^{t'+T} + \frac{1}{T} \int_0^T a_{11}(\tau) d\tau \\ \beta_2 = -\frac{1}{T} \ln(u)|_{t'}^{t'+T} + \frac{1}{T} \int_0^T a_{22}(\tau) d\tau \end{cases} \quad (\text{C.7})$$

where β_1 and β_2 are the two Floquet exponents of the second-order system.

Bibliography

- [1] R.W. Adams, *Filtering in the log domain* , 63rd Convention A.E.S., New York, May 1979, preprint 1470.
- [2] L.Y. Adrianova, *Introduction to linear systems of differential equations* , American Math. Soc., Providence, 1995.
- [3] M.A.G. de Anda, *A study of the time-varying eigenvalues and their application in circuit design*, Ph.D. thesis, Delft University of Technology, 2003.
- [4] R. Bellman, J. Bentsman and S.M. Meerkov, *Stability of fast periodic systems* , IEEE Trans. AC, Vol. 30(3), pp. 289-291, 1985.
- [5] S. Bittanti, A.J. Laub and J.C. Willems (Eds), *The Riccati Equation* , Springer-Verlag, 1991.
- [6] H.K. Carlin, *Singular network elements*, IEEE Trans. CAS, Vol. 11(3), pp. 67-72, 2001.
- [7] T.H.A.J. Cordenier, *Ontwerp van een negative-feedback, class-B, eindversterker vor de 1 V lange golf radio*, Master's thesis, Delft University of Technology, 1998.
- [8] F.M. Diepstraten, F.C.M. Kuijstermans, A. van Staveren, P. van der Kloet, F.L. Neerhoff, C.J.M. Verhoeven and A.H.M van Roermund, *Dynamic Behaviour of Dynamic Translinear circuits; the Linear Time-Varying Approximation*, IEEE Trans. CAS-I, Vol. 48(11), pp. 1333-1337, 2001.
- [9] E.M. Drakakis, A.J. Payne and C. Toumazou, *"Log-domain state-space": A systematic transistor-level approach for log-domain filtering*, IEEE Trans. CAS-II, Vol. 46(3), pp. 290-305, March 1999.
- [10] T. Falk, F.C.M. Kuijstermans and A. van Staveren, *Investigation of the stability properties of a class of oscillators using Lyapunov transformations*, Proceedings NDES'99, pp. 221-224, Rønne, Denmark, July 1999.
- [11] M. Farkas, *Periodic Motions* , Springer-Verlag, New York, 1994.
- [12] R. Fox, M. Nagarajan and J. Harris, *Practical design of single-ended log-domain filter circuits* , Proceedings ISCAS'97, Vol. 1, pp. 341-344, May 1997.
- [13] D.R. Frey, *Exponential State Space Filters: A Generic Current Mode Design Strategy*, IEEE Trans. on Circuits and Systems I, Vol. 43(1), pp. 34-42, 1996.
- [14] D.R. Frey, *Log-domain filtering: An approach to current mode filtering* , Proceedings Inst. Elect. Eng. G., Vol. 140(6), pp. 406-416, Dec. 1993.
- [15] D.R. Frey and L. Steigerwald, *An adaptive notch filter using log filtering* , Proceedings ISCAS'96, Vol. I, pp. 297-300, May 1996.
- [16] D.R. Frey, *Explicit log domain root-mean-square detectors* , U.S. Patent 5 585 757, Dec. 1996.

- [17] I. Getreu, *Modeling the Bipolar Transistor*, Elsevier, Amsterdam, 1978.
- [18] B. Gilbert, *Translinear circuits: A proposed classification*, Elec. Letters, Vol. 11(1), pp. 14-16, Jan. 1975.
- [19] J.K. Hale, *Oscillations in nonlinear systems*, McGraw-Hill, New York, 1963.
- [20] E.W. Kamen, *The poles and zeros of a linear time-varying system*, Lin. Algebra and its Appl., Vol 98, pp. 263-289, 1988.
- [21] P. van der Kloet, F.L. Neerhoff, *On eigenvalues and poles for second-order linear time-varying systems*, Proceedings NDES'97, pp. 300-305, Moscow, 1997.
- [22] P. van der Kloet, F.L. Neerhoff and M. de Anda, *The dynamic characteristic equation*, Proceedings NDES'2002, pp. 77-80, Delft, the Netherlands, 2002.
- [23] P. van der Kloet, F.L. Neerhoff, *Private communications*, 1998.
- [24] F.C.M. Kuijstermans, A. van Staveren, P. van der Kloet, F.L. Neerhoff, C.J.M. Verhoeven, *Dynamic Exponent-based Electronics*, Proceedings CSSP'97, pp. 307-315, Mierlo, 1997.
- [25] F.C.M. Kuijstermans, F.M. Diepstraten, W.A. Serdijn, P. van der Kloet, A. van Staveren, and A.H.M. van Roermund, *The linear time-varying approach applied to a first-order dynamic translinear filter*, Proceedings ISCAS'99, Vol. VI, pp. 69-72, Orlando, June 1999.
- [26] E.K. de Lange, A. van Staveren, O. De Feo, F.L. Neerhoff, M. Hasler and J.R. Long, *Predicting nonlinear distortion in common-emitter stages for amplifier design*, Proceedings NDES'02, pp. 2-41-2-44, 2002.
- [27] T. Larsen, *Determination of Volterra transfer functions of non-linear multi-port networks*, Int. J. Circuit Theory and Applications, Vol. 21(2), pp. 107-131, 1993.
- [28] V.W. Leung, M. El-Gamal and G.W. Roberts, *Effects of transistor non-idealities on log-domain filters*, Proceedings ISCAS'98, Vol. I, pp.109-112, May 1998.
- [29] *MATLAB Reference Guide*, The Mathworks Inc., Nattick, Mass., 1992.
- [30] *Mathcad Plus 6.0*, Professional edition.
- [31] J. Mulder, W.A. Serdijn, A.C. van der Woerd and A.H.M van Roermund, *Dynamic Translinear circuits - An overview*, Proceedings ISIC, pp. 31-38, Singapore, September 1997.
- [32] J. Mulder, W.A. Serdijn, A.C. van der Woerd and A.H.M van Roermund, *Dynamic Translinear and Log-domain Circuits: analysis and synthesis*, Kluwer Academic Publishers, Boston, 1999.
- [33] J. Mulder, M.H.L. Kouwenhoven, W.A. Serdijn, A.C. van der Woerd and A.H.M van Roermund, *Nonlinear analysis of noise in static and dynamic translinear circuits*, IEEE Trans. on CAS II, Vol. 46(3), pp. 266-278, March 1999.
- [34] J. Mulder, A.C. van der Woerd, W.A. Serdijn and A.H.M van Roermund, *An RMS-DC converter based on the dynamic translinear principle*, Proceedings ESSIRC'96, pp. 312-315, Sept. 1996.
- [35] J. Mulder, A.C. van der Woerd, W.A. Serdijn and A.H.M van Roermund, *General Current-Mode Analysis Method for Translinear Filters*, IEEE Trans. on Circuits and Systems I, Vol. 44(3), pp. 193-197, 1997.
- [36] J. Mulder, W.A. Serdijn and A.H.M van Roermund, *Analysis and synthesis of dynamic translinear circuits*, Proceedings ECCTD'97, Budapest 1997.
- [37] M.S. Nakla and J. Vlach, *A piecewise harmonic balance technique for the determination of the periodic response of nonlinear systems*, IEEE Trans. on Circuits and Systems, Vol. 23(2), pp. 58-91, 1976.

- [38] L.K. Nanver, E.J.G. Goudena and H.W. van Zeijl, *DIMES-01, a baseline BIFET process for smart sensors experimentation*, Sensors and Actuators Physical, Vol. 36(2), pp. 139-147, 1993.
- [39] E.H. Nordholt, *Design of High-Performance Negative-Feedback amplifiers*, Elsevier, Amsterdam, 1983.
- [40] D. Perry and G.W. Roberts, *The design of log-domain filters based on the operational simulation of LC ladders*, IEEE Trans. on CAS I, Vol. 43(11), pp. 763-773, Nov. 1996.
- [41] S. Pookaiyaudom and J. Mahattanakul, *A 3.3 volt high frequency capacitorless electronically tunable log-domain oscillator*, Proceedings ISCAS'95, Vol. I, pp. 829-832, May 1995.
- [42] D.H. Sattinger, *Topics in Stability and Bifurcation Theory*, Springer Verlag, Berlin, 1973.
- [43] E. Seevinck, *Companding current-mode integrator: A new circuit principle for continuous-time monolithic filters*, Electron. Lett., Vol 26(2), pp. 2046-2047, Nov. 1990.
- [44] W.A. Serdijn, M. Broest, J. Mulder, A.C. van der Woerd and A.H.M. van Roermund, *A low-voltage ultra-low-power current-companding integrator for audio filter applications*, Proceedings ESSIRC'96, pp. 412-415, Sept. 1996.
- [45] W.A. Serdijn, J. Mulder, A.C. van der Woerd and A.H.M. van Roermund, *A wide-tunable translinear second-order oscillator*, IEEE Journal of Solid-State Circuits, Vol. 33(2), pp. 195-201, February 1998.
- [46] W.A. Serdijn, J. Mulder and A.H.M. van Roermund, *Dynamic translinear circuits*, Proceedings Workshop on Advances in Analog Circuit Design, April 1998.
- [47] A. van Staveren, T.H.A.J. Cordenier, F.C.M. Kuijstermans, P. van der Kloet, F.L. Neerhoff, C.J.M. Verhoeven and A.H.M. van Roermund, *The Linear Time-Varying Approach applied to the design of a Negative-Feedback Class-B Output Amplifier*, Proceedings ISCAS'99, Vol. II, pp. 204-207, Orlando, June 1999.
- [48] A. Thanachayanont, A. Payne and S. Pookaiyaudom, *A current-mode phase-locked loop using a log-domain oscillator*, Proceedings ISCAS'97, Vol. I, pp. 277-280, June 1997.
- [49] C.J.M. Verhoeven, A. van Staveren and G.L.E. Monna, *Structured electronic design, negative-feedback amplifiers*, Lecture notes et04-33, Delft University of Technology, 1996.
- [50] L. Weiss and W. Matthis, *Nonlinear non equilibrium thermodynamics of nonlinear electrical networks*, Proc. ECCTD'97, pp. 185-190, 1997
- [51] J.R. Westra, C.J.M. Verhoeven and A.H.M. van Roermund, *High-performance oscillators and oscillator systems*, Kluwer Academic Publishers, Dordrecht, the Netherlands, January 2000.
- [52] M.Y. Wu, *On the stability of linear time-varying systems*, Int. J. Systems Sci., Vol. 15(2), pp.137-150, 1984.
- [53] M.Y. Wu, *A new concept of eigenvalues and eigenvectors and its applications*, IEEE Trans. Automat. Control, Vol. 25(4), pp. 824-826, 1980.
- [54] J. Zhu and C.D. Johnson, *New results in the reduction of linear time varying dynamical systems*, SIAM J. Contr. and Optm., Vol. 27(3), pp. 476-494, 1989.

Summary

Over the last years interest in the design of nonlinear electronic circuits has been steadily increasing. The use of nonlinear relations as primitives for the synthesis of electronics inherently implies that we have to deal with analysis and synthesis of dynamic nonlinear circuits. For circuits with a strong nonlinearity no structured design approach is available.

A general approach to the structured design of nonlinear circuits was presented in Chapter 2. Nonlinearities were classified based on their instantaneous behaviour and dynamic behaviour. The general synthesis/analysis approach presented handles the nonlinear design complexity by dividing the design process in two main steps: a high-level synthesis/analysis step and a low-level analysis/synthesis step.

The first step of the presented general synthesis/analysis approach consists of a high-level synthesis/analysis step and is covered in Chapter 3. In this step a topology implementing the wanted (nonlinear) function is found. Simple models and if possible a synthesis path specific to the nonlinearities are used in order to perform a fast exploration of the design space. Several modeling approaches for implementing this high-level design step were considered. An expansion in basic functions, chosen to fit the nonlinear building blocks used, appears to be the best option for implementing this step.

The second step of the design approach is dealt with in Chapter 4. In this low-level analysis/synthesis step the quality of the topologies is investigated and the effect of non-idealities on the instantaneous behaviour, noise behaviour and dynamic behaviour is determined. In the low-level step we might need to use more detailed models than in the high-level step, in order to cover the perturbed behaviour. However, since large-signal behaviour is covered in the high-level step, only the effect of small deviations needs to be modeled, and knowledge from the high-level step should be used to decrease complexity. Also we would like a modeling approach which provides a close link between the model and the physical layer, in order to give the designer insight in what to do to improve performance, if necessary. The linear time-varying small-signal model—or, if the signals are sufficiently small, the linear time-invariant small-signal model—

has these properties by letting the model be dependent on the input signals and only modeling the effect of small deviations. It is a good modeling candidate in the context of low-level analysis/synthesis, and is the focus of this thesis.

The linear time-varying (LTV) approach, as treated in Chapter 5, generalizes the conventional linear time-invariant (LTI) small-signal modeling approach by describing the behaviour of a nonlinear circuit in the neighbourhood of an (input-signal dependent) dynamic bias trajectory rather than a (DC-input dependent) bias point. The linear time-varying small-signal model is obtained by linearizing the behaviour of the nonlinear circuit in its signal-dependent dynamic bias trajectory. This modeling approach is exact in the dynamic bias trajectory, despite of the (time-varying) linearization involved, because the next point in the linearization is determined by the signal-dependent dynamic bias trajectory, which incorporates the large-signal behaviour of the nonlinearities in the time evolution of the state variables.

The derivation of the linear time-varying small-signal model (also called the variational equation) was given, and also the special case of linear time-invariant small-signal models and linear time-invariant circuits was treated. It was shown how deviations in instantaneous behaviour, internally generated noise and deviation in dynamic behaviour can be incorporated in the LTV small-signal model. The determination of the dynamic behaviour of the state-variables from the homogeneous variational equation, and its description in terms of time-domain modes, is the first and most important step in any analysis using the LTV small-signal model. Any subsequent analysis of the effect of deviations in amplitude behaviour and of internally generated noise from the nonhomogeneous variational equation uses these results: the same time-domain modes are present in the small-signal and noise expressions derived from the nonhomogeneous variational equation. Therefore, this thesis focuses on the description of the dynamic behaviour of nonlinear circuits using the time-domain modes of the homogeneous variational equation.

For linear systems with constant coefficients these time-domain modes were shown to be defined by the eigenvalues and eigenvectors of the constant state-transition matrix \mathbf{A} . The solutions are stable if all eigenvalues have a negative real part. This property is well-known from the familiar frequency domain description of LTI systems: the solutions are stable if all poles have negative real part, and these poles equal the eigenvalues of \mathbf{A} . For linear systems with periodic coefficients the modes are defined by periodic eigenvectors and Floquet exponents. The solutions are stable if all Floquet exponents have negative real parts, and the Floquet exponents of an LTI system equal the eigenvalues of \mathbf{A} . For linear systems with arbitrary time-varying coefficients the modes are defined by dynamic eigenvalues and eigenvectors, which can be obtained from a generalized characteristic equation. When the coefficients are slowly-varying, a frozen time approach can be used and quasi-static eigenvalues and eigenvectors

are obtained. The solutions of a general LTV system are stable if the Lyapunov exponents of all its modes are negative. This stability criterion based on Lyapunov exponents was shown to simplify to the stability criterion based on Floquet exponents for periodic LTV systems and to the stability criterion based on poles for LTI systems.

The concept of dynamic eigenvalues and eigenvectors, and stability analysis using Lyapunov and Floquet exponents, was applied to the variational equation for nonlinear circuits exhibiting first-order and second-order dynamic behaviour, respectively. For first-order variational equations the dynamic eigenvalue was obtained easily. For second-order variational equation a method was shown which uses the solution of a Riccati differential equation in order to derive the dynamic eigenvalues. A transformation method was given in Appendix C in order to obtain this solution, even if it contains singularities.

The linear time-varying approach was applied in the design of three classes of circuits. First in Chapter 6 we applied the linear time-varying approach to the design of a negative-feedback amplifier with class-B output stage. Though the intended transfer is linear, an LTV small-signal model is necessary in order to be able to incorporate the effect of the strongly nonlinear class-B output stage on the dynamic behaviour. Since the main source of nonlinear effects in the negative-feedback class-B output amplifier is the class-B output stage, we first analyzed this push-pull class-B output stage separately. By considering three regions of operation of the class-B stage (relatively low frequencies with instantaneous behaviour; relatively high frequencies and large input amplitudes with behaviour dominated by diffusion capacitors; relatively high frequencies and small signal amplitudes with behaviour dominated by junction capacitors), we were able to find some explicit expressions for the dynamic bias trajectory, dynamic eigenvalue and Floquet exponent of the class-B stage. The approximated results were compared with exact results, obtained using numerical evaluation of the complete nonlinear differential equation and corresponding variational equation, and the results were found to be in good agreement. We were able to generate a plot of the Floquet exponent versus the input signal amplitude, for various input signal frequencies, in which we were able to give explicit expressions for the asymptotes. This enables a fast evaluation of the dynamic behaviour of the class-B stage. The push-pull class-B output stage was applied in a low-voltage low-power balanced transimpedance amplifier, and the linear time-varying approach was used for examining the dynamic behavior. The measured bandwidth of the built amplifier was in correspondence with the calculated Floquet exponents. An intuitive explanation of the transfer characteristics could be given, using the knowledge of the class-B stage dynamic behaviour.

Second, in Chapter 7 we applied the linear time-varying approach to analyze the dynamic behaviour of dynamic translinear (DTL) circuits in the presence of parasitics. High-level synthesis/analysis methods are available for DTL cir-

circuits, based on ideal models. By lack of a suitable modeling method, the effect of parasitic capacitances has not yet been rigorously incorporated before. DTL synthesis and analysis are based on the nonlinear input-output relation of the transistor. Therefore, the system behaviour in the presence of parasitics is often defined by nonlinear differential equations, even if the ideal overall transfer function is linear. We used the LTV approach for handling these nonlinear differential equations for the low-level analysis/synthesis of two example DTL circuits: a first-order DTL filter and a DTL oscillator. Through the example of a first-order linear DTL filter it has been shown that the linear time-varying approach is a useful method for analyzing DTL circuits in the presence of parasitics. We applied the linear time-varying approach to analyze the dynamic behaviour of the DTL filter in the presence of parasitic capacitors and compared the results with the quasi-static and LTI approach. The dynamic eigenvalue of the DTL filter was shown to converge to the designed ideal linear pole if the parasitics vanish, which is a required property. The time-varying pole of the quasi-static approach does not have this property. If the DTL filter is operating under slowly-varying conditions the quasi-static pole was shown to be equal to the dynamic eigenvalue. The example of a DTL oscillator was chosen because the nonlinearity in the differential equation describing this circuit is not a consequence of parasitic effects, but rather a conscious design choice. Neither the quasi-static nor the LTI approach can be applied to analyze this oscillator. Its operation is based on an instantaneous control action, and as a consequence it is neither a slowly varying nor a linear time-invariant system. Therefore, only the linear time-varying approach is applicable. The dynamic eigenvalues, which contain periodic singularities, were derived using the transformation method described in Appendix C. The Floquet exponents were derived from these dynamic eigenvalues; they correspond to the properties of a stable limit cycle. This confirms the consistency of the method used.

Third, in Chapter 8 we applied the linear time-varying approach to the differential pair. When driven with a sufficiently large input signal, this commonly used amplifier stage implements the limiter function and inherently behaves strongly nonlinear. First we ignored the base-resistances, which resulted in a first-order nonlinear model for the differential pair. The dynamic bias trajectory for a sinusoidal input signal was determined, and from this the dynamic eigenvalue and Floquet exponent was calculated. We found that the Floquet exponent is equal to the transit frequency of the transistor for the specific tail bias-current. This is quite different from the LTI-model of the differential pair without base-resistances, for which the pole cancels out and which predicts a frequency independent transfer. The latter result is physically not very realistic. We expect to see at least the finite speed of the transistors used, and the Floquet exponent obtained with the LTV approach does have this property. We also found that even for a differential pair which is completely switching the

Floquet exponent still almost equals the transit-frequency curve of the transistors. We can conclude that in this first-order analysis the nonlinearity of the limiting differential pair has no significant effect on the stability analysis and that the LTI-pole provides a good estimate of the Floquet exponent. When the base-resistances are not neglected, a second-order state-space model of the differential pair results. Again a dynamic bias trajectory and dynamic eigenvalues were derived. In order to obtain the dynamic eigenvalues, a Riccati quadratic differential equation has to be solved. The solution turned out to have singularities, and the transformation method elaborated in appendix C had to be used. Using this method the dynamic eigenvalues were obtained. The second transformation variable $m(t)$, which defines the dynamic eigenvector, turned out to increase exponentially with time. Therefore, a Floquet exponent could not be determined.

Through the design examples treated the LTV approach has been shown to be a good modeling candidate for low-level analysis/synthesis. Especially the explicit asymptotes and expressions for the Floquet exponent of the class-B stage and of the dynamic translinear filter would be very useful in nonlinear circuit design. A topic of future research should be to find a method for deriving the dynamic eigenvalues which does not result in singularities. The singularities appear to be caused by the separate determination of closely coupled dynamic eigenvalues. A method should be found which is similar to the LTI-handling of complex poles. Another open problem was the non-periodicity of the second transformation variable $m(t)$ for a periodic variational equation. A method should be found which keeps this second transformation variable normalized, such that it only changes the orientation of the dynamic eigenvectors, and not the modulus.

Samenvatting

Ontwerp van niet-lineaire circuits de lineair-tijdvariante methode

De afgelopen jaren neemt de belangstelling voor het ontwerp van niet-lineaire schakelingen steeds meer toe. Het gebruik van niet-lineaire overdrachten als bouwsteen voor de synthese van elektronica brengt met zich mee dat we moeten omgaan met de analyse en synthese van dynamische niet-lineaire circuits. Voor sterk niet-lineaire schakelingen is nog geen gestructureerde ontwerpmethode beschikbaar.

Een algemene methode voor het gestructureerd ontwerpen van niet-lineaire schakelingen wordt gepresenteerd in Hoofdstuk 2. Niet-lineairiteiten werden geclassificeerd op grond van hun instantane gedrag en dynamische gedrag. De beschreven algemene ontwerpmethode houdt de ontwerpcomplexiteit van niet-lineaire schakelingen hanteerbaar door het ontwerpproces op te splitsen in twee stappen: een hoog-niveau synthese/analyse stap en een laag-niveau analyse/synthese stap.

De eerste stap van de algemene ontwerpmethode, zoals behandeld in Hoofdstuk 3, bestaat uit een hoog-niveau synthese/analyse stap. In deze stap wordt een topologie bepaald die de gewenste (niet-lineaire) functie kan implementeren. Simpele modellen en indien mogelijk een synthesemethode toegespitst op de specifieke niet-lineairiteiten worden gebruikt om de ontwerpruimte snel te kunnen doorzoeken. Verschillende modelleringsmethodes om deze hoog-niveau stap te implementeren zijn in beschouwing genomen. Een expansie in basisfuncties die een directe afbeelding op de gebruikte niet-lineaire bouwblokken hebben, lijkt de beste optie te zijn voor het implementeren van deze stap.

De tweede stap van de ontwerpmethode wordt behandeld in Hoofdstuk 4. In deze laag-niveau analyse/synthese stap wordt de kwaliteit van de topologiën onderzocht, en het effect van niet-idealiteiten op het instantane gedrag, ruis gedrag en dynamisch gedrag wordt bepaald. In de laag-niveau stap hebben we in principe modellen met meer details nodig, om het afwijkende gedrag te kunnen

beschrijven. Maar aangezien het groot-sigitaal gedrag al wordt meegenomen in de hoog-niveau stap, hoeven we alleen het effect van kleine afwijkingen te modelleren, en informatie uit de hoog-niveau stap kan worden gebruikt om de complexiteit kleiner te maken. Ook zouden we graag een modelleringsmethode gebruiken die een directe link tussen het model en de fysieke implementatie oplevert, om de ontwerper inzicht te geven waar ingegrepen kan worden om de kwaliteit te verbeteren, indien nodig. Het lineair-tijdvariante klein-sigitaal model—of, als de signalen klein genoeg zijn, het lineair-tijdinvariante klein-sigitaal model—heeft deze eigenschappen doordat het model afhankelijk is van hetingangssigitaal en alleen het effect van kleine afwijkingen modelleert. Het is een goede modelleringskandidaat in de context van laag-niveau analyse/synthese en is het belangrijkste onderwerp van dit proefschrift.

De lineair-tijdvariante (LTV) methode, zoals behandeld in hoofdstuk 5, generaliseert de conventionele lineair-tijdinvariante (LTI) modelleringsmethode door het gedrag van een niet-lineaire schakeling niet te beschrijven in de omgeving van een (DC-sigitaalafhankelijk) instelpunt, maar in de omgeving van een (sigitaalafhankelijke) dynamische instelbaan. Het lineair-tijdvariante klein-sigitaal model wordt verkregen door het gedrag van de niet-lineaire schakeling te lineariseren in de sigitaalafhankelijke dynamische instelbaan. Deze modelleringsmethode is exact in de dynamische instelbaan, ook al wordt er een linearisatie gebruikt, omdat de volgende stap in de linearisatie wordt bepaald door de dynamische instelbaan en die bevat de informatie over het groot-sigitaal gedrag van de niet-lineairiteiten

De afleiding van het lineair-tijdvariante klein-sigitaal model (ook wel de variatievergelijking genoemd) is gegeven, en ook de speciale gevallen van lineair-tijdinvariante klein-sigitaal modellen and lineair-tijdinvariante schakelingen zijn behandeld. Er is aangegeven hoe afwijkingen in instantaan gedrag, ruis gedrag en dynamisch gedrag kunnen worden meegenomen in het LTV model. Het bepalen van het dynamisch gedrag van de toestandsvariabelen met behulp van de homogene variatievergelijking en de beschrijving van dit gedrag met tijddomein modi, is de eerste en meest belangrijke stap in elke analyse met behulp van het lineair-tijdvariante klein-sigitaal model. Elke verdere analyse van het effect van afwijkingen van het instantane gedrag en van het ruisgedrag met behulp van de niet-homogene variatievergelijking bouwt verder op deze resultaten: dezelfde tijddomein modi zijn ook aanwezig in de klein-sigitaal en ruis expressies die afgeleid kunnen worden van de niet-homogene variatievergelijking. Daarom spitst dit proefschrift zich toe op de beschrijving van het dynamisch gedrag van niet-lineaire schakelingen met behulp van de tijddomein modi van de homogene variatievergelijking.

Voor lineaire systemen met constante coëfficiënten hebben we laten zien dat deze tijddomein modi bepaald worden door de eigenwaarden en eigenvectoren van de constante toestands-transitiematrix \mathbf{A} . De oplossingen zijn stabiel als

alle eigenwaarden een negatieve reële waarde hebben. Deze eigenschap is ook bekend van de conventionele frequentiedomein beschrijving van LTI systemen: de oplossingen zijn stabiel als alle polen een negatieve reële waarde hebben, en deze polen zijn gelijk aan de eigenwaarden van \mathbf{A} . Voor lineaire systemen met periodieke coëfficiënten worden de modi bepaald door periodieke eigenvectoren en Floquet exponenten. De oplossingen zijn stabiel als alle Floquet exponenten een negatieve reële waarde hebben, en de Floquet exponenten van een LTI systeem worden gegeven door de eigenwaarden van \mathbf{A} . In het algemene geval van lineaire systemen met tijdvariërende coëfficiënten worden de modi bepaald door dynamische eigenwaarden en eigenvectoren, die afgeleid kunnen worden van een gegeneraliseerde karakteristieke vergelijking. Als de coëfficiënten langzaam variëren dan kan een "bevroren tijd" methode gebruikt worden en worden quasi-statische eigenwaarden en eigenvectoren verkregen. De oplossingen van een algemeen LTV systeem zijn stabiel als de Lyapunov exponenten van al de modi negatief zijn. Dit stabiliteitscriterium gebaseerd op Lyapunov exponenten simplificeert tot het stabiliteitscriterium gebaseerd op Floquet exponenten voor periodieke LTV systemen en tot het stabiliteitscriterium gebaseerd op polen voor LTI systemen.

Het concept van dynamische eigenwaarden en eigenvectoren, en stabiliteitsanalyse met behulp van Lyapunov en Floquet exponenten, is toegepast op de variatievergelijking van niet-lineaire schakelingen met eerste-orde en tweede-orde dynamisch gedrag. Voor eerste-orde variatievergelijkingen is de dynamische eigenwaarde gemakkelijk te bepalen. Voor tweede-orde variatievergelijkingen is er een methode beschreven die de oplossing van een Riccati differentiaalvergelijking gebruikt om de dynamisch eigenwaarden af te leiden. In Appendix C is een transformatiemethode behandeld om de oplossing van de Riccati differentiaalvergelijking te vinden, zelfs als hij singulariteiten bevat.

De lineair-tijdvariante methode is toegepast bij het ontwerp van drie klassen van schakelingen. Ten eerste hebben we in Hoofdstuk 6 de lineair-tijdvariante methode toegepast bij het ontwerp van een negatief-teruggekoppelde versterker met een klasse-B uitgangstrap. Hoewel de bedoelde overdracht lineair is moeten we toch een LTV klein-sigitaal model gebruiken om het effect van de sterk niet-lineaire klasse-B uitgangstrap op het dynamisch gedrag te kunnen beschrijven. Omdat de belangrijkste bron van niet-lineaire effecten in de negatief-teruggekoppelde versterker wordt gevormd door de klasse-B uitgangstrap, hebben we deze push-pull klasse-B uitgangstrap eerst apart geanalyseerd. Door drie werkingsgebieden van de klasse-B trap te onderscheiden (relatief lage frequenties met instantaan gedrag; relatief hoge frequenties en grote signaalamplitudes met gedrag gedomineerd door diffusiecapaciteiten; relatief hoge frequenties en kleine signaalamplitudes met gedrag gedomineerd door junctiecapaciteiten) waren we in staat expliciete uitdrukkingen te vinden voor de dynamische instelbaan, dynamische eigenwaarde en Floquet exponent van de klasse-B trap. Deze be-

naderde resultaten werden vergeleken met exacte resultaten, verkregen door numerieke evaluatie van de complete niet-lineaire differentiaalvergelijking en bijbehorende variatievergelijking, en de resultaten bleken goed overeen te komen. We konden een figuur van the Floquet exponent versus de ingangsignaalamplitude genereren, voor verschillende ingangsignaalfrequenties, waarin we expliciete uitdrukkingen voor de asymptoten konden geven. Dit maakt een snelle evaluatie van het dynamisch gedrag van de klasse-B trap mogelijk. De push-pull klasse-B uitgangstrap werd toegepast in een laagspanning laagvermogen gebalanceerde transimpedantie versterker, en de lineair-tijdvariante methode werd gebruikt om het dynamisch gedrag te onderzoeken. De gemeten bandbreedte van de gerealiseerde versterker kwam overeen met de berekende Floquet exponenten. We konden een intuïtieve verklaring voor de overdrachtskarakteristieken geven, met gebruik van onze kennis van het dynamisch gedrag van de klasse-B trap.

Ten tweede hebben we in Hoofdstuk 7 de lineair-tijdvariante methode gebruikt om het dynamisch gedrag van dynamisch-translineaire (DTL) schakelingen te beschrijven, als er parasitaire capaciteiten aanwezig waren. Hoog-niveau synthese/analyse methodes zijn beschikbaar voor DTL schakelingen, gebaseerd op ideale modellen. Door gebrek aan een geschikte modelleringsmethode is het effect van parasitaire capaciteiten niet systematisch meegenomen. DTL synthese en analyse zijn gebaseerd op de niet-lineaire ingang-uitgang relatie van de transistor. Daarom wordt het systeemgedrag bij de aanwezigheid van parasitaire capaciteiten vaak beschreven door niet-lineaire differentiaalvergelijkingen, ook al is de ideale overdrachtsfunctie lineair. We hebben de LTV methode gebruikt om deze niet-lineaire differentiaalvergelijkingen te behandelen bij de laag-niveau analyse/synthese van twee voorbeelden van DTL schakelingen: een eerste-orde DTL filter en een DTL oscillator. Door het voorbeeld van een eerste-orde lineair DTL filter hebben we laten zien dat de lineair-tijdvariante methode een bruikbare methode is om DTL circuits te analyseren bij de aanwezigheid van parasitaire capaciteiten. We hebben de lineair-tijdvariante methode toegepast om het dynamisch gedrag van het DTL filter bij aanwezigheid van parasitaire capaciteiten te analyseren en hebben de resultaten vergeleken met de quasi-statische en LTI methode. De dynamische eigenwaarde van het DTL filter bleek te convergeren naar de ontworpen ideale lineaire pool als we de parasitaire capaciteiten steeds kleiner veronderstelden, wat een noodzakelijke eigenschap is. De tijd-variërende pool van de quasi-statische methode heeft deze eigenschap niet. Als het DTL filter in het langzaam variërende regime gebruikt werd bleek de quasi-statische pool gelijk te zijn aan de dynamische eigenwaarde. Het voorbeeld van de DTL oscillator werd gekozen omdat de niet-lineariteit in de differentiaalvergelijking die deze schakeling beschrijft geen gevolg is van parasitaire effecten, maar een bewuste ontwerpkeuze is. Noch de quasi-statische, noch de LTI methode kan worden toegepast om deze oscillator te analyseren, aangezien zijn manier van werken is gebaseerd op een instantaan bijstuurgedrag, en het di-

entengevolge noch een langzaam variërend noch een lineair-tijdinvariant systeem is. Daarom kunnen we alleen de lineair-tijdvariante methode gebruiken. De dynamische eigenwaarden, die periodieke singulariteiten bevatten, werden bepaald met behulp van de transformatie methode beschreven in Appendix C. De Floquet exponenten afgeleid van deze dynamische eigenwaarden kwamen overeen met de eigenschappen van een stabiele limitcycle. Dit bevestigt de consistentie van de gebruikte methode.

Ten derde, zoals beschreven in Hoofdstuk 8, hebben we de lineair-tijdvariante methode toegepast op de verschiltrap. Als deze aangestuurd wordt met een voldoende groot ingangssignaal, dan implementeert deze veelgebruikte versterkertrap de limietfunctie en vertoont sterk niet-lineair gedrag. In eerste instantie hebben we de basis-weerstand verwaarloosd, waardoor we een eerste-orde niet-lineair model voor de verschiltrap verkregen. De dynamische instelbaan voor een sinusöide ingangssignaal werd bepaald en daarmee berekenden we de dynamische eigenwaarde en Floquet exponent. De Floquet exponent bleek gelijk te zijn aan de overgangsfrequentie van de transistor voor de specifieke staartstroom. Dit is heel verschillend van het LTI model van de verschiltrap zonder basisweerstand, waarvoor de pool wegvalt en een frequentie-onafhankelijke overdracht voorspeld wordt. Dit laatste is natuurlijk fysiek niet erg realistisch. We verwachten in ieder geval de beperkte snelheid van de gebruikte transistoren te zien, en de Floquet exponent verkregen met de lineair-tijdvariante methode heeft deze eigenschap. Ook bleek dat zelfs voor een verschiltrap die volledig schakelde de Floquet exponent nog steeds vrijwel gelijk was aan de overgangsfrequentie van de transistoren. We kunnen concluderen dat in deze eerste-orde analyse de niet-lineariteit van de schakelende verschiltrap geen significante invloed heeft op de stabiliteitsanalyse en dat de LTI pool een goede benadering voor de Floquet exponent is. Als de basisweerstand niet worden verwaarloosd verkrijgen we een tweede-orde toestandsbeschrijving van de verschiltrap. We bepaalden weer de dynamische instelbaan en dynamische eigenwaarden. Om de dynamische eigenwaarden te verkrijgen moest een Riccati kwadratische differentiaalvergelijking opgelost worden. De oplossing bleek singulariteiten te bevatten, en de transformatie methode beschreven in Appendix C moest worden gebruikt. Op deze manier konden de dynamische eigenwaarden worden bepaald. De tweede transformatievariabele $m(t)$, die de dynamische eigenvector definieert, bleek exponentieel toe te nemen in de tijd. Daarom kon de Floquet exponent niet bepaald worden.

Door de behandelde ontwerpvoorbeelden hebben we laten zien dat de LTV methode een goede kandidaat is als modelleringsmethode voor laag-niveau analyse/synthese. In het bijzonder de expliciete asymptoten en uitdrukkingen voor de Floquet exponent voor de klasse-B trap en het dynamisch-translineaire filter zouden erg nuttig zijn bij het ontwerp van niet-lineaire schakelingen. Een onderwerp van verder onderzoek is het vinden van een methode om de dy-

namische eigenwaarden te bepalen die niet in singulariteiten resulteert. De singulariteiten lijken veroorzaakt te worden door het apart bepalen van sterkgekoppelde dynamisch eigenwaarden. Een methode zou gevonden moeten worden vergelijkbaar met de manier waarop complexe polen in LTI systemen behandeld worden. Een ander open probleem was de niet-periodiciteit van de tweede transformatievariabele $m(t)$ voor een periodieke variatievergelijking. Er zou een methode gezocht moeten worden om deze tweede transformatievariabele genormaliseerd te houden, zodat alleen de oriëntatie van de dynamische eigenvectoren verandert en niet de modulus.

Acknowledgements

Realizing a thesis is a lengthy and exhausting activity. It would not have been possible to finish this thesis without the support and stimulation of a lot of people.

First of all, I would like to thank dr.ir. Arie van Staveren, my advisor and co-promotor who kept me going even when I had lost confidence myself, and my promotor prof.dr.ir. A.H.M. van Roermund, for their stimulating discussions and the time they invested in proof-reading the concept versions of this manuscript. I would also like to thank my early-day advisor dr.ir. Chris Verhoeven, for introducing me to the Electronics Research Laboratory and to the subject of this thesis.

I would also like to express my gratitude to dr.ir. Fred Neerhoff, dr.ir. Piet van der Kloet and Miguel de Anda, M.Sc., who worked in the same field of research, for numerous discussions we had and for contributing a lot to the theoretical background of this work. My thanks go also to the students who contributed to this work: Fabio Diepstraten, Thomas Cordenier and Richard Koek.

Thanks also to all my colleagues of the Electronics Research Laboratory during my thesis work, for providing a pleasant and stimulating working atmosphere, and in particular to my roommates Paul de Jong, Martijn Goossens, Jan Mulder, Roelof Klunder and Erhan Yildiz.

I'm very grateful to my friends and family, especially to my mother and late father, who always supported me and stimulated me to study and develop myself. Finally, thanks and love go to my girlfriend Carola, whose support and patience were crucial.

List of publications

1. F.C.M. Kuijstermans, A. van Staveren, P. van der Kloet, F.L. Neerhoff and C.J.M. Verhoeven, *Dynamic Exponent-based Electronics*, Proceedings CSSP'97, pp. 307-315, Mierlo, the Netherlands, Nov. 1997.
2. P. van der Kloet, F.L. Neerhoff, F.C.M. Kuijstermans, A. van Staveren and C.J.M. Verhoeven, *Generalizations for the Eigenvalue and Pole Concept with respect to Linear Time-Varying Systems*, Proceedings CSSP'97, pp. 291-296, Mierlo, the Netherlands, Nov. 1997.
3. F.C.M. Kuijstermans, A. van Staveren, P. van der Kloet, F.L. Neerhoff and C.J.M. Verhoeven, *Dynamic Behaviour of Nonlinear Circuits: the Linear Time-Varying Approach*, Proceedings NDES'98, pp. 279-285, Budapest, July 1998.
4. F.C.M. Kuijstermans, F.M. Diepstraten, W.A. Serdijn, P. van der Kloet, A. van Staveren, and A.H.M. van Roermund, *Dynamic Behaviour of a First-Order Dynamic Translinear Filter: the Linear Time-Varying Approach*, Proceedings CSSP'98, pp. 323-330, Mierlo, the Netherlands, Nov. 1998.
5. A. van Staveren, T.H.A.J. Cordenier, F.C.M. Kuijstermans, P. van der Kloet, C.J.M. Verhoeven and A.H.M. van Roermund, *Design of a Negative-Feedback Class-B Output Amplifier: the Linear Time-Varying Approach*, Proceedings CSSP'98, pp. 521-527, Mierlo, the Netherlands, Nov. 1998.
6. F.C.M. Kuijstermans, F.M. Diepstraten, W.A. Serdijn, P. van der Kloet, A. van Staveren, and A.H.M. van Roermund, *The Linear Time-Varying Approach applied to a First-Order Dynamic Translinear Filter*, Proceedings ISCAS'99, Vol. VI, pp. 69-72, Orlando, June 1999.
7. A. van Staveren, T.H.A.J. Cordenier, F.C.M. Kuijstermans, P. van der Kloet, F.L. Neerhoff, C.J.M. Verhoeven and A.H.M. van Roermund, *The Linear Time-Varying Approach applied to the design of a Negative-Feedback*

- Class-B Output Amplifier*, Proceedings ISCAS'99, Vol. II, pp. 204-207, Orlando, June 1999.
8. T. Falk, F.C.M. Kuijstermans and A. van Staveren, *Investigation of the Stability Properties of a Class of Oscillators using Lyapunov Transformations*, Proceedings NDES'99, pp. 221-224, Rønne, Denmark, July 1999.
 9. P. van der Kloet, F.C.M. Kuijstermans, F.L. Neerhoff, A. van Staveren and C.J.M. Verhoeven, *A Note on Dynamic Eigenvalues and Slowly-Varying Systems*, Proceedings ISTET'99, pp. 141-144, Magdeburg, September 1999.
 10. A. van Staveren, F.C.M. Kuijstermans, P. van der Kloet, F.L. Neerhoff, C.J.M. Verhoeven and A.H.M. van Roermund, *Analyzing Non-linear Circuits using the Linear Time-Varying Approach*, Proceedings ISTET'99, pp. 337-341, Magdeburg, September 1999.
 11. M. de Anda, F.C.M. Kuijstermans, A. van Staveren, P. van der Kloet and F.L. Neerhoff, *Determination of the Steady-State Behaviour of the State Variables of a Second-Order filter with Syllabic Companding*, Proceedings CSSP'99, pp. 9-16, Mierlo, November 1999.
 12. F.M. Diepstraten, F.C.M. Kuijstermans, W.A. Serdijn, P. van der Kloet, A. van Staveren, F.L. Neerhoff, C.J.M. Verhoeven and A.H.M. van Roermund, *Dynamic Behaviour of Dynamic Translinear Circuits: the Linear Time-Varying Approximation*, IEEE Transactions on Circuits and Systems - part I, Vol. 48(11), pp. 1333-1337, November 2001.

Biography

Frank Kuijstermans was born in Oud Gastel, the Netherlands, on November 9th 1970. In 1989, after completing the Atheneum at the "Thomas More College" in Oudenbosch (cum laude), he started his studies at the Delft University of Technology. In 1994 he received his M.Sc. degree in Electrical Engineering (cum laude). After his graduation he joined the Electronics Research Laboratory of the Delft University of Technology as a Ph.D. student, to start the research that culminated in this thesis. In 2000 he joined the National Semiconductor Corporation Delft Design Centre as an analog circuit designer, and currently he is still employed there.